1-1-2007

Studies on polyurethane adhesives and surface modification of hydrophobic substrates.

Jayaraman, Krishnamoorthy
University of Massachusetts Amherst

STUDIES ON POLYURETHANE ADHESIVES AND SURFACE MODIFICATION OF HYDROPHOBIC SUBSTRATES

A Dissertation Presented

by

JAYARAMAN KRISHNAMOORTHY

Submitted to the Graduate School of the
University of Massachusetts Amherst in partial fulfillment
of the requirements for the degree of

DOCTOR OF PHILOSOPHY

September 2007

Polymer Science and Engineering

UMI Number:`3289266

UMI®

STUDIES ON POLYURETHANE ADHESIVES AND SURFACE MODIFICATION OF HYDROPHOBIC SUBSTRATES

A Dissertation Presented

by

JAYARAMAN KRISHNAMOORTHY

Approved as to style and content by:

_____
Shaw Ling Hsu, Chair

_____
Thomas J. McCarthy, Chair

_____
Alfred J. Crosby, Member

_____
D. Venkataraman, Member

_____
Shaw Ling Hsu, Department Head
Polymer Science and Engineering

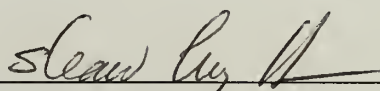# STUDIES ON POLYURETHANE ADHESIVES AND SURFACE MODIFICATION OF HYDROPHOBIC SUBSTRATES

A Dissertation Presented

by

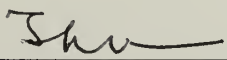JAYARAMAN KRISHNAMOORTHY
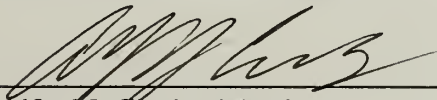
Approved as to style and content by:

_____
Shaw Ling Hsu, Chair

_____
Thomas J. McCarthy, Chair

_____
Alfred J. Crosby, Member

_____
D. Venkataraman, Member
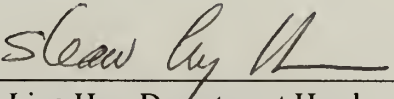
_____
Shaw Ling Hsu, Department Head
Polymer Science and Engineering

ACKNOWLEDGMENTS

I would like to express my gratitude to my advisors, Prof. McCarthy and Prof. Hsu for their encouragement and guidance throughout my graduate career. Tom and Dr. Hsu have different yet effective approaches in training me as a scientist and in improving my communication skills. Tom has allowed me to experiment with my synthetic skills and I thank him for encouraging me and allowing me to learn from my mistakes. Dr. Hsu's question "What will you write (in a paper) if you do this experiment?" is the one that I ask myself whenever I design my experiments. I thank him for guiding me to ask the right questions. I could not have expected a friendlier thesis committee. Thanks to Prof. Crosby and Prof. Venkataraman (DV) for their helpful suggestions and for making me 'feel at home' during my thesis committee meetings. They are great teachers and I appreciate their teaching methods, be it DV's 'NMR jeopardy' or Prof. Crosby's group discussion. I enjoyed the conversations I had with DV. Coming from similar backgrounds, his perspective helped to make my career and personal decisions easier.

I am indebted to all the teachers who have taught me since my childhood days. I would like to thank Prof. T. N. Guru Row for encouraging me to continue my education and research. Special thanks are due to Wei for taking me under her wings and helping me to get started in the lab in my first year. Prof. Coughlin has been a 'go-to' person for me in the final stages of my graduation and I thank him for his insight and amiable nature. This thesis would not have been possible with out the help of Kwasi, Prof. Vachet (in HPLC-MS), Deepak, Prof. Winter (in rheological studies) and Tomoko (in IR studies). I thank them for their help.

ABSTRACT

STUDIES ON POLYURETHANE ADHESIVES AND SURFACE MODIFICATION OF HYDROPHOBIC SUBSTRATES

SEPTEMBER 2007

JAYARAMAN KRISHNAMOORTHY, B.Sc., UNIVERSITY OF MADRAS

M.S., INDIAN INSTITUTE OF SCIENCE, BANGALORE, INDIA

Ph.D., UNIVERSITY OF MASSACHUSETTS AMHERST

Directed by: Professor Shaw L. Hsu and Professor Thomas J. McCarthy

This thesis work deals with (a) Curing of reactive, hot-melt polyurethane adhesives and (b) Adsorption studies using different interactions. Research on polyurethanes involves characterization of polyurethane prepolymers and a novel mechanism to cure isocyanate-terminated polyurethane prepolymer by a "trigger" mechanism. Curing of isocyanate-terminated polyurethane prepolymers has been shown to be influenced by morphology and environmental conditions such as temperature and relative humidity. Although the initial composition, final morphology and curing kinetics are known, information regarding the intermediate prepolymer mixture is yet to be established. Polyurethane prepolymers prepared by the reaction of diisocyanates with the primary hydroxyls of polyester diol (PHMA) and secondary hydroxyls of polyether diol (PPG) were characterized. The morphology and crystallization kinetics of a polyurethane prepolymer was compared with a blend of PPG prepolymer (the product obtained by the reaction of PPG with diisocyanate) and a PHMA prepolymer (the product obtained by the reaction of PHMA with diisocyanate) to study the effect of copolymer formed in the polyurethane prepolymer on the above-mentioned properties.

Although the morphology of the polyurethane prepolymer is determined in the first few minutes of application, the chemical curing of isocyanate-terminated prepolymer occurs over hours to days. In the literature, different techniques are described to follow the curing kinetics. But there is no established technique to control the curing of polyurethane prepolymer. To make the curing process independent of environmental factors, a novel approach using a trigger mechanism was designed and implemented by using ammonium salts as curing agents. Ammonium salts that are stable at room temperature but decompose on heating to yield active hydrogen-containing compounds, NH_3 and H_2O, were used as 'Trojan horses' to cure the prepolymer chemically.

Research on adsorption studies involved making functionalized, thickness-controlled, wettability-controlled multilayers on hydrophobic substrates and the adsorption of carboxylic acid-terminated poly(styrene-*b*-isoprene) on alumina/silica substrates. Poly(vinyl alcohol) has been shown to adsorb onto hydrophobic surfaces irreversibly due to hydrophobic interactions. This thin semicrystalline coating is chemically modified using acid chlorides, butyl isocyanate and butanal to form thicker and hydrophobic coatings. The products of the modification reactions allow adsorption of a subsequent layer of poly(vinyl alcohol) that could subsequently be hydrophobized. This 2-step (adsorption/chemical modification) allows layer-by-layer deposition to prepare coatings with thickness, chemical structure and wettability control on any hydrophobic surface.

Research on adsorption characteristics of carboxylic acid-terminated poly(styrene-*b*-isoprene) involved syntheses of block copolymers with the functional

group present at specific ends. Comparative adsorption studies for carboxylic acid-terminated and hydrogen-terminated block copolymers was carried out on alumina and silica substrates.

TABLE OF CONTENTS

LIST OF TABLES

LIST OF FIGURES

CHAPTER 1

INTRODUCTION

1.1 Polyurethanes as reactive, hot-melt adhesives

Polyurethanes (PUR) find their use in variety of applications including adhesives, coatings, elastomers, fibers and foams. The main reason behind the diversity of applications of polyurethanes is the segmented nature of PURs and the rich chemistry of isocyanates. Hard segments of the PUR impart strength whereas the soft segments provide flexibility, making the PUR elastomeric by nature. By tuning the characteristics of the hard and soft segments, different properties can be realized from PURs. Though the name 'polyurethanes' seek to generalize the functional group present to urethane (carbamate), other functional groups are also present. Hard segments are obtained by the reaction of diisocyanates with small molecule diol, diamine or water. Urea is the functional group obtained by the reaction of amine/water with isocyanate. Functionality in the soft segment is determined by the temperature range for operation, solvent and weather resistance. The polymers predominantly used for soft segments are hydroxyl-terminated polyester, polyether or polycarbonate. Apart from the segmented structure, PURs can also form highly crosslinked networks due to rich isocyanate chemistry. Figure 1.1 shows the possible chain extension and crosslinking chemistry in polyurethanes. A wide variety of catalysts are available to control the products formed in polyurethanes, ranging from tertiary amines to tin compounds.

Polyurethanes find application in reactive, hot-melt adhesives because of their ability to combine the fast setting property of a hot-melt adhesive and the cohesive

1

strength of a crosslinked polymer. In general, reactive, hot-melt polyurethanes involve reacting excess diisocyanate with polyols in the presence of a high T_g component. High T_g component helps in fast vitrification of the adhesive and the polyols provide physical crosslinks and elastic properties through a semi-crystalline component and/or an amorphous component. Excess isocyanate cures chemically over a period of time to yield the chemically crosslinked system.
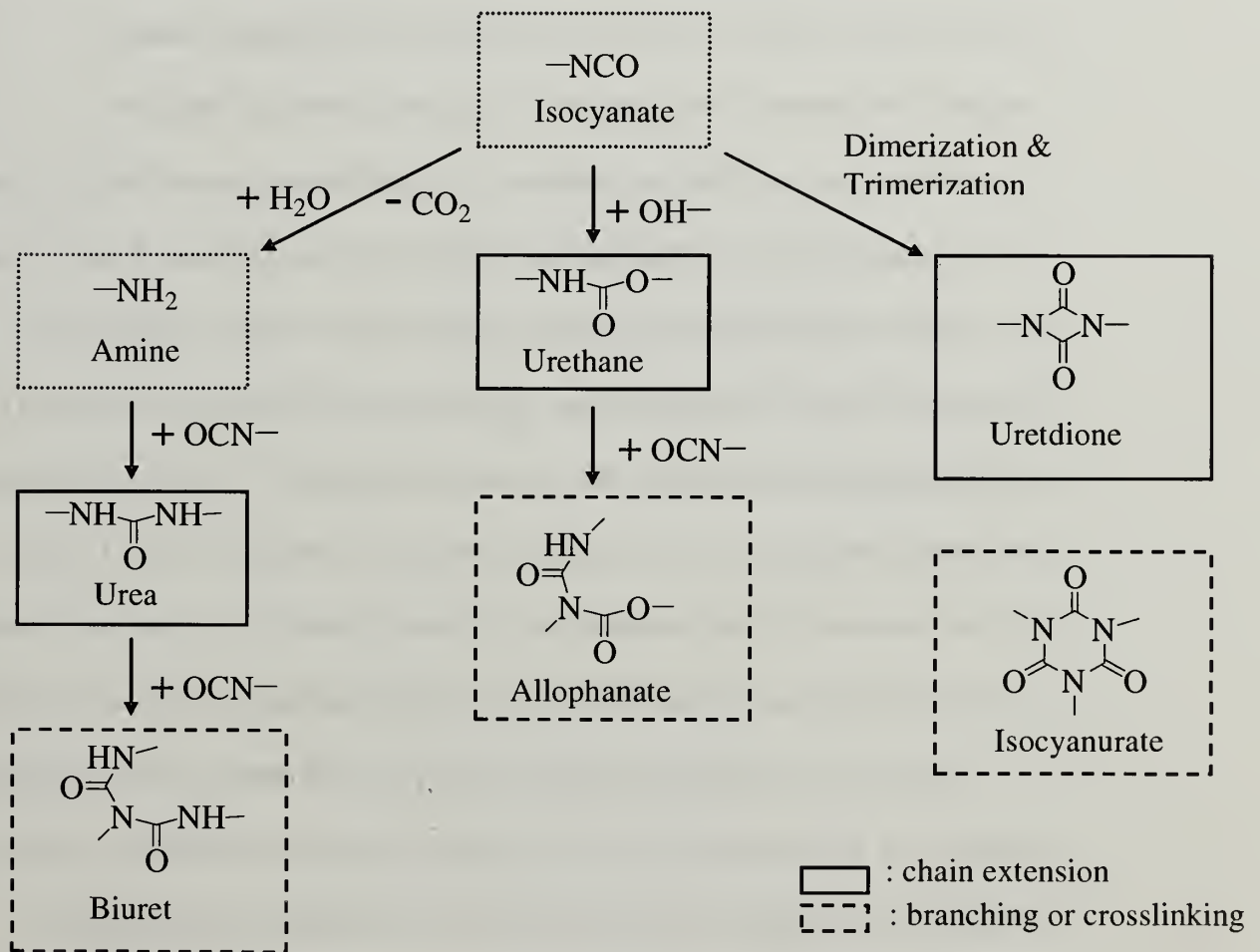
Figure 1.1 Isocyanate chemistry involved in chain extension and crosslinking in polyurethanes.

Apart from the chemical crosslinks, morphology also plays an important role in determining the mechanical strength of the adhesives. Morphology that is more interpenetrating/co-continuous offers better mechanical properties than the domain-matrix structure.[1] Compatibilization is one of the easy ways to achieve co-continuous morphology. A compatibilizer acts as a surfactant and reduces the interfacial tension between the phases. This increases the 'adhesion' between the phases and helps in better stress transfer. With all the above-mentioned advantages, compatibilization can be tuned by the molecular weight of the components and type of copolymer used as compatibilizer (either a block copolymer or a graft copolymer).[2-4] Reactive compatibilization is an effective technique to compatibilize an immiscible blend that involves reaction of the functional groups during the processing stage. Reactive, hot-melt polyurethane adhesives are typically a ternary blend which is reacted with isocyanate during the processing stage.[5-8] Reaction of NCO with hydroxyl groups of polyols changes the morphology and crystallization kinetics.[9,10] Chapter 2 of this thesis deals with quantification of the copolymer formed by the reaction of NCO with the polyols, polyester diol and polyether diol. Influence of this *in-situ* copolymer formation on the morphology and crystallization kinetics of polyurethane prepolymer is studied.

Reaction of isocyanate-terminated prepolymer with water to form crosslinked product is the second step involved in the curing of reactive, hot-melt polyurethane adhesives. In the literature, different techniques are described to characterize the conversion of isocyanate during the curing process.[11-17] But, there exists none to control the curing. However, these kinds of controlled curing by blocking/deblocking isocyanates are well-known phenomena in solvent-borne coatings. Blocking involves

3

reaction of NCO with an active hydrogen compound to yield a product that would generate NCO on deblocking by a change in temperature or pH. A review by Wicks *et. al.* describes the various blocking/deblocking mechanisms available for coating applications.[18] However, these techniques are not applicable for reactive, hot-melt, polyurethane adhesives because curing involves reaction of an active, hydrogen-containing compound with isocyanate. Chapter 3 of this thesis deals with curing of isocyanate-terminated prepolymer by a trigger mechanism where curing process is made independent of environmental conditions.

1.2 Surface modification using adsorption phenomena

Surface modification of polymers plays an important role in wide variety of fields such as adhesion, coatings, tribology and thin-film technology to name a few. Surface modification involves incorporation of functional groups to meet the needs of the specific application without compromising the bulk properties of the material. Conventional ways to modify the surface involve either chemical treatment or plasma/corona treatment.[19] Multilayer formation on different substrates is another way to maintain 'similar surfaces' with varying bulk properties. Multilayer, instead of monolayer is necessary because 'memory effects' persist over short length scales. The literature describes different methods to fabricate multilayers. Ionic interactions, H-bond interactions, charge transfer, repetitive adsorption/drying, biological interactions and various complex formation methods were studied for multilayer film construction.[20-26] Although these methods extend multilayer assembly to neutral molecules with specific interactions, they individually lack latitude in terms of substrate choice and multilayer

functionality and collectively do not comprise a versatile method, but rather a collection of specific syntheses. Moreover, these techniques are not applicable for low-energy surfaces as there are no favorable interactions leading to adsorption on these substrates. Chapter 4 of this thesis deals with forming thickness-controlled, wettability-controlled, functionalized multilayers on hydrophobic substrates by using the adsorption characteristics of poly (vinyl alcohol) on hydrophobic substrates using hydrophobic interactions.

Adsorption of polymer onto a substrate is determined by two factors : (a) Loss of translational entropy, polymer/solvent interactions and solvent/adsorbent interactions and (b) Adsorbent/polymer interactions.[27] Chapter 5 of this thesis deals with adsorption of hemi-telechelic block copolymers of carboxylic acid-terminated poly(styrene-*b*-isoprene) and H-terminated poly(styrene-*b*-isoprene) on alumina and silica substrates and the study of the influence of the enthalpic interaction between –COOH and alumina/silica on adsorption of hemi-telechelic block copolymers.

1.3 Thesis overview

This thesis deals with two different fields : (a) Reactive, hot-melt polyurethanes and (b) Surface science. Chapter 1 presents an introduction to the topics discussed in the thesis. In Chapter 2, polyurethane prepolymer, synthesized by the reaction of PPG and PHMA diols with diisocyanate, is characterized for the presence of copolymer of PPG and PHMA. Morphology and crystallization kinetics of the polyurethane prepolymer are compared with the blend of PPG prepolymer (obtained by the reaction of PPG with diisocyanate) and PHMA prepolymer (obtained by the reaction of PPG with

diisocyanate). Chapter 3 presents a proof of concept for the curing of isocyanate-terminated PPG prepolymer by a trigger mechanism. Ammonium salts, that are stable at room temperature but decompose at elevated temperatures to give active hydrogen-containing compounds are used as curing agents. In Chapter 4, functionalized, thickness-controlled, wettability-controlled multilayers are formed on hydrophobic substrates by using the adsorption of poly (vinyl alcohol) (PVOH) and the modification of PVOH by chemical means in a cyclic manner. In Chapter 5, hemi-telechelic block copolymers of poly(styrene-b-isoprene) containing carboxylic acid terminal groups are synthesized by a living, anionic polymerization technique. Adsorption studies are carried out on alumina and silica substrates and the effect of terminal carboxylic acid group on adsorption characteristics is studied. Chapter 6 summarizes and discusses future directions of this thesis work.

1.4 References

(1)   Qiao, L.; Leibig, C.; Hahn, S. F.; Winey, K. I. "Isolating the effects of morphology and chain architecture on the mechanical properties of triblock copolymers" *Ind Eng Chem Res* **2006**, *45*, 5598-5602.

(2)   Folkes, M. J.; Hope, P. S. *Polymer blends and alloys*; Chapman & Hall, 1993.

(3)   Otterson, D. M.; Kim, B. H.; Lavengood, R. E. "The Effect of Compatibilizer Level on the Mechanical-Properties of a Nylon 6/Abs Polymer Blend" *J Mater Sci* **1991**, *26*, 1478-1484.

(4)   Pernot, H.; Baumert, M.; Court, F.; Leibler, L. "Design and properties of co-continuous nanostructured polymers by reactive blending" *Nat Mater* **2002**, *1*, 54-58.

(5)   Jeong, Y. G.; Hashida, T.; Wu, G. L.; Hsu, S. L.; Paul, C. W. "Analysis of the multistep solidification process in polymer blends" *Macromolecules* **2006**, *39*, 274-280.

(6)   Jeong, Y. G.; Ramalingam, S.; Archer, J.; Hsu, S. W.; Paul, C. W. "Influence of copolymer configuration on the phase behavior of ternary blends" *Journal of Physical Chemistry B* **2006**, *110*, 2541-2548.

(7)   Duffy, D. J.; Stidham, H. D.; Hsu, S. L.; Sasaki, S.; Takahara, A.; Kajiyama, T. "Effect of polyester structure on the interaction parameters and morphology development of ternary blends: Model for high performance adhesives and coatings" *J Mater Sci* **2002**, *37*, 4851-4859.

(8)   Duffy, D. J.; Heintz, A. M.; Stidham, H. D.; Hsu, S. L.; Suen, W.; Chu, W.; Paul, C. W. "Influence of polymer structure on melt miscibility of ternary polymer blends: A model for high performance polyurethane adhesives and coatings" *Journal of Adhesion* **2003**, *79*, 1091-1107.

(9)   Duffy, D. J.; Heintz, A. M.; Stidham, H. D.; Hsu, S. L.; Suen, W.; Paul, C. W. "The competitive influence of specific interactions and extent of reaction on the miscibility of ternary reactive polymer blends: model for polyurethane adhesives" *International Journal of Adhesion and Adhesives* **2005**, *25*, 39-46.

(10)   Jeong, Y. G.; Hashida, T.; Nelson, C. M.; Hsu, S. L.; Paul, C. W. "Morphology evolution and associated curing kinetics in reactive blends" *International Journal of Adhesion and Adhesives* **2006**, *26*, 600-608.

(11)   Comyn, J.; Brady, F.; Dust, R. A.; Graham, M.; Haward, A. "Mechanism of moisture-cure of isocyanate reactive hot melt adhesives" *International Journal of Adhesion and Adhesives* **1998**, *18*, 51-60.

(12)   Chen, D. B.; Qi, X.; Zhou, Z. H.; Zhong, A. Y.; Du, Z. Y. "Curing behavior of acrylate-urethane system" *J Appl Polym Sci* **1996**, *62*, 1715-1721.

(13)   Cui, Y. J.; Hong, L.; Wang, X. L.; Tang, X. Z. "Evaluation of the cure kinetics of isocyanate reactive hot-melt adhesives with differential scanning calorimetry" *J Appl Polym Sci* **2003**, *89*, 2708-2713.

(14)   Dimier, F.; Sbirrazzuoli, N.; Vergnes, B.; Vincent, M. "Curing kinetics and chemorheological analysis of polyurethane formation" *Polym Eng Sci* **2004**, *44*, 518-527.

(15)   Lepene, B. S.; Long, T. E.; Meyer, A.; Kranbuehl, D. E. "Moisture-curing kinetics of isocyanate prepolymer adhesives" *Journal of Adhesion* **2002**, *78*, 297-312.

(16)   Sun, X. D.; Sung, C. S. P. "Cure characterization in polyurethane and model urethane reactions by an intrinsic fluorescence technique" *Macromolecules* **1996**, *29*, 3198-3202.

(17)   Jeong, Y. G.; Hashida, T.; Hsu, S. L.; Paul, C. W. "Factors influencing curing Behavior in phase-separated structures" *Macromolecules* **2005**, *38*, 2889-2896.

(18)   Wicks, D. A.; Wicks, Z. W. "Blocked isocyanates III: Part A. Mechanisms and chemistry" *Prog Org Coat* **1999**, *36*, 148-172.

(19)   Chan, C.-M. *Polymer surface modification and characterization*; Hanser Publishers.

(20)   Decher, G.; Hong, J. D.; Schmitt, J. "Buildup of Ultrathin Multilayer Films by a Self-Assembly Process .3. Consecutively Alternating Adsorption of Anionic and Cationic Polyelectrolytes on Charged Surfaces" *Thin Solid Films* **1992**, *210*, 831-835.

(21)   Decher, G.; Lehr, B.; Lowack, K.; Lvov, Y.; Schmitt, J. "New Nanocomposite Films for Biosensors - Layer-by-Layer Adsorbed Films of Polyelectrolytes, Proteins or DNA" *Biosens Bioelectron* **1994**, *9*, 677-684.

(22)   Serizawa, T.; Hashiguchi, S.; Akashi, M. "Stepwise assembly of ultrathin poly(vinyl alcohol) films on a gold substrate by repetitive adsorption/drying processes" *Langmuir* **1999**, *15*, 5363-5368.

(23)   Serizawa, T.; Hamada, K.; Kitayama, T.; Fujimoto, N.; Hatada, K.; Akashi, M. "Stepwise stereocomplex assembly of stereoregular poly(methyl methacrylate)s on a substrate" *Journal of the American Chemical Society* **2000**, *122*, 1891-1899.

(24)   Shimazaki, Y.; Mitsuishi, M.; Ito, S.; Yamamoto, M. "Preparation of the layer-by-layer deposited ultrathin film based on the charge-transfer interaction" *Langmuir* **1997**, *13*, 1385-1387.

(25)   Stockton, W. B.; Rubner, M. F. "Molecular-level processing of conjugated polymers .4. Layer-by-layer manipulation of polyaniline via hydrogen-bonding interactions" *Macromolecules* **1997**, *30*, 2717-2725.

(26)   Wang, L. Y.; Wang, Z. Q.; Zhang, X.; Shen, J. C.; Chi, L. F.; Fuchs, H. "A new approach for the fabrication of an alternating multilayer film of poly(4-vinylpyridine) and poly(acrylic acid) based on hydrogen bonding" *Macromolecular Rapid Communications* **1997**, *18*, 509-514.

(27)   Adamson, A. W.; Gast, A. P. *Physical chemistry of surfaces*, 1997.

CHAPTER 2

CAUSE AND EFFECT OF COPOLYMER FORMATION IN POLYURETHANE

PREPOLYMERS

2.1 Introduction

One-component polyurethane systems used as hot melt adhesives have many attractive physical properties. These formulations have substantial environmental benefits, such as being solvent-free and not producing volatile organic compounds. These polyurethanes also are fast setting, durable, adhere well to a broad range of substrates and are chemically stable.[1,2] Typically, a three-component blend is used, with each component serving a specific purpose to achieve the desired physical properties. The three polymer components commonly employed are polyether, polyester and polyacrylate.[3,4] Polyether is used for its low T_g properties whereas crystallizable polyester is used to control the green strength (initial viscosity) and mechanical properties. Polyacrylate is used for green strength and to enhance the overall physical properties at elevated temperatures.

A substantial number of studies have clarified the miscibility behavior of the various components and morphological features formed.[5-8] The degree of crystallinity and the size of crystallites formed are the controlling factors in determining the effective viscosity thus their applicability as an one component adhesive.[9] These studies are based on the non-reactive components. In actual reactive blends, the situation is more complex. The reaction of diisocyanates and reactive polyols introduces a degree of

complexity that has not been discussed previously for polyurethanes. Besides with the increase in molecular weight and introduction of urethane groups, copolymerization can also occur. The presence of a copolymer that acts as a surfactant reduces the interfacial tension between the immiscible components. All of these effects should influence the morphology of the blends. Therefore, any structural feature that would affect the crystallization behavior would be important to identify and characterize.

Although a large number of studies have been carried out to characterize the reaction products of an isocyanate and an alcohol, only a few studies have been carried out to characterize the products of actual reactive polyurethanes.[10-22] The molecular weight distribution of the prepolymer based on poly(propylene glycol) (PPG) and bis(4-isocyantophenyl) methane (MDI) and the different products formed have been determined recently.[23] In the reactive system under study, poly(propylene glycol) (PPG), a polyether and poly(hexamethylene adipate) (PHMA), a polyester are used as macrodiols. These two macrodiols possess two different types of hydroxyl groups, primary hydroxyl in PHMA and secondary hydroxyl in PPG, with significant differences in reactivity towards isocyanates. This difference in reactivity and the stoichiometric excess of NCO leads to the formation of PPG and PHMA homopolymers, both chain-extended by the urethane functionality and also possible copolymers of PPG and PHMA.

In theory, introduction of copolymers is a simple, economical way to compatibilize two immiscible polymers.[24] Compatibilization changes the morphology of the immiscible blend and has a significant impact on the mechanical properties of the blend. When a block copolymer is added to an immiscible blend, entropy would dictate

11

random distribution of the copolymer. But the presence of the block copolymer at the interface overcomes the unfavorable interaction between the immiscible homopolymers, thereby reducing the interfacial tension.[25,26] Practically, compatibilization can be accomplished by suitably changing the chemistry of the end groups or having conditions that would facilitate copolymer formation. Such compatibilization studies have been extensively carried out with the formation of amide bonds and to a lesser extent with ester bonds while processing. Compatibilization of non-polar polyolefins and polar polyamides has been brought about by the formation of amide bonds between the amine functionality in the polyamide and maleic anhydride incorporated in the polyolefin. Transesterification was employed to compatibilize the ester based systems. Although this technique is widely used, few attempts have been made to quantify the amount of copolymer formed in such systems. [27-30] However, no such compatibilization or quantification has been studied for polyurethane systems in spite of their importance and application.

In this study, we demonstrate a general strategy to quantify the amount of copolymer formed in polyether-based and polyester-based polyurethane prepolymer systems and study how changes in miscibility can be brought about by the presence of copolymers. The changes in the crystallization rate and morphology of the product are then compared to the blends of polyester- based polyurethane (PHMA prepolymer) and polyether-based polyurethane (PPG prepolymer).

2.2 Experimental Section

2.2.1 Materials

Poly (propylene glycol) (PPG) was obtained from ARCH chemical ($M_n = 1900$ g/mol, $M_w/M_n = 1.01$, $T_g = -66$ °C and hydroxyl value (Number of mg of KOH containing same number of hydroxyl groups as in 1 g of the material) = 56). Poly (hexamethylene adipate) (PHMA) was obtained from Dow chemical ($M_n = 1600$ g/mol, $M_w/M_n = 1.59$, $T_m = 55$ °C, $T_g = -61$ °C and hydroxyl value = 34).[31] MDI was used as received (Aldrich, 98%).

2.2.2 Prepolymer synthesis

Polyurethane prepolymer was synthesized as follows. PPG and PHMA were introduced to a three-neck round bottom flask fitted with a mechanical stirrer, vacuum adapter and a rubber septum. Contents of the flask were evacuated at 60 °C coupled with nitrogen purge in a cyclical manner to remove any trace amount of moisture over a period of 24 h. The temperature of the flask was then increased to 120 °C under nitrogen purge. A calculated amount of MDI was added through the septum and the reaction allowed to proceed for 3 h under nitrogen. The prepolymer was synthesized with a PPG/PHMA ratio of 1:1 (by mass) and a NCO/OH ratio of 1.68 with the OH contribution from both PPG and PHMA. Polyurethane prepolymer thus obtained was isocyanate terminated. To facilitate the characterization of the prepolymer, dry methanol was added and stirred for 24 h to obtain methyl-terminated prepolymer. Inactive polyurethane prepolymer, thus obtained, was recovered by rotary evaporation.

13

PPG and PHMA prepolymers were prepared by reaction of the corresponding macromonomer with MDI at 120 °C for 3 h with a NCO/OH ratio of 1.68. Conditions for the synthesis of these prepolymers were the same as mentioned for the polyurethane prepolymer.

2.2.3 Characterization

A Bruker DPX300 spectrometer (300 MHz ^{1}H NMR) was used to record NMR spectra. Acetone-d_6 was used as solvent. An acquisition time of 2.0 s was employed to collect the data and was found to be ample to allow all the protons to relax. The final spectrum was signal-averaged over 16 scans. Fourier Tranform Infrared (FT-IR) spectroscopy was carried out on a Perkin Elmer Spectrum 2000 system using transmission mode. Samples were cast from $CHCl_3$ solution onto a NaCl salt plate and dried under vacuum at 50 °C for 3 h. Spectra recorded were signal averages of 32 scans. Time-resolved IR measurements, to follow the crystallization process, were obtained using a Perkin-Elmer 2000 FT-IR spectrometer in reflection-absorption mode. The spectral resolution was 4 cm^{-1} and the infrared spectra were obtained every 14 s to follow the crystallization process. Samples were melted and transferred to a specially designed cell maintained at a predetermined temperature to have a ΔT ($T_m - T$) of 18 °C. The molecular weight distribution was obtained using a Waters GPC equipped with a differential refractometer using THF as the eluent at a flow rate of 1.0 mL/min. Optical microscopy of the samples was carried out using an Olympus Vanox optical microscope equipped with a Kodak EASYSHARE LS443 zoom digital camera. Thermal analysis was carried out using a TA Instruments Q1000 instrument. A heating

rate of 10 °C/min was used for the thermal measurements. The degree of crystallinity was estimated by comparing the melting enthalpy (ΔH) of an isothermally crystallized sample with the equilibrium melting enthalpy of PHMA ($\Delta H°$).

Filtration was carried out by dissolving/dispersing approximately 1g of polyurethane prepolymer in 10 ml of methanol and filtering the solution/dispersion through a sintered glass funnel. More methanol was added to wash the remains and the residue was dissolved in acetone. The filtrate and residue were dried over a water bath. The filtration products were characterized by NMR, GPC and FT-IR.

The residue of the filtration process was extracted with a mixture of 12.5/1 methanol/chloroform (v/v) using a Soxhlet extractor over 60 h. Due to the high temperature in the sample chamber (because of conduction), part of the residue, which was otherwise insoluble at room temperature in the solvent mixture, was obtained in the extract flask. The solvent mixture was filtered to separate the extract and the insoluble part. The extracted component was obtained from the solution by rotary evaporation. The insoluble component of the extraction process was combined with the residue left in the thimble. It was not possible to verify the amount of sample left in the thimble.

2.3 Results and discussion

2.3.1 Cause of the copolymer formation

Polyurethane prepolymer was obtained by the reaction of diisocyanate (MDI) with the blend of macrodiols, PPG and PHMA. PHMA has primary hydroxyl groups that have higher reactivity with isocyanate compared to the secondary hydroxyl group of

15

PPG.[32] In theory, it is possible to have PPG homopolymer, PHMA homopolymer, copolymer of PPG and PHMA linked by the urethane bond and unreacted MDI as shown in Figure 2.1. It is imperative to identify the different components of the polyurethane prepolymer to account for the observed physical properties.

Filtration is an easy yet effective technique to purify or separate the constituents of the synthesized prepolymer. PHMA is sparingly soluble in methanol whereas PPG is highly soluble. Employing this contrast in solubility, the PPG component of the polyurethane prepolymer can be obtained in the filtrate leaving the PHMA component in the filtration residue. Copolymer, if present, can be obtained either in the filtration residue or the filtrate depending on the volume fraction of the constituents in the copolymer. Components obtained from filtration were compared with PPG and PHMA prepolymers.
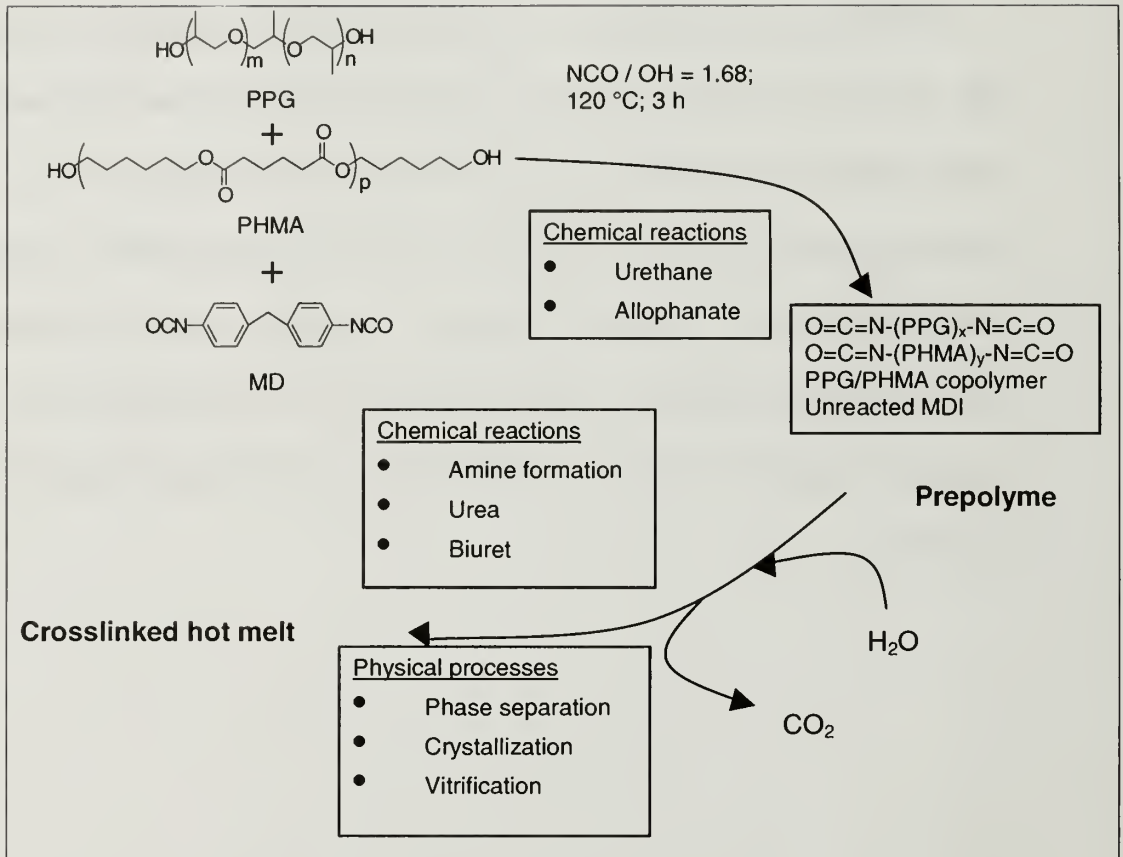
Figure 2.1 Processes involved in crosslinked, hot melt polyurethane adhesives
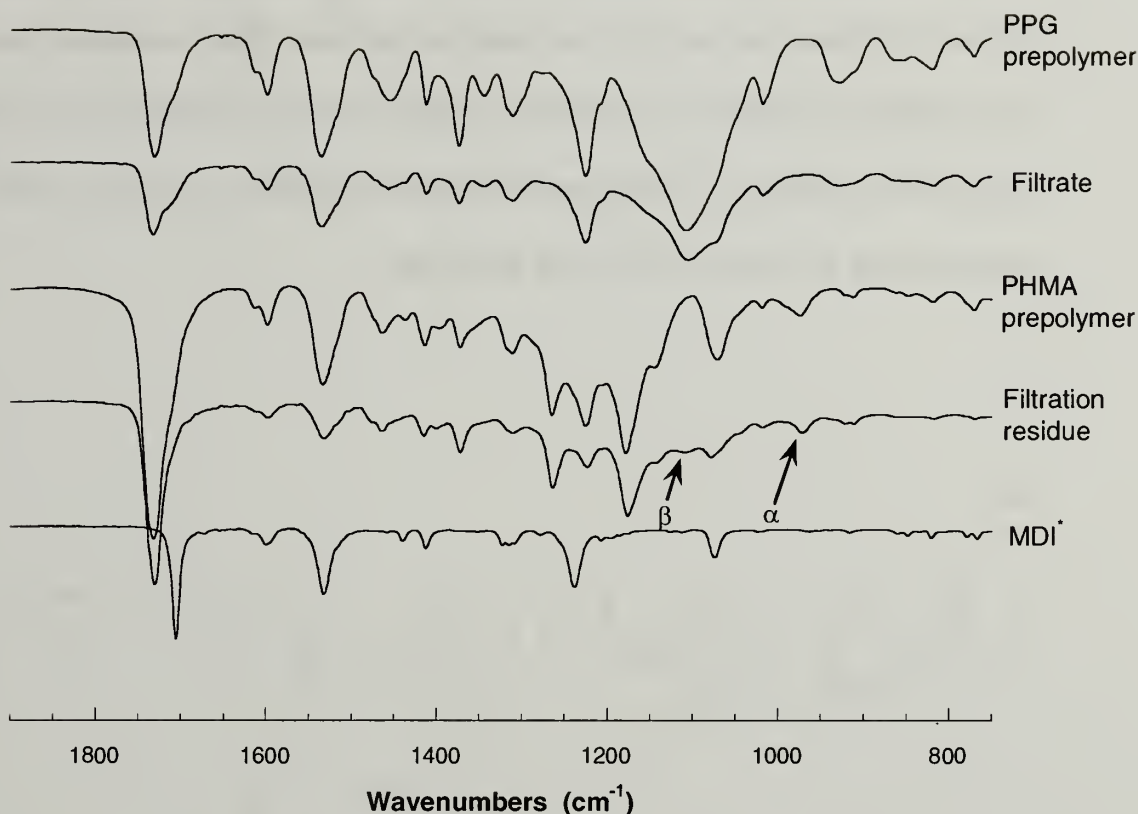
Figure 2.2 IR analyses of different prepolymer systems and filtration products. β shows the C-O-C stretching band at 1108 cm⁻¹ and α shows the PHMA crystallization band at 973 cm⁻¹. MDI* denotes methanol-reacted MDI.

The filtration residue and filtrate were analyzed for functional groups by infrared spectroscopy. The 1108 cm⁻¹ band is characteristic of the backbone stretching of the C-O-C functional group, which is indeed found to be extremely intense in the filtrate as shown in Figure 2.2. In contrast, the intensity of this band is weak in the filtration residue indicating the presence of PPG in the filtration residue. Its presence in the residue can only be attributed to the PPG in the copolymer of PPG and PHMA. The band at 973 cm⁻¹ is the CH_2 skeletal backbone deformation band that is sensitive to conformational order. This conformational order is identified with the crystalline state

18

of PHMA.[8] From Figure 2.2, it is clear that PHMA in the filtration residue crystallizes whereas the filtrate does not show any crystallization peak. This observation confirms the crystallinity of PHMA in the filtration residue but rules out crystallization of PHMA in the filtrate. However, it is important to note that the absence of crystalline PHMA does not imply an absence of PHMA in the filtrate.

(a)
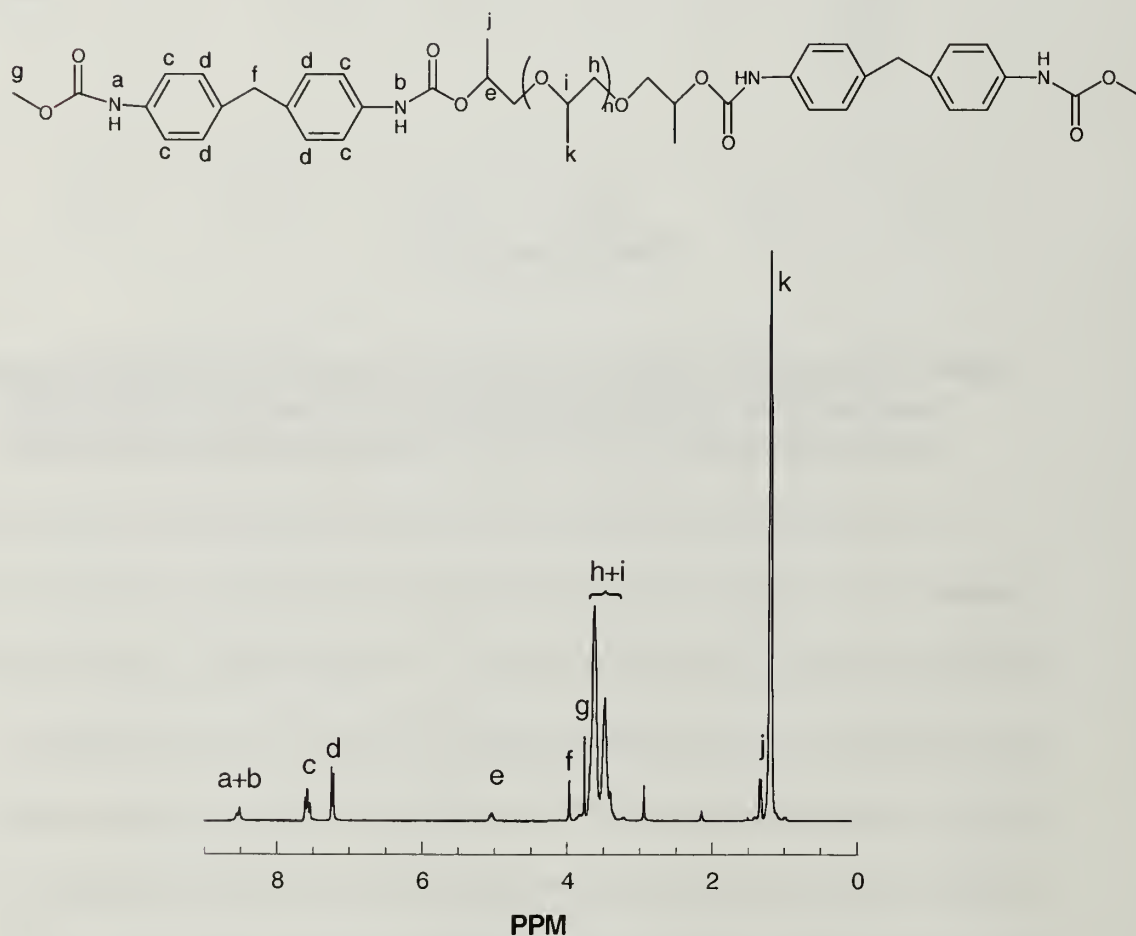
(b)
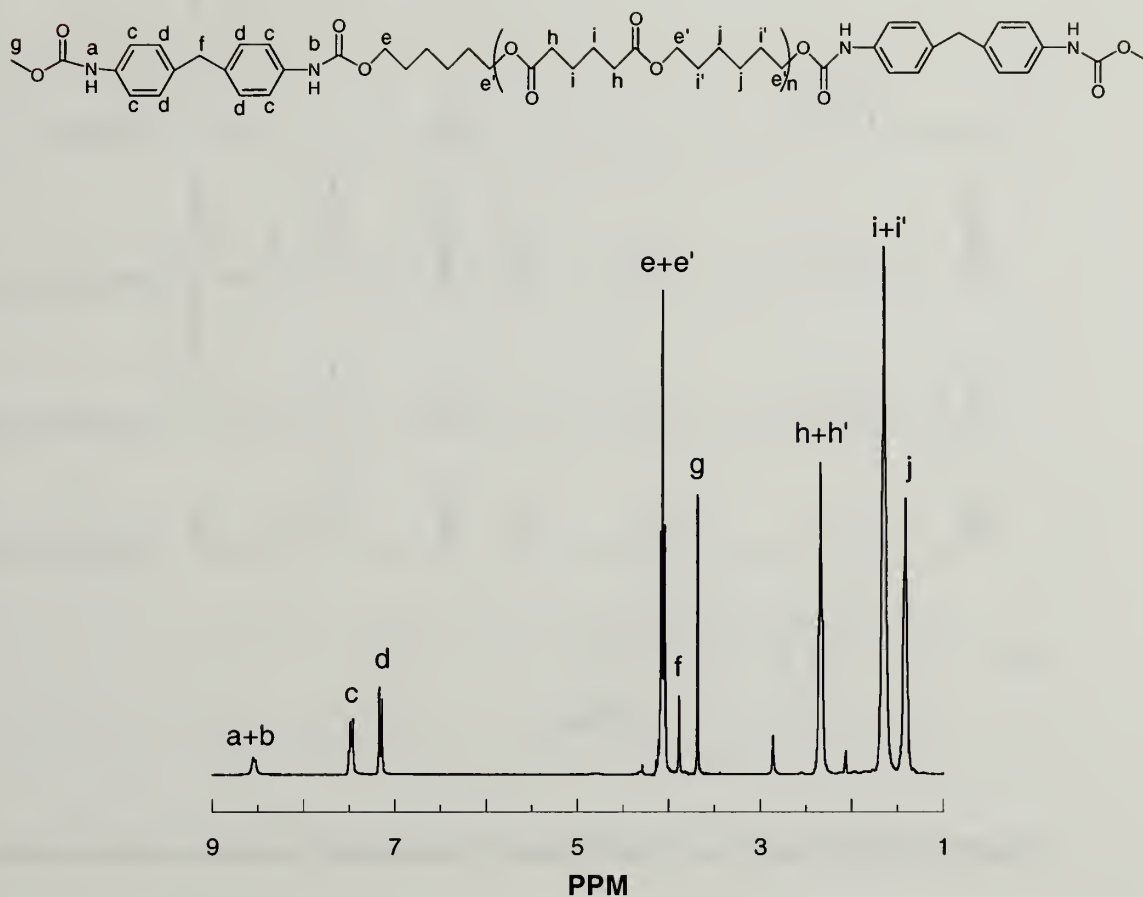
Figure 2.3 NMR spectra of (a) PPG prepolymer and (b) PHMA prepolymer and the corresponding assignments for the protons.
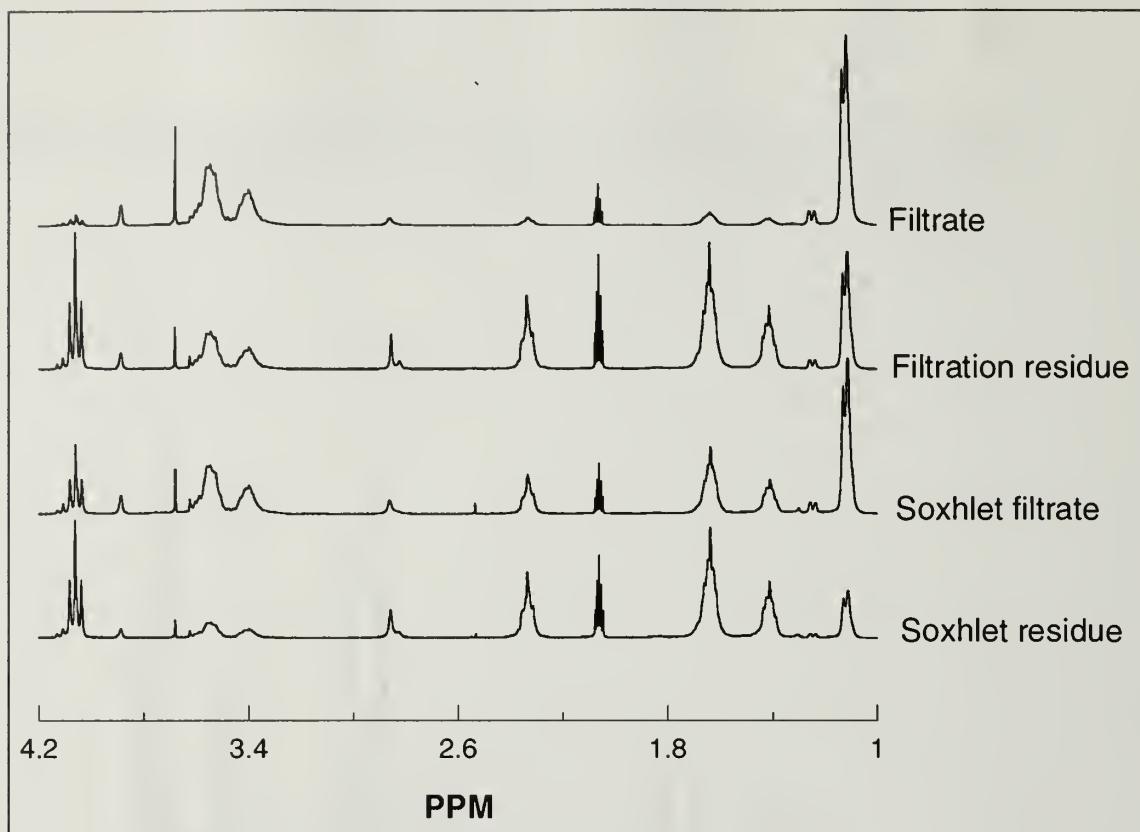
Figure 2.4 NMR analyses of the different constituents of polyurethane prepolymer.

Proton NMR was used to quantify the copolymer in the filtration residue and the filtrate. Figure 2.3 shows the NMR spectrum of PPG and PHMA prepolymers and the corresponding peak assignments. The methylene protons adjacent to the ester carbonyl (at 2.2-2.5 ppm) were used as the signature for the PHMA component and the methyl protons to assign the PPG component (1.0-1.3 ppm). Aromatic protons of MDI were used to calculate the MDI contribution. Figure 2.4 shows the NMR spectra of different constituents of the polyurethane prepolymer. From the spectra of filtration products, mass ratios of PPG/PHMA were calculated using the molar mass of the monomers of PHMA (228 g/mol) and PPG (58 g/mol). For the filtrate, PPG/ PHMA (mass ratio) was

determined to be 8.27 and for the residue, PPG/PHMA was 0.33. Table 2.1 tabulates the

mass of the individual components from the observed amount for the filtrate and the

residue. Based on the amount of PPG present in the residue relative to the total mass of

polyurethane prepolymer used for filtration (0.1156 g/0.9260 g), the contribution of

PPG to the copolymer of PPG-PHMA is approximately 12% of the total mass of the

polyurethane prepolymer. Calculations from NMR were based on isocyanate-terminated

prepolymers, but the observed mass was obtained from methanol-terminated

prepolymers. This discrepancy does not affect our inference as the amount of unreacted

MDI was low and the mass increase of the prepolymer due to isocyanate-methanol

adduct formation was less than 1%. Estimation of mass contributions of PPG and

PHMA in filtration products through NMR studies has an error of 5% with respect to

the initial composition used in the synthesis of polyurethane prepolymer.

Table 2.1 Estimation of mass of individual components from NMR studies and filtration technique.

	Filtrate			Filtration residue		
	MDI	PPG	PHMA	MDI	PPG	PHMA
Observed mass	0.4391 g/ 0.9620 g			0.5213 g /0.9620 g		
Mole ratio	2.4305	32.52	1	1	9.18	7.092
Weight ratio	2.67	8.27	1	1	2.125	6.4534
Estimated mass (g)		0.304	0.0368		0.1156	0.3512

To verify the validity of the filtration technique and the results obtained from NMR, a blend of PPG prepolymer and PHMA prepolymer (1:1 by mass) was mixed in methanol thereby replicating the same condition as the polyurethane prepolymer in methanol. The blend solution was filtered and NMR was performed on the filtrate and the residue. In the filtrate, PPG/PHMA was 16.74 and in the residue, PPG/PHMA was 0.03. PPG/PHMA ratio in the filtrate of the blend filtration shows the efficiency of the filtration process. This control experiment confirms our premise that PPG in the residue of polyurethane prepolymer is due to copolymer of PPG and PHMA.

Although the presence of copolymer in the residue was confirmed by the NMR studies, the presence of PHMA homopolymer needs to be excluded. To isolate the PHMA homopolymer and the PPG-PHMA copolymer, soxhlet extraction was carried out using 12.5/1 (v/v) methanol/chloroform. From Figure 2.4, it is obvious that the soxhlet residue and the extract have both PPG and PHMA. The extract of the process has a PPG/ PHMA ratio of 1.22 and the insoluble part has PPG/PHMA = 0.24. This experiment shows that the copolymer was inseparable from the PHMA homopolymer. Therefore, based on the NMR data, PPG contribution to the copolymer is 12% of the total mass of the polyurethane prepolymer.

(a)
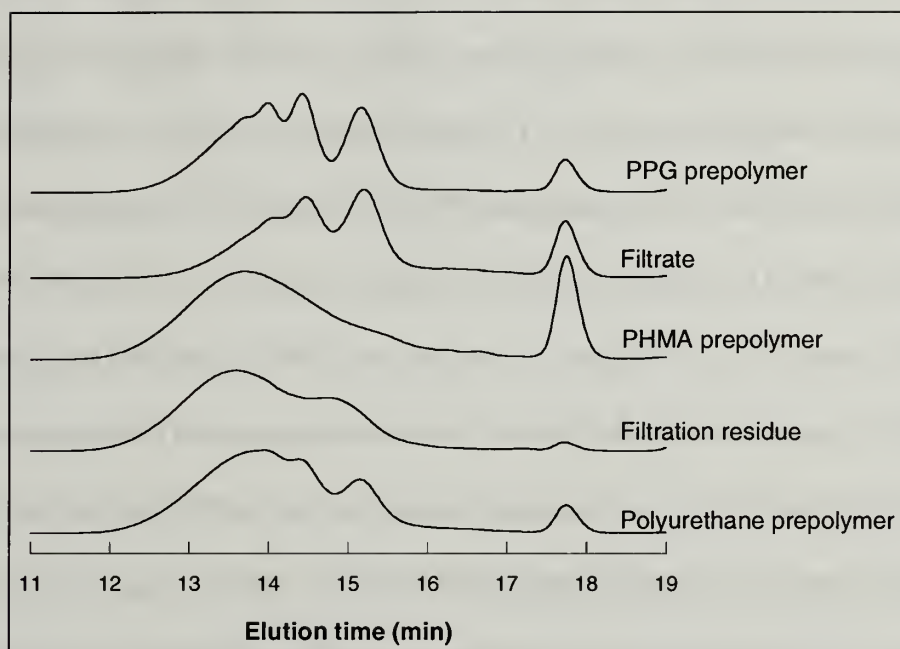
(b)
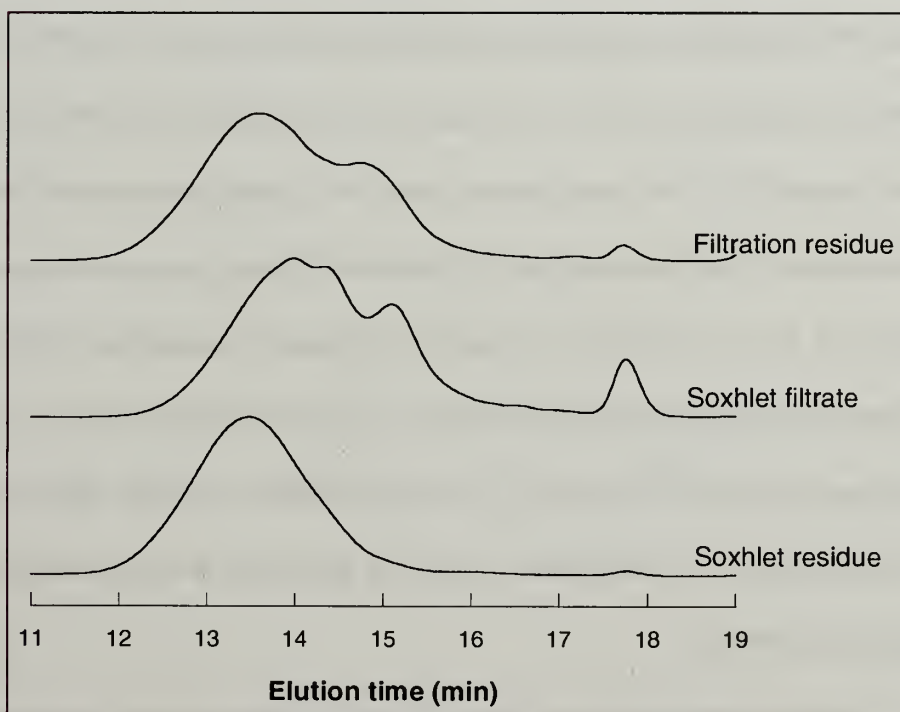
Figure 2.5 GPC analyses for (a) Comparison of MWD of the prepolymers with the filtration products and (b) Comparison of MWD of the soxhlet extraction products with the filtration residue.

24

The molecular weight distribution (MWD) of the prepolymers and the different constituents obtained by filtration were analyzed by GPC. Macromonomer PHMA has a molecular weight distribution of 1.59 that translates into a broad distribution for the PHMA prepolymer. Macromonomer PPG has a PDI of 1.01 that translates into well-defined MWD for PPG prepolymer. Products formed were OCN-MDI-(PPG-MDI)$_n$-NCO, where n = 1-4.[23] Figure 2.5 compares the MWD of the PPG prepolymer and PHMA prepolymer with the polyurethane prepolymer and its filtration products. The filtration residue of the polyurethane prepolymer has a MWD profile that resembles the PHMA prepolymer and the filtrate MWD profile is similar to that of the PPG prepolymer. However, due to the different reactivity of alcohol groups of PHMA and PPG with isocyanate, MWD values of the filtration products were different from those of the PPG and PHMA prepolymers. PHMA should react faster than PPG on account of PHMA's primary hydroxyls; so consumption of isocyanate by the PHMA should be faster than by PPG. This results in the formation of copolymer between PPG and PHMA as determined by the rate constants for reaction of primary and secondary alcohol with isocyanate. Since NCO/OH = 1.68, after the complete consumption of PHMA hydroxyls and partial consumption of PPG hydroxyls, remaining PPG hydroxyls react with the isocyanate functionality. However, NCO/OH is different from the initial value of 1.68. This difference in NCO/OH leads to MWD of the filtrate different from the PPG prepolymer's MWD.

Soxhlet extraction of the filtration residue yields two components with different molecular weight distributions. The extract of the process has a lower molecular weight

compared to the filtration residue and has a MWD profile similar to the filtration residue

whereas the soxhlet residue has an unimodal distribution but higher than the M_w of the

filtration residue.

(a)   **(b)**
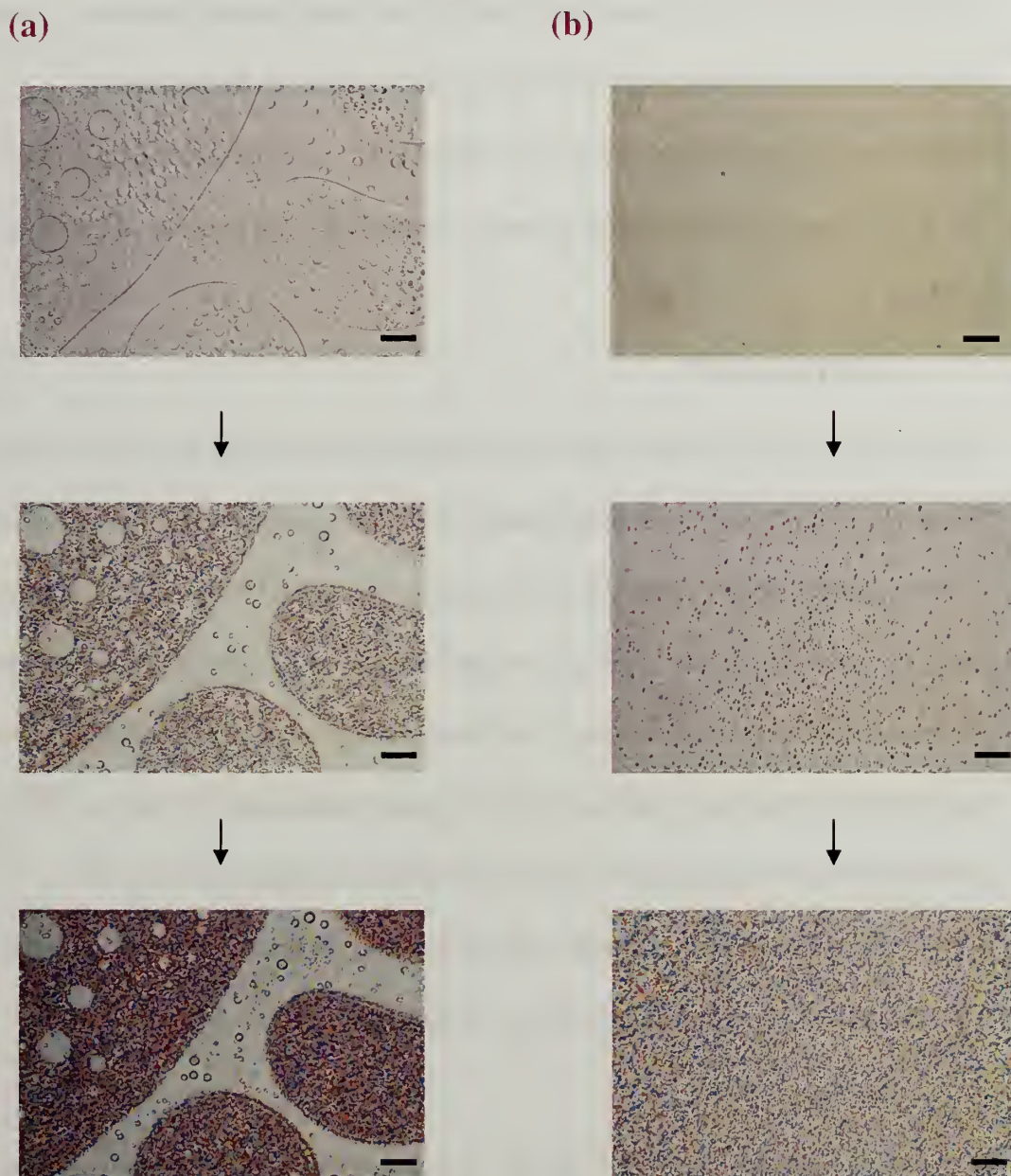
Figure 2.6 Optical micrographs showing morphology evolution when cooled from
120 ˚C to 22 ˚C for (a) The blend of PHMA prepolymer and PPG prepolymer and
(b) The polyurethane prepolymer. Scale bar corresponds to 100 μm.

2.3.2 Effect of the copolymer formation

Copolymer formation affects the morphology and crystallization kinetics of polyurethane prepolymer in a profound way. Figure 2.6 compares the morphology of a PPG prepolymer/ PHMA prepolymer blend and the polyurethane prepolymer. The blend is phase separated with the domains formed in the length scale of hundreds of microns whereas the polyurethane prepolymer has a 'macroscopically homogeneous' morphology. This phase separation in the blend is due to an unfavorable χ-parameter which translates into high interfacial tension between the components of the blend as given by

$$\gamma = (kT/a^2) \, (\chi/6)^{1/2} \tag{1}$$

where γ is the interfacial tension between the phases, and a is the monomer length.[33] However, in the polyurethane prepolymer, interfacial tension between the components is greatly reduced because of copolymer formation. The extent of decrease in interfacial tension is a function of the molecular weights of the homopolymers and copolymer in the system and the concentration of copolymer. Reduction in interfacial tension with concentration occurs until a critical micellar concentration (cmc) is reached.[25] Park et. al. have shown for a polystyrene/polybutadiene blend compatibilized by the poly(styrene-*b*-butadiene) copolymer, dependence of the interfacial tension on the concentration of copolymer approximately follows the relationship

$$\gamma/\gamma_0 \sim \exp\,(-c\varphi) \tag{2}$$

where γ and γ_0 are the interfacial tensions with and without the copolymer, φ is the concentration of the copolymer and c is a constant.[34] Beyond cmc, copolymer molecules tend to form micelles and the domain size remains constant. In the polyurethane system

studied here, even though the exact copolymer amount is not known, it is high enough to reduce the interfacial tension between the PPG and PHMA components. Although the polyurethane prepolymer appears optically homogenous at 120 °C when viewed using white light, there exists micron/submicron domains. This explains the observed morphology evolution for the polyurethane prepolymer.
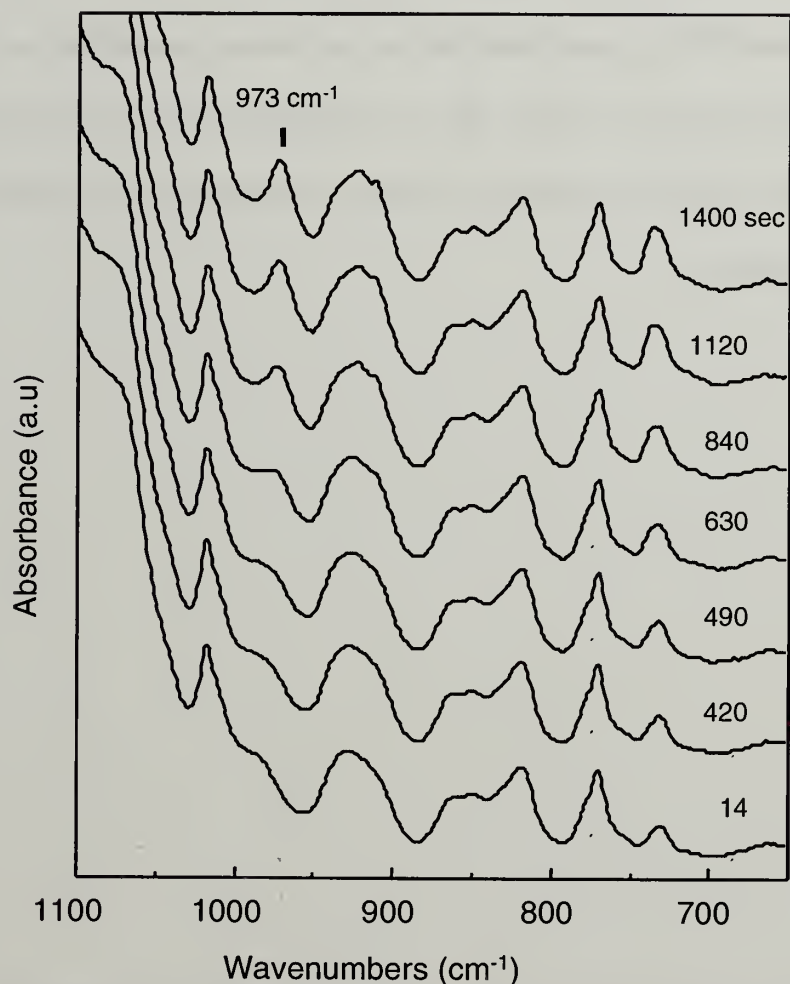
Figure 2.7 Kinetics of PHMA crystallization in the polyurethane prepolymer as followed by the deformation band at 973 cm⁻¹.

The observed morphological features explain the crystallization trend in the blend and the polyurethane prepolymer system. Figure 2.7 shows the time-dependent

infrared spectra of the systems studied with a supercooling (difference between melting temperature and crystallization temperature) of $\Delta T = 18\ ^{\circ}C$. Depression in the melting temperature of PHMA occurs in the polyurethane due to the copolymer formation. To arrive at any meaningful conclusion, the degree of supercooling and not the absolute crystallization temperature is the appropriate parameter to follow the crystallization kinetics. Crystallization of PHMA was faster in the blend system of PPG prepolymer/PHMA prepolymer than the polyurethane prepolymer as followed by the deformation band at 973 cm^{-1}. This crystallization band was normalized with respect to the carbonyl stretching band and calibrated to the degree of crystallinity from thermal measurements.
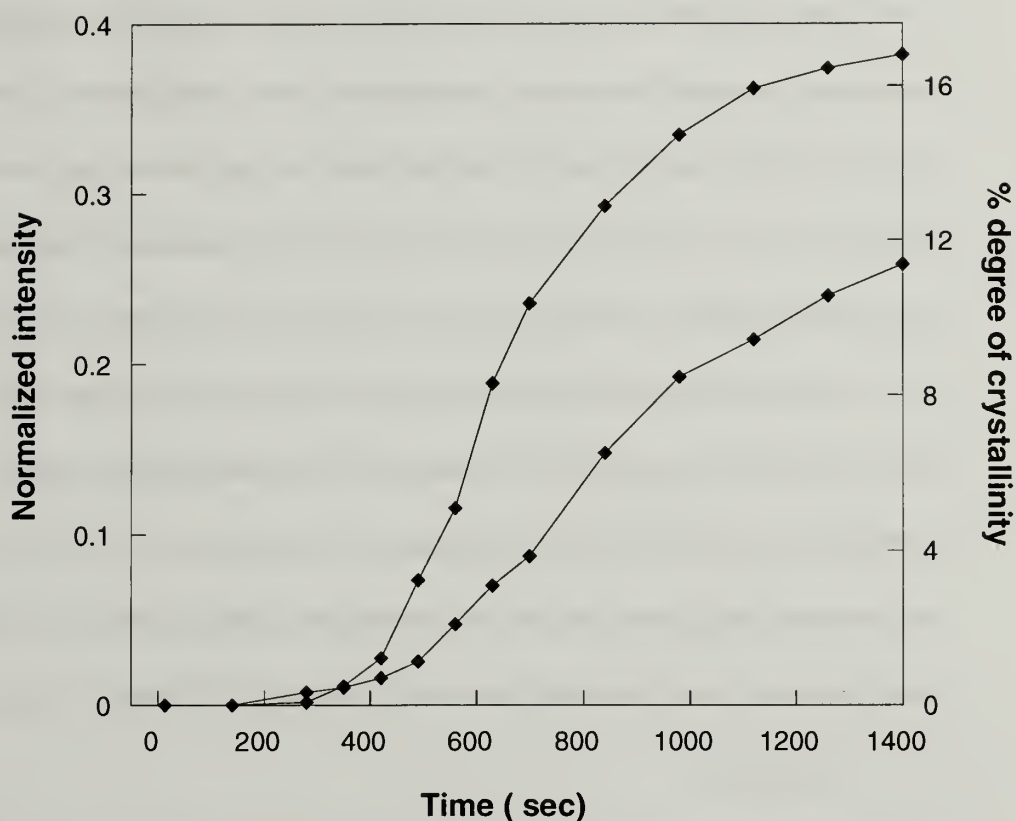
Figure 2.8 Crystallization kinetics of PHMA in (a) The blend of PHMA prepolymer and PPG prepolymer and (b) The polyurethane prepolymer as measured by following the deformation band at 973 cm^{-1}.

Figure 2.8 compares quantitatively the crystallization kinetics of the different systems. In the miscible system, the crystallization kinetics is slow and the degree of crystallinity reaches a value of ~12%, while in the immiscible blend system, the degree of crystallinity is ~ 16.5% after 1400 seconds. This observation can be qualitatively explained by considering the two processes involved in the crystallization: nucleation and growth. For nucleation to occur, presence of heterogeneities and/or a critical concentration of crystallizable component has to be attained and for crystal growth, polymer chains need to be transported to the growth front. From the kinetics plot, there

is not much of a difference in the nucleation rate as observed by the induction time for crystallization. In the literature, crystallization studies of such compatibilized systems are directed towards fractionated crystallization where homogeneous crystallization is observed at high supercooling.[35,36] In this study, our goal was to study the crystallization kinetics at fixed supercooling and not fractionated crystallization. Hence at the given supercooling, PHMA-rich domains of the blend or the polyurethane prepolymer should be governed by the same nucleation mechanism. This nucleation mechanism in micron/submicron domains is also confirmed by the morphological studies where crystallization of PHMA starts at the domain. However growth is slower in the polyurethane prepolymer than the PPG prepolymer /PHMA prepolymer blend. This observation can be explained by the reptation model.[37,38] Effective transport rate, v_r

$$v_r = f_c / \xi_r \tag{3}$$

where f_c is the force for pushing molecules to the growth front and ξ_r is the friction coefficient associated with the reptation correlated to the segmental size of the reptation model. In the polyurethane systems, correlation length, ξ_r, the average distance between contact points of crystallizable polymer chains, is high as the concentration of PHMA is diluted by the presence of PPG from the copolymer and the PHMA has to be transported to the growth front. Thus growth is affected by the presence of copolymer which in turn affects the crystallization kinetics. The same reasons also explain the observed trend in the phase separated blend system of PPG prepolymer/ PHMA prepolymer. Because of the high concentration of PHMA in the PHMA-rich domains of the blend, which are larger than the domains of polyurethane prepolymer, ξ_r is lower than in the polyurethane

prepolymer. Thus, a lower friction coefficient results in faster crystal growth in the blend.

2.4 Conclusions

Polyurethane prepolymer prepared from PPG, PHMA and MDI was separated by filtration and soxhlet extraction techniques and analyzed for the copolymer formed during the prepolymer formation by FT-IR, GPC and NMR techniques. Secondary hydroxyls of PPG have lower reaction rates than the primary hydroxyls of PHMA during urethane formation with isocyanates. From NMR studies, the contribution of PPG to the copolymer is determined to be 12% of the total mass of the polyurethane prepolymer. Presence of the copolymer alters the otherwise macrophase-separated PHMA prepolymer/PPG prepolymer blend into a compatibilized polyurethane system. This compatibilization results in slower PHMA crystallization kinetics in the polyurethane prepolymer than in the blend of PPG prepolymer/PHMA prepolymer.

2.5 References

(1)   Forschner, T. C.; Gwyn, D. E.; Xiao, H. X.; Suthar, B.; Sun, L. Q.; Frisch, K. C. "Polyurethane hot melt adhesives based on 1,3-PDO" *Adhes Age* **1999**, *42*, 20.

(2)   Vick, C. B.; Okkonen, E. A. "Strength and durability of one-part polyurethane adhesive bonds to wood" *Forest Prod J* **1998**, *48*, 71.

(3)   Jeong, Y. G.; Hashida, T.; Wu, G. L.; Hsu, S. L.; Paul, C. W. "Analysis of the multistep solidification process in polymer blends" *Macromolecules* **2006**, *39*, 274-280.

(4)   Jeong, Y. G.; Ramalingam, S.; Archer, J.; Hsu, S. L.; Paul, C. W. "Influence of copolymer configuration on the phase behavior of ternary blends" *J Phys Chem B* **2006**, *110*, 2541-2548.

(5)   Duffy, D. J.; Stidham, H. D.; Hsu, S. L.; Sasaki, S.; Takahara, A.; Kajiyama, T. "Effect of polyester structure on the interaction parameters and morphology development of ternary blends: Model for high performance adhesives and coatings" *J Mater Sci* **2002**, *37*, 4851-4859.

(6)   Duffy, D. J.; Heintz, A. M.; Stidham, H. D.; Hsu, S. L.; Suen, W.; Chu, W.; Paul, C. W. "Influence of polymer structure on melt miscibility of ternary polymer blends: A model for high performance polyurethane adhesives and coatings" *Journal of Adhesion* **2003**, *79*, 1091-1107.

(7)   Duffy, D. J.; Heintz, A. M.; Stidham, H. D.; Hsu, S. L.; Suen, W.; Paul, C. W. "The competitive influence of specific interactions and extent of reaction on the miscibility of ternary reactive polymer blends: model for polyurethane adhesives" *Int J Adhes Adhes* **2005**, *25*, 39-46.

(8)   Hashida, T.; Jeong, Y. G.; Hua, Y.; Hsu, S. L.; Paul, C. W. "Spectroscopic study on morphology evolution in polymer blends" *Macromolecules* **2005**, *38*, 2876.

(9)   Jeong, Y. G.; Pagodina, N. V.; Jiang, C.; Hsu, S. L.; Paul, C. W. "Effects of polyester-poor phase microstructures on viscosity development of polymer blends" *Macromolecules* **2006**, *39*, 4907-4913.

(10)   Brame, E. G.; Ferguson, R. C.; Thomas, G. J. "Identification of Polyurethanes by High Resolution Nuclear Magnetic Resonance Spectrometry" *Anal Chem* **1967**, *39*, 517.

(11)   Prabhakar, A.; Chattopadhyay, D. K.; Jagadeesh, B.; Raju, K. V. S. N.
         "Structural investigations of polypropylene glycol (PPG) and isophorone
         diisocyanate (IPDI)-based polyurethane prepolymer by 1D and 2D NMR
         spectroscopy" *J Polym Sci Pol Chem* **2005**, *43*, 1196.

(12)   Pegoraro, M.; Galbiati, A.; Ricca, G. "H-1 nuclear magnetic resonance study of
         polyurethane prepolymers from toluene diisocyanate and polypropylene glycol"
         J Appl Polym Sci **2003**, *87*, 347.

(13)   Sumi, M.; Chokki, Y.; Nakai, Y.; Nakabayashi, M.; Kanzawa, T. "Studies on
         the Structure of Polyurethane Elastomers .1. Nmr Spectra of the Model
         Compounds and Some Linear Polyurethanes" *Makromolekul Chem* **1964**, *78*,
         146.

(14)   Chokki, Y. "Studies on Structure of Polyurethane Elastomers, .4. Nmr-Spectra
         of Linear Polyurethane Based on 2,4-Tolylenediisocyanate" *Makromol Chem*
         1974, *175*, 3425.

(15)   Chokki, Y.; Sumi, M.; Nakabaya.M. "Studies on Structure of Polyurethane
         Elastomers .3. Characterization of Linear Polyurethanes by Nmr-Spectroscopy -
         Components and Molecular-Weight" *Makromolekul Chem* **1972**, *153*, 189.

(16)   Okuto, H. "Studies on Structure of Polyurethane Elastomers .2. High Resolution
         Nmr Spectroscopic Determination of Allophanate and Biuret Linkages in Cured
         Polyurethane Elastomer - Degradation by Amine" *Makromolekul Chem* **1966**,
         98, 148.

(17)   Yeager, F. W.; Becker, J. W. "Determination of Composition and Molecular-
         Weight of Polyester Urethanes by High-Resolution Proton Magnetic-Resonance
         Spectrometry" *Anal Chem* **1977**, *49*, 722.

(18)   Vanderweij, F. W. "Kinetics and Mechanism of Urethane Formation Catalyzed
         by Organotin Compounds .2. The Reaction of Phenyl Isocyanate with Methanol
         in Dmf and Cyclohexane under the Action of Dibutyltin Diacetate" *J Polym Sci
         Pol Chem* **1981**, *19*, 3063.

(19)   Vanderweij, F. W. "Kinetics and Mechanism of Urethane Formation Catalyzed
         by Organotin Compounds .1. The Reaction of Phenyl Isocyanate with Methanol
         in Dibutyl Ether under the Action of Dibutyltin Diacetate" *J Polym Sci Pol
         Chem* **1981**, *19*, 381.

(20)   Wong, S. W.; Frisch, K. C. "Catalysis in Competing Isocyanate Reactions .2.
         Competing Phenyl Isocyanate Reactions Catalyzed with N,N',N"-
         Pentamethyldipropylenetriamine" *J Polym Sci Pol Chem* **1986**, *24*, 2877.

(21)   Mehl, J. T.; Murgasova, R.; Dong, X.; Hercules, D. M.; Nefzger, H. "Characterization of polyether and polyester polyurethane soft blocks using MALDI mass spectrometry" *Anal Chem* **2000**, *72*, 2490.

(22)   Murgasova, R.; Brantley, E. L.; Hercules, D. M. "Characterization of polyester-polyurethane soft and hard blocks by a combination of MALDI, SEC, and chemical degradation" *Macromolecules* **2002**, *35*, 8338.

(23)   Heintz, A. M.; Duffy, D. J.; Hsu, S. L.; Suen, W.; Chu, W.; Paul, C. W. "Effects of reaction temperature on the formation of polyurethane prepolymer structures" *Macromolecules* **2003**, *36*, 2695.

(24)   Paul, D. R. *Polymer Blends (Eds. D. R. Paul and S. Newmann), Vol. 1, Academic Press* **2000**.

(25)   Noolandi, J.; Hong, K. M. "Interfacial Properties of Immiscible Homopolymer Blends in the Presence of Block Copolymers" *Macromolecules* **1982**, *15*, 482-492.

(26)   Leibler, L.; Orland, H.; Wheeler, J. C. "Theory of Critical Micelle Concentration for Solutions of Block Co-Polymers" *J Chem Phys* **1983**, *79*, 3550.

(27)   Guegan, P.; Macosko, C. W.; Ishizone, T.; Hirao, A.; Nakahama, S. "Kinetics of Chain Coupling at Melt Interfaces" *Macromolecules* **1994**, *27*, 4993.

(28)   Ide, F.; Hasegawa, A. "Studies on Polymer Blend of Nylon-6 and Polypropylene or Nylon-6 and Polystyrene Using Reaction of Polymer" *J Appl Polym Sci* **1974**, *18*, 963.

(29)   Campbell, J. R.; Hobbs, S. Y.; Shea, T. J.; Watkins, V. H. "Poly(Phenylene Oxide) Polyamide Blends Via Reactive Extrusion" *Polym Eng Sci* **1990**, *30*, 1056.

(30)   Freluche, M.; Iliopoulos, I.; Millequant, M.; Flat, J. J.; Leibler, L. "Graft copolymers of poly(methyl methacrylate) and polyamide-6: Synthesis by reactive blending and characterization" *Macromolecules* **2006**, *39*, 6905-6912.

(31)   Heintz, A. M. *Ph. D Thesis, University of Massachusetts, 2003*.

(32)   Szycher , M. *Handbook of Polyurethanes*, Chapter 4.

(33)   Helfand, E.; Tagami, Y. "Theory of Interface between Immiscible Polymers" *Journal of Polymer Science Part B-Polymer Letters* **1971**, *9*, 741.

(34)   Park, D. W.; Roe, R. J. "Effect of Added Block Copolymer on the Phase-Separation Kinetics of a Polymer Blend .2. Optical Microscopic Observations" *Macromolecules* **1991**, *24*, 5324.

(35)   Ikkala, O. T.; Holstimiettinen, R. M.; Seppala, J. "Effects of Compatibilization on Fractionated Crystallization of PA6/PP Blends" *J Appl Polym Sci* **1993**, *49*, 1165.

(36)   Tol, R. T.; Mathot, V. B. F.; Groeninckx, G. "Confined crystallization phenomena in immiscible polymer blends with dispersed micro- and nanometer sized PA6 droplets, part 2: reactively compatibilized PS/PA6 and (PPE/PS)/PA6 blends" *Polymer* **2005**, *46*, 383.

(37)   de Gennes, P. G. "Reptation of a Polymer Chain in Presence of Fixed Obstacles" *J Chem Phys* **1971**, *55*, 572.

(38)   de Gennes, P. G. "Dynamics of Entangled Polymer-Solutions .1. Rouse Model" *Macromolecules* **1976**, *9*, 587.

CHAPTER 3

TROJAN HORSE APPROACH TO POLYURETHANE CURING

3.1 Introduction

Polyurethane (PUR) is one of the most studied polymers in the scientific community. PURs find their use in variety of applications including foams, coating, adhesives and fibers. The main reason behind the diverse applications of these materials is the segmented nature of PURs. Hard segments of the PUR impart strength whereas the soft segments provide flexibility, making the PUR elastomeric by nature. By tuning the characteristics of the hard and soft segments, different properties can be realized from PURs. Application in adhesion requires unique properties. It is preferred to have a thermoplastic material for processing but the strength of chemical crosslinking of a thermoset is needed for real-world application. Apart from the chemical crosslinking, physical crosslinking can also occur if a crystallizable diol is used for PUR synthesis. These processes of chemical crosslinking by isocyanate moieties and physical crosslinking due to crystallization are called curing. There are two steps involved in the curing of reactive hot melt adhesives. In the first step, an isocyanate terminated prepolymer is obtained by reacting the macrodiol(s) with an excess of isocyanate. This isocyanate-terminated prepolymer is applied for adhesive application and allowed to cure. Water from the atmosphere reacts with the isocyanate to form an urea that can form a biuret, a crosslink. The formation of biuret crosslinks is an important step in PUR curing.

Curing of PUR is dependent on the relative humidity of the ambient conditions. A number of studies have been carried out to follow the curing kinetics by FT-IR, DSC, intrinsic fluorescence spectroscopy, frequency-dependent dielectric sensing technique and rheology. [1-5] Comyn et. al., proposed diffusion-limited curing kinetics defined by an empirical equation

$$z = (2VPpt)^{0.5}$$

where z is the cure depth, V is the volume of the prepolymer , P is the permeability coefficient of water in the cured prepolymer, p is the water vapor pressure and t is the reaction time.[6] This theory of diffusion-controlled curing kinetics is contested by Jeong *et. al.* who showed the curing is both a reaction rate-controlled and diffusion-controlled process with the rate-determining reaction being that between the water and isocyanate.[7] It was also shown that the curing kinetics is dependent on the relative humidity, temperature of curing and morphology of the prepolymer. However, it would be interesting to not have the environmental factors control the curing kinetics.

Controlled curing of PUR for coating processes is a well-studied subject. Blocked isocyanates synthesized by reacting -NCO with reagents including oximes, sodium bisulphite, active methylene containing compounds like dialkyl malonate, acetoacetic ester (to form ester-amide) and hindered alcohols can be deblocked by either thermal means or by changing the pH.[8] This process of deblocking releases free isocyanate, which can react with a diol to form a cured product. However, these reactions are carried out in solution and significant amounts of volatile compounds, sometimes up to 50% of the total volume, are released during the curing process making the process environmentally unfriendly. In research described in this chapter, we studied

ammonium salts as curing agents for the curing of reactive hot melt adhesives by a trigger mechanism. A dispersion of ammonium salt and isocyanate-terminated PPG prepolymer was made which is stable at room temperature, but curing can be effected by the release of ammonia and/or water that occurs upon heating the dispersion to a predetermined temperature. Figure 3.1 is a pictorial version of the conventional curing mechanism and compares that with the curing process as effected by the trigger mechanism.
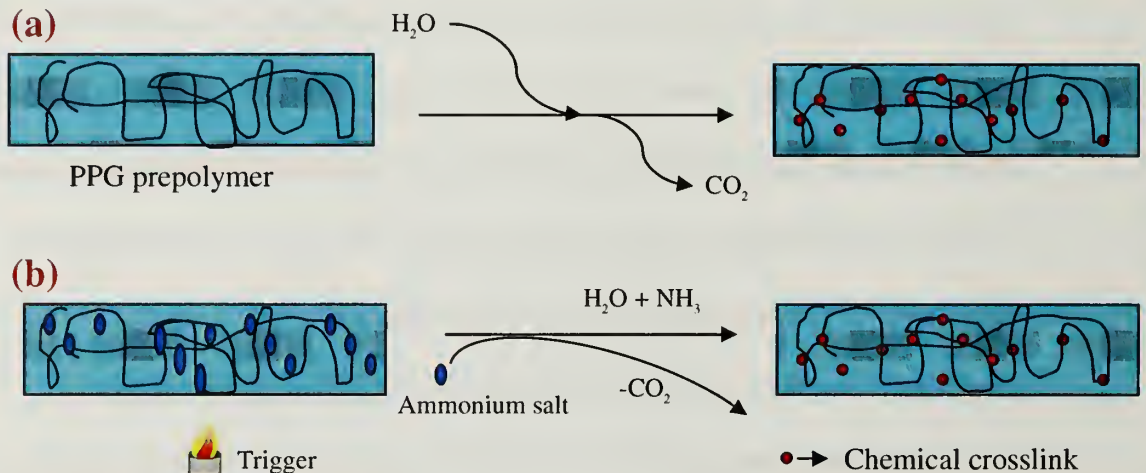
Figure 3.1 Pictorial representation of (a) conventional curing mechanism and (b) curing process by trigger mechanism.

3.2 Experimental section

3.2.1 Materials

Poly (propylene glycol) (PPG) was obtained from ARCH chemical ($M_n = 1900$ g/mol, $M_w/ M_n = 1.01$, $T_g = -66\ °C$ and hydroxyl value = 56). MDI, NH_4HCO_3 and NH_2COONH_4 were used as received (either from Aldrich or Fisher).

3.2.2 Prepolymer synthesis

Isocyanate-terminated PPG prepolymer was synthesized as follows. PPG was taken in a two-neck round bottom flask fitted with a stop-cock-controlled purge/vacuum adapter. Contents of the flask were evacuated at 60 °C coupled with a nitrogen purge in a cyclical manner to remove any trace amount of moisture over a period of 24 h. The temperature of the flask was then increased to 120 °C under nitrogen. A calculated amount of MDI was added and the reaction allowed to proceed for 3 h under nitrogen. The isocyanate-terminated prepolymer was synthesized with a NCO/OH ratio of 2. To facilitate the characterization of the prepolymer and for TGA studies, dry methanol was added and stirred for 24 h to obtain methyl-terminated, inactive PPG prepolymer.

3.2.3 Characterization

TGA studies were performed using a TA instruments TGA 2950 under nitrogen with a heating rate of 10 °C/min. HPLC studies were carried out with an Agilent -HP 1100 series instrument using a diode array detector. The mixed solvent system used for elution started with a mixture of CH_3CN and water (50 : 50 by volume), reached 100% CH_3CN in 20 minutes and 10 more minutes of elution with CH_3CN was carried out. To avoid reaction of the isocyanate group in the sample reacting with adventitious moisture, dibutyl amine was added to react with the isocyanate functionality. MS was performed in positive ion mode using Bruker's Esquire~ LC instrument. Rheological studies were performed with a constant stress of 10 Pa. Curing of PPG prepolymer with NH_4HCO_3 was followed in a Rheologica instruments' Viscotech with a frequency range of 0.062832 rad/sec (0.01 Hz) to 6.2832 rad/sec (1 Hz) and the studies using

NH_2COONH_4 were performed using an AR2000 instrument with a frequency range of 0.6283 (0.1 Hz) to 62.83 (10 Hz). DSC studies were performed using a TA instruments DSC Q 100 instrument at a heating rate of 10 $^{\circ}$C/min.

3.3 Results and discussion

Curing of isocyanate-terminated polyurethane prepolymers involves reaction of isocyanate with active hydrogen containing molecules to form cross-linked products. The active hydrogen-containing molecules, called the reactive component (RC), obtained by the decomposition of ammonium salts are ammonia and/or water. Ammonium salts used in this study are ammonium bicarbonate (NH_4HCO_3) and ammonium carbamate (NH_2COONH_4). RCs formed by the decomposition of the ammonium salts are given by the following equations.

$$NH_4HCO_3 \longrightarrow NH_3 + H_2O + CO_2$$

$$NH_2COONH_4 \longrightarrow 2\,NH_3 + CO_2$$
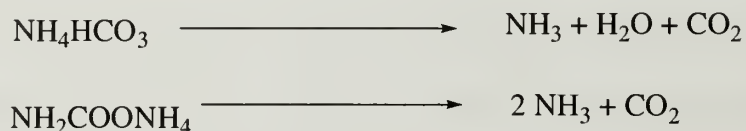
TGA studies were carried out to determine the onset of decomposition of the ammonium salt and also to follow the decomposition kinetics of the salt in the presence of PPG prepolymer. To avoid the isocyanate-terminated PPG prepolmer reacting with the RCs, inactive PPG prepolymer was used for TGA srudies. Finely ground ammonium salts were dispersed in the inactive PPG prepolymer to carry out the TGA studies. Figure 3.2 shows the TGA analyses of an NH_4HCO_3/PPG prepolymer mixture. It is clear from Figure 3.2a that decomposition of NH_4HCO_3 starts at approximately 60 $^{\circ}$C. However, when a mixture containing 8% NH_4HCO_3 and inactive PPG prepolymer was used, as shown in Figure 3.2b, 2 stages of mass loss were observed. The first mass

41

loss corresponds to decomposition of NH_4HCO_3 and the subsequent removal of NH_3 and the second mass loss corresponds to elimination of water, which is a decomposition product of NH_4HCO_3. Decomposition kinetics of the salt was followed at predetermined temperatures above the decomposition temperature of the salt. From Figure 3.2c, it is clear that the decomposition of salt has an expected trend with the decomposition at 80 °C faster than the one at 60 °C. However, the significant aspect of the decomposition kinetics at all temperatures studied is the gradual decomposition of the salt. This is pertinent for efficient curing, as abrupt release of all the RC, particularly gaseous NH_3 would result in either incomplete conversion of NCO groups as the RCs can escape from the reaction medium (if reaction rate of the RC with NCO is slower than the diffusion rate of the RC) or reaction of NCO with RC with degree of conversion of NCO greater than 50% (if reaction rate of NCO with RC is faster than the diffusion rate of RC). For good mechanical properties, it is preferred to have high crosslink density, hence degree of conversion of NCO with RC should be lower than 50% to facilitate chain extension and crosslinking by the reaction of remaining NCO with the product of NCO and RC.

(a)

(b)
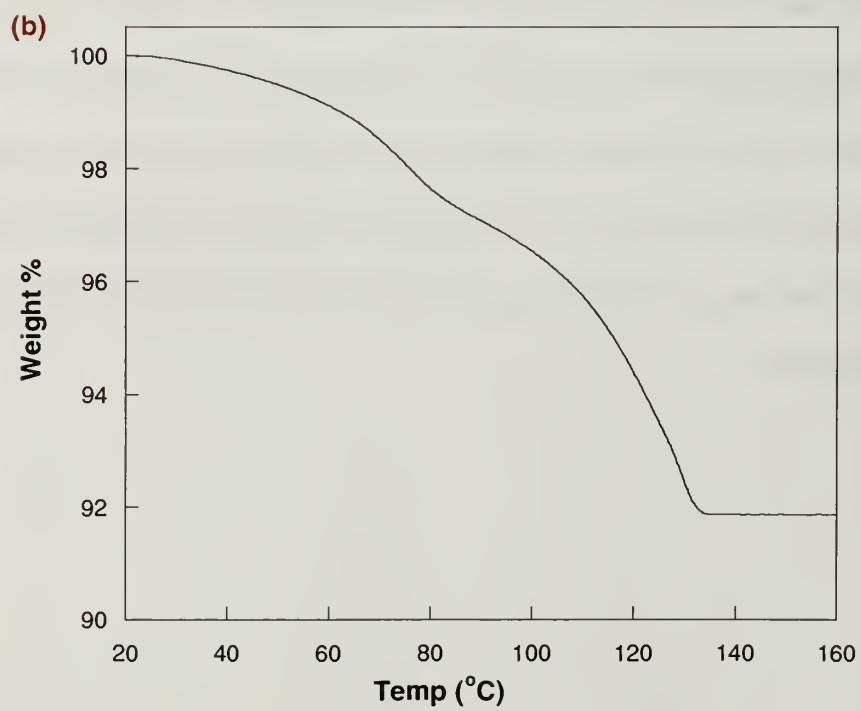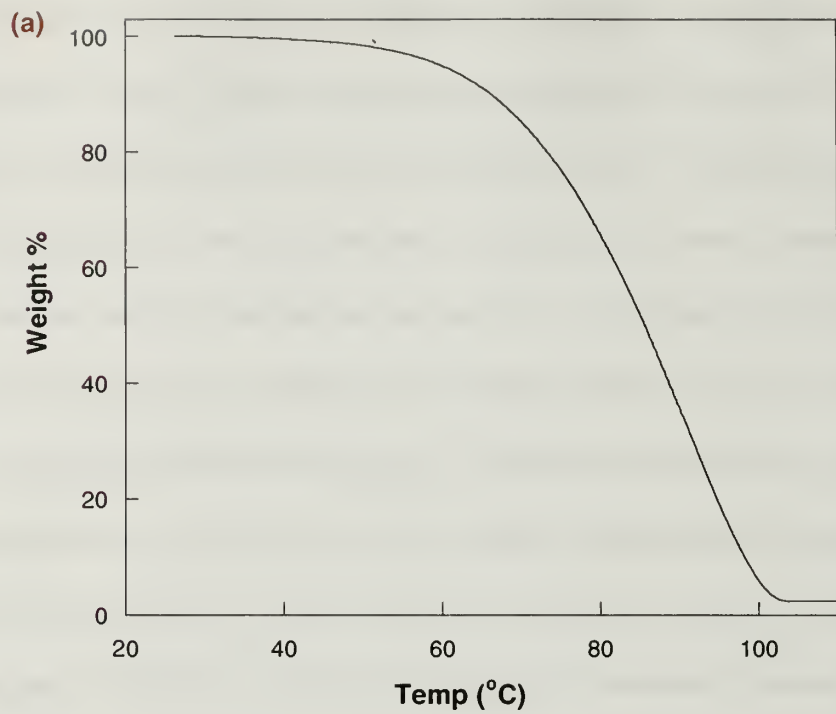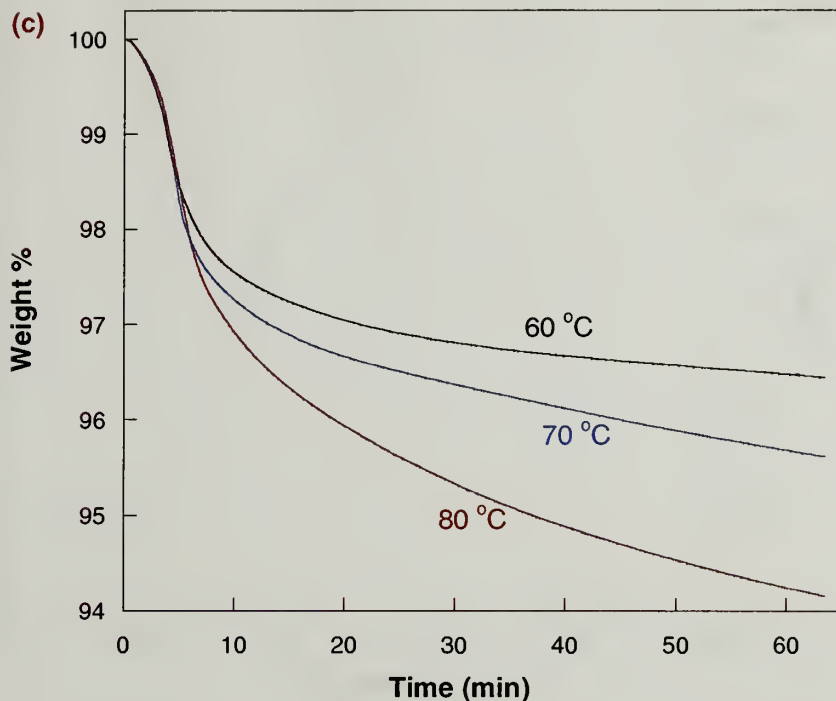
Figure 3.2 TGA analyses of (a) NH_4HCO_3, (b) mixture containing inactive PPG prepolymer and 8% NH_4HCO_3 and (c) decomposition kinetics of the mixture under isothermal conditions. Isothermal temperature is given in the graph.
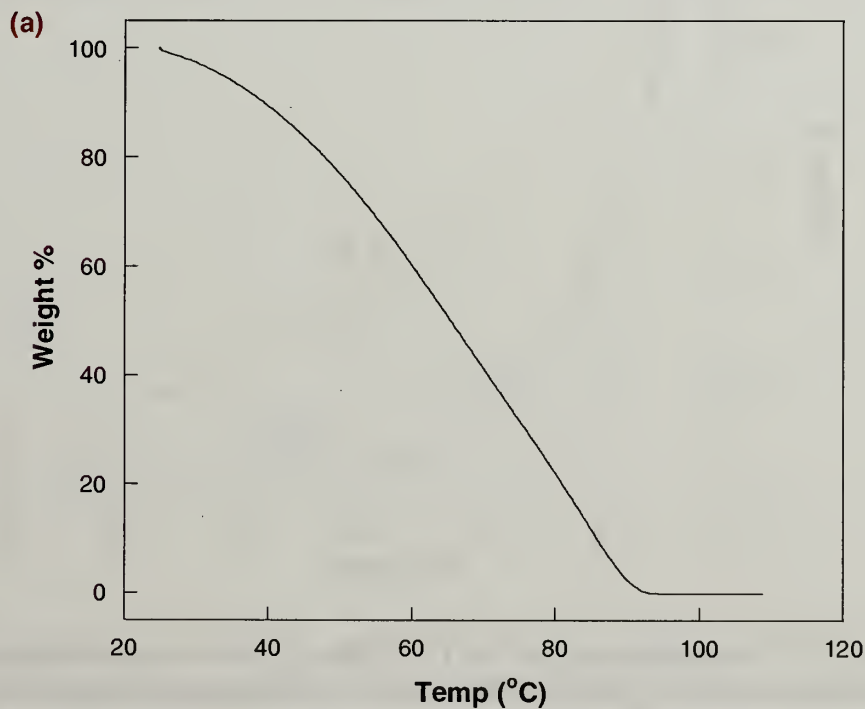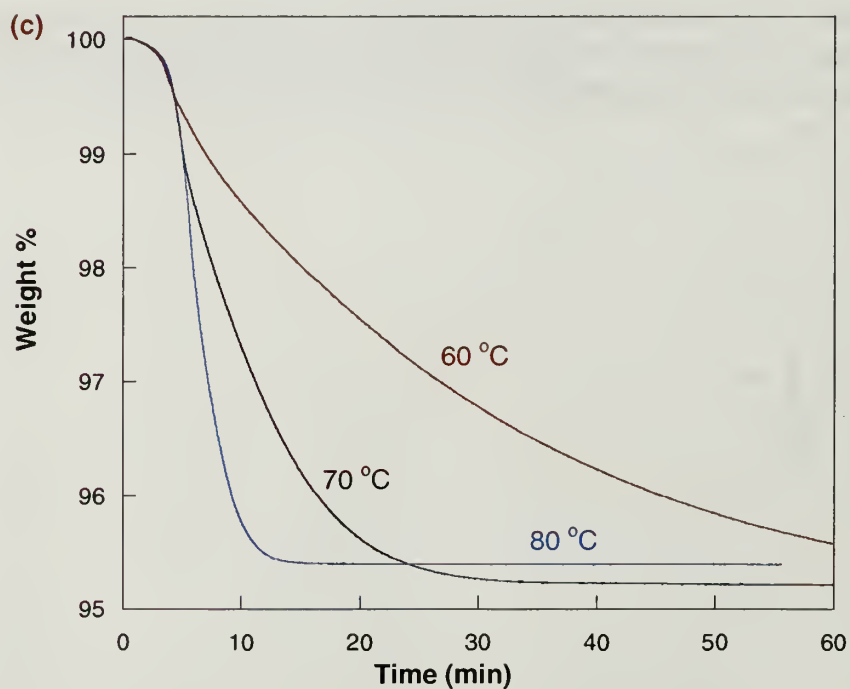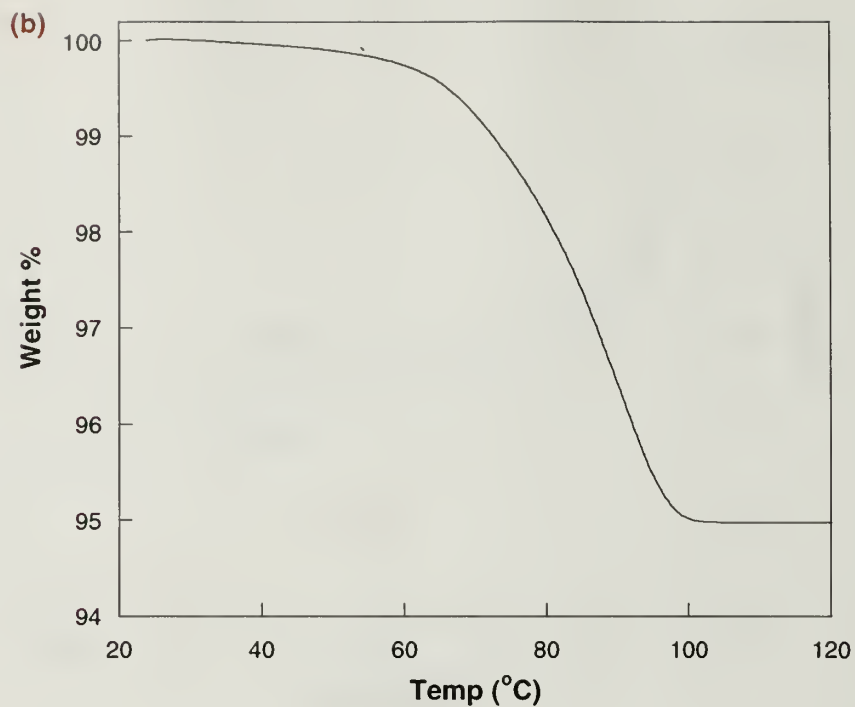
Figure 3.3 TGA analyses of (a) NH_2COONH_4, (b) mixture containing inactive PPG prepolymer and 5% NH_2COONH_4 and (c) decomposition kinetics of the mixture under isothermal conditions. Isothermal temperature is given in the graph.

Figure 3.3 shows the TGA analyses for NH_2COONH_4. NH_2COONH_4 begins to decompose at room temperature, but NH_2COONH_4 in the mixture, as seen in Figure 3.3b, begins to decompose only above 60 °C. From the decomposition kinetics as shown in Figure 3.3c, it is observed that at 60 °C and 70 °C, decomposition of NH_2COONH_4 in the mixture is gradual whereas at 80 °C, decomposition of NH_2COONH_4 is abrupt. It is interesting to note that NH_4HCO_3 which is stable at room temperature decomposes faster in the presence of PPG prepolymer whereas NH_2COONH_4 which starts to decompose at room temperature is stable in the presence of PPG prepolymer up to 60 °C.

(a)

RNCO

RNCO + Salt, RT, 12 d

RNCO / RC = 1, 70 °C, 24 h

RNCO / RC = 2, 70 °C, 24 h

RNCO / RC = 0.5, 70 °C, 24 h

RNCO + Salt, RT, 30 d

Time (min)
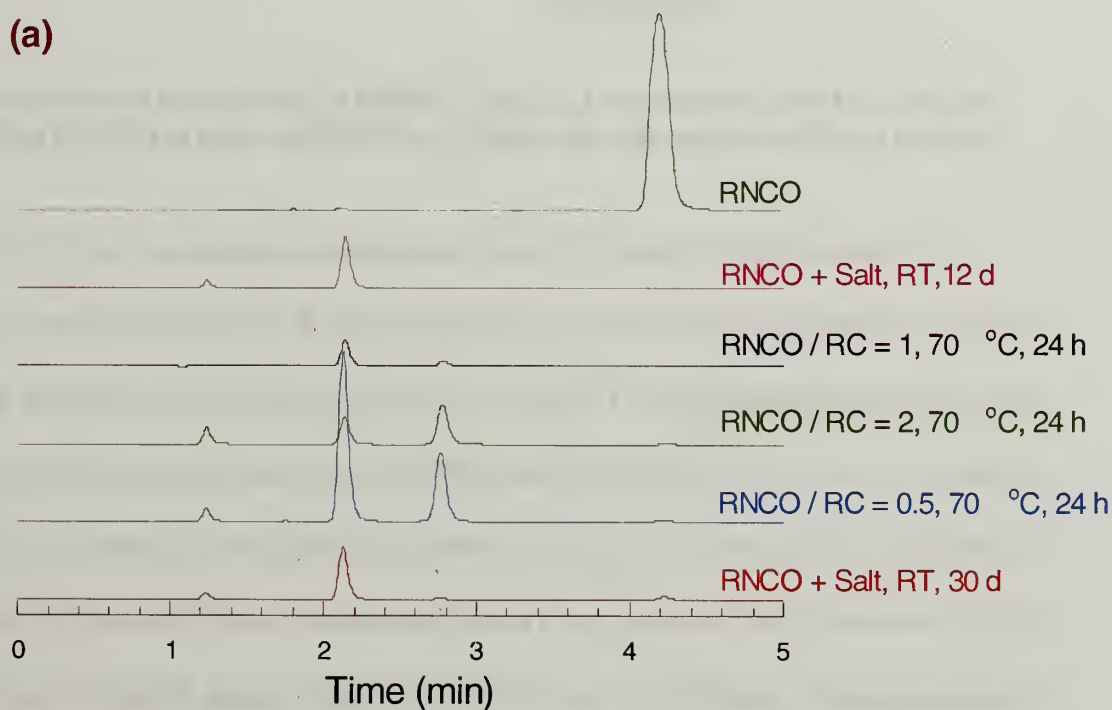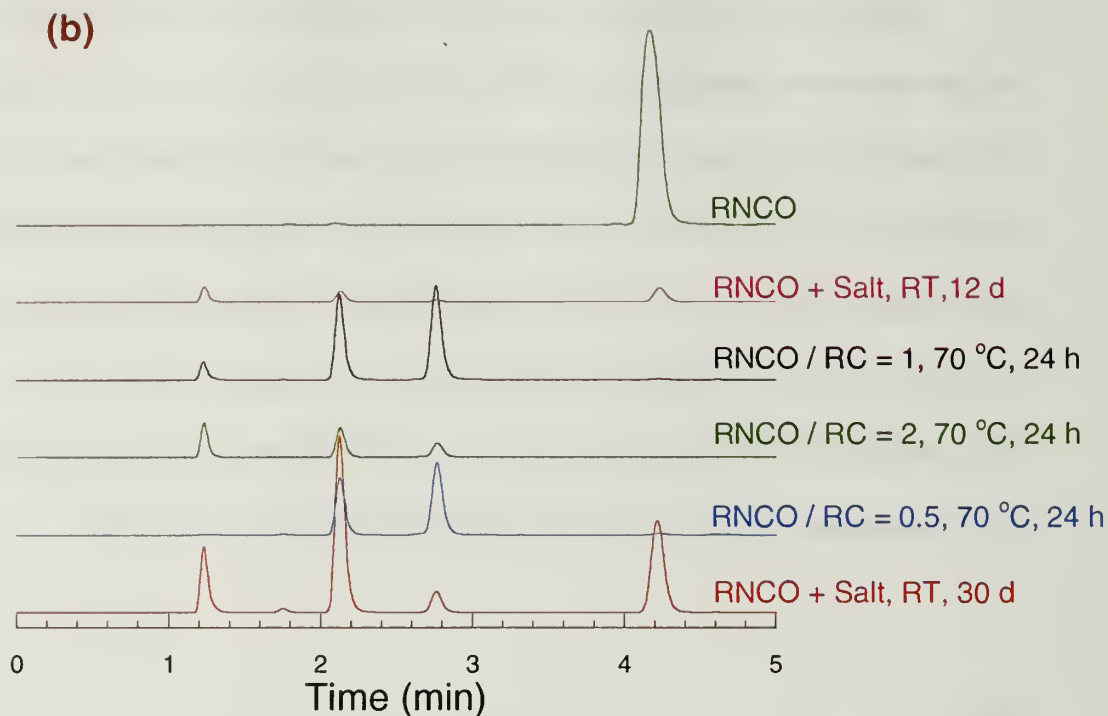
Figure 3.4 HPLC analyses of C_6H_5NCO (RNCO)/ ammonium salt mixture at various conditions when the salt used is (a) NH_4HCO_3 and (b) NH_2COONH_4.

To be an effective trigger for curing, ammonium salts must not react with the isocyanate-terminated prepolymer at room temperature, but should decompose and react at a predetermined temperature. To study the efficacy of the trigger mechanism, model studies were carried out. Phenyl isocyanate (RNCO) was used as isocyanate source and the stability of the ammonium salts in the presence of RNCO was followed by HPLC-MS. To avoid the RNCO reacting with adventitious water or any other active-hydrogen containing species, dibutyl amine was added to the eluent system. Figure 3.4 shows the HPLC analyses of ammonium salts with RNCO at different conditions. RNCO-dibutyl amine adduct elutes at 4.2 minutes. From Figure 3.4a, it is obvious that after 12 days at room temperature, no isocyanate groups are left behind when NH_4HCO_3 is used as the curing agent. However, NH_2COONH_4 (Figure 3.4b) is more stable than NH_4HCO_3

47

indicated by the presence of eluting species at 4.2 minutes when stored at room temperature over a period of 30 days. This shows the efficiency of ammonium salts to act as controlled curing agents in polyurethane curing processes. On heating the RNCO/ammonium salt mixture, with varying ratios of NCO/RC, at 70 °C different species are formed that elute at different times, which confirms the ability of ammonium salts to cure the prepolymer on heating.
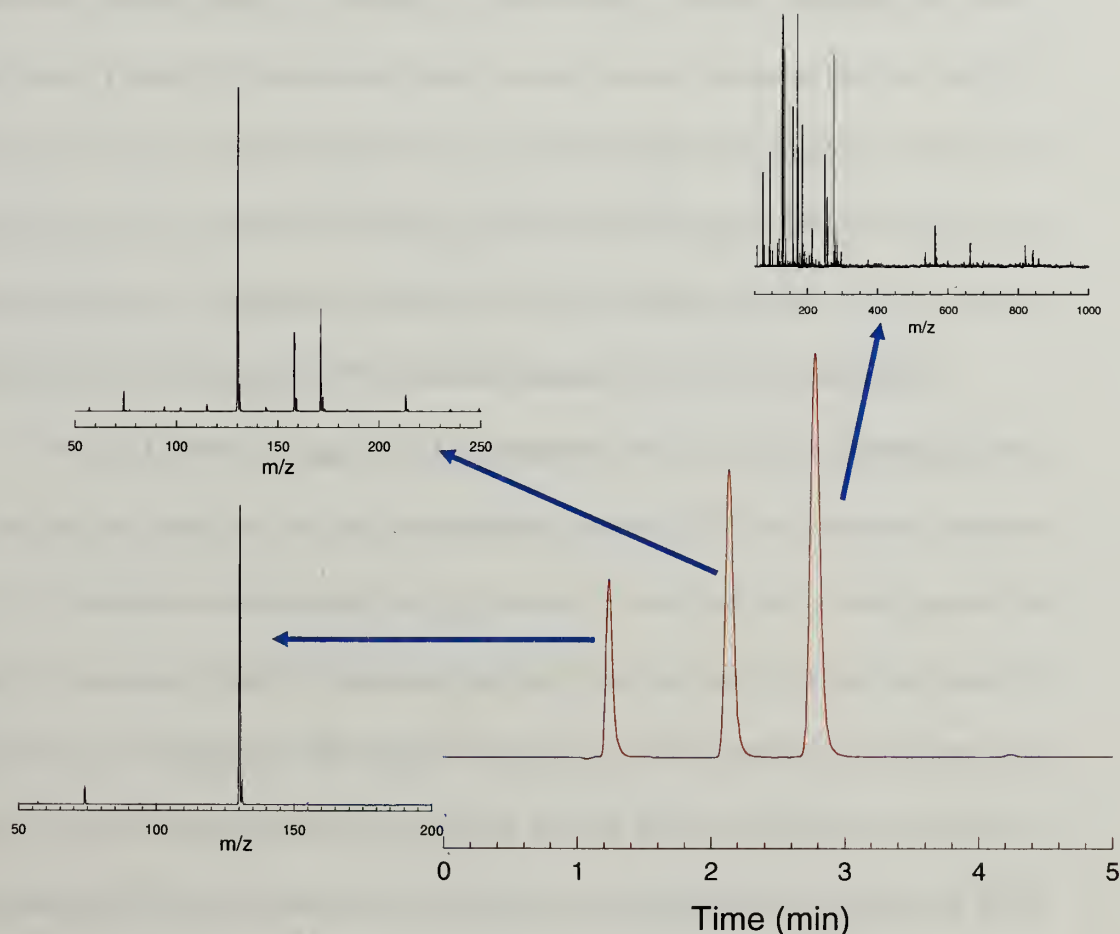
Figure 3.5 HPLC-MS analyses of RNCO/NH₄HCO₃ with NCO/RC =2 at 70 °C.

HPLC-MS was carried out to analyze the products formed by the reaction of ammonium salt, NH_4HCO_3. Figure 3.5 shows HPLC-MS analyses of the products formed by the reaction of C_6H_5NCO with NH_3 and H_2O, formed by the decomposition of

NH_4HCO_3. The molecular weight of C_6H_5NCO is 119 g/mol and dibutyl amine is 129 g/mol. From the MS analyses, it is obvious that dibutyl amine elutes at 1.2 min (m/z of 130). For the species that eluted around 2.2 min, m/z is 213. This molecular weight corresponds to formation of urea formed by the reaction of H_2O with C_6H_5NCO. For the species that eluted at 2.8 min, mass spectrometry shows a variety of peaks with the maximum m/z value of 857. It is not clear whether the peak at 857 is a parent peak or one of the fragments from the parent molecule. However, it clearly shows the existence of higher molecular weight species that are equal to or above 857 g/mol. Considering the molecular weight of C_6H_5NCO (119 g /mol), 857 g/mol yields a chemical species that is formed by the condensation of multiple C_6H_5NCO molecules. This experiment confirms the crosslinking ability of the decomposition products of the ammonium salt.

Curing kinetics of the isocyanate-terminated PPG prepolymer was followed by small amplitude oscillatory shear experiments. G' (Storage modulus), G" (Loss modulus) and tan δ (= G"/G') are the parameters that are used to define the progress of the curing process and the onset of gelation. Figure 3.6a shows the evolution of G' and G" with time and it is clear that as curing time increases, G' and G" increase. To begin with, isocyanate-terminated PPG prepolymer is liquid-like resulting in G" greater than G'. However as the system starts to cure, becoming more elastic than viscous, G' equals G" at the gel point. After the gel point, material is more solid-like with G' greater than G". At the gel point, G' and G" are proportional to $\omega^{0.5}$.[9] The gel point of the system is best determined by the transition of tan δ from > 1 to < 1. At gel point, tan δ is independent of ω, at low frequencies, as seen in Figure 3.6b. Though the exact gel point

is missed, it is clear from the tan δ vs ω that at low frequencies, tan δ is independent of
the frequency.
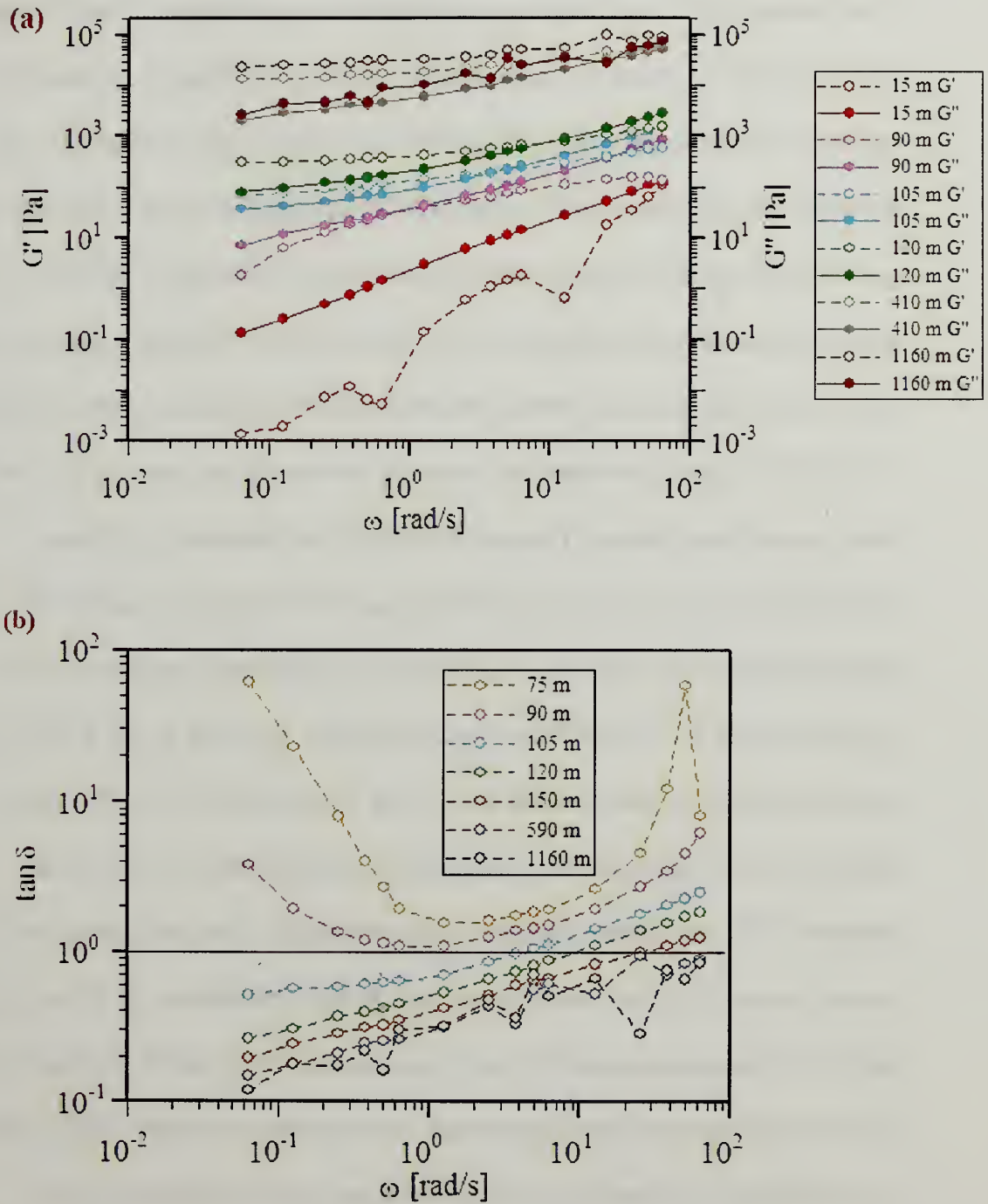
Figure 3.6 Representative rheological data obtained for RC/NCO =4 at 70 °C using
NH₄HCO₃ showing (a) Evolution of G' and G'' with curing and (b) Evolution of
tan δ with curing. Line shown is to identify tan δ =1.

To determine the gel point to characterize the curing kinetics, G' and G" at the frequency 0.628 rad/sec (0.1 Hz) is plotted against the curing time. Frequency of 0.1 Hz is used because it is in the frequency range which is independent of G'and G" during gelation. Figure 3.7 shows the curing kinetics of PPG prepolymer by the reaction of isocyanate with NH_3 and H_2O, evolved from the decomposition of NH_4HCO_3, for different curing temperatures and different RC/NCO ratios. As expected, gelation time, t_{gel} decreases with an increase in curing temperature or an increase in RC/NCO. Either temperature or salt concentration would increase the rate at which RCs are generated and is consistent with the t_{gel} values obtained for the curing caused by the decomposition of NH_4HCO_3. It is also worthwhile to study the mechanical properties of the cured PPG-based polyurethane polymer. Though the G' and G" are measured at different temperatures, 60 to 80 °C, these temperatures are well above the T_g (around -40 °C) and should not affect the qualitative comparisons. Final mechanical properties of the polymer cured at 70 °C (RC/NCO = 2 and RC/NCO = 4) and 60 °C (for RC/NCO = 4) are better than the polymer cured at 80 °C or 60 °C (for RC/NCO =2). This can be explained by the three factors that determine the curing kinetics of isocyanate-terminated PPG prepolymer. They are (1) decomposition of the ammonium salts (2) reaction between NCO and the RCs, obtained by the decomposition of the ammonium salts and (3) reaction between NCO and the product of NCO and RC. In ideal scenario, to obtain maximum mechanical properties, less than 50% of available NCO groups need to react with RC to account for both chain extension and crosslinking. At low temperature and low salt concentration, generation of RC is slow, making the curing process dependent on decomposition kinetics. At high temperature and high salt

51

concentration, RC production is fast, resulting in higher degrees of conversion of isocyanate groups (NCO conversion > 50%) causing lowered crosslink density. This argument is validated by looking at the curing kinetics at 60 °C. After 1000 min, for RC/NCO = 2, mechanical properties have not reached the maximum whereas for RC/NCO =4, a plateau seems to have been reached with maximum mechanical properties obtained for this system. This confirms the concentration effect of RC on curing kinetics. At 70 °C, decomposition kinetics and reaction kinetics are optimum, resulting in superior mechanical properties. However at 80 °C, decomposition kinetics is fast, resulting in an NCO conversion of greater than 50 % and lower crosslink density.

(a)

53

(b)

@ 60 °C; t_{gel} =225 min

@ 70 °C; t_{gel} =90 min
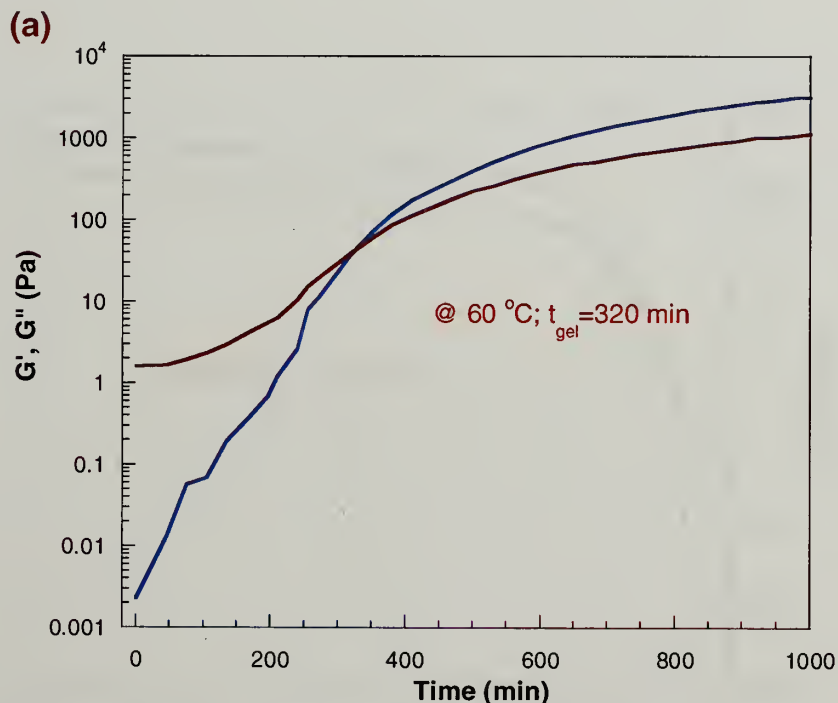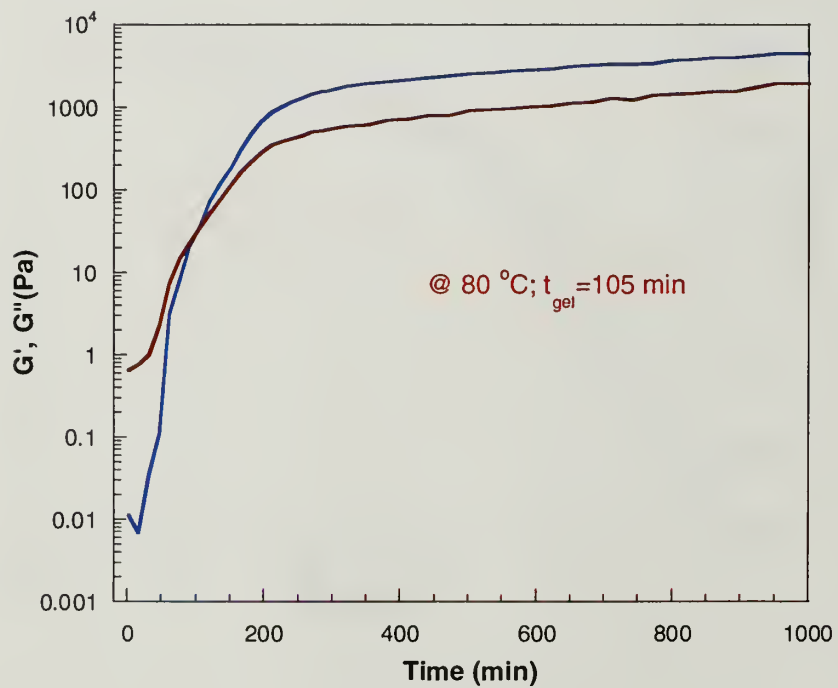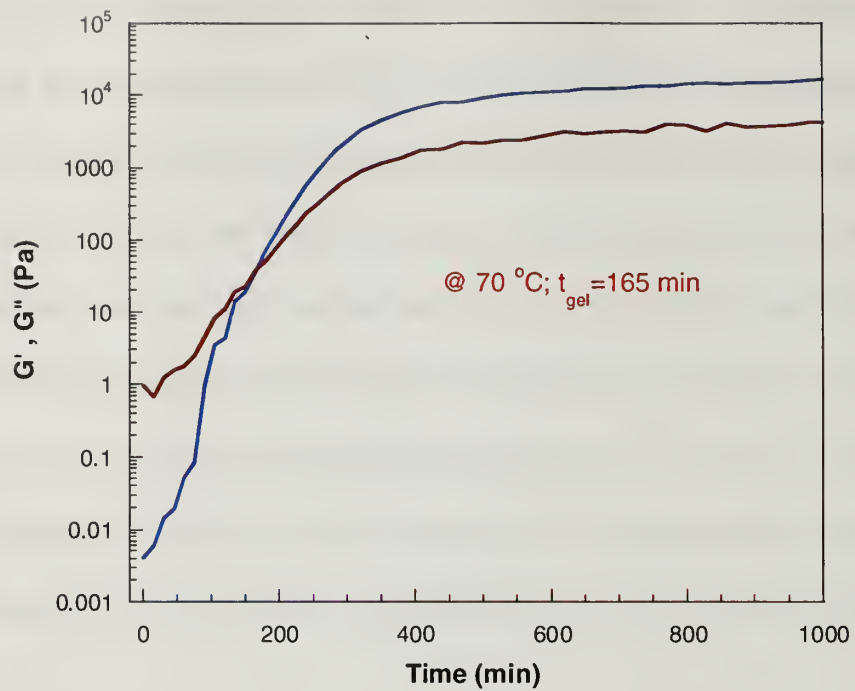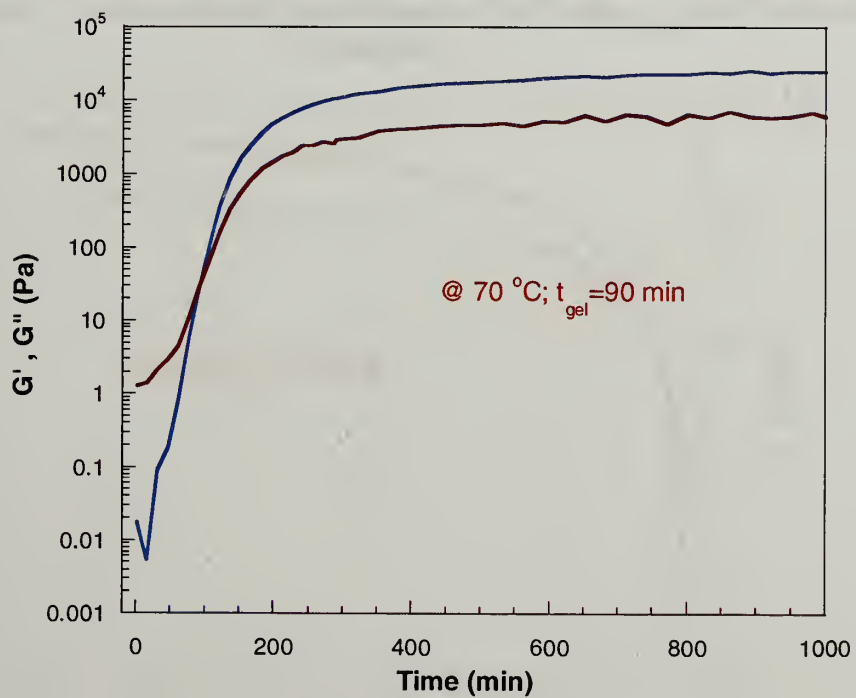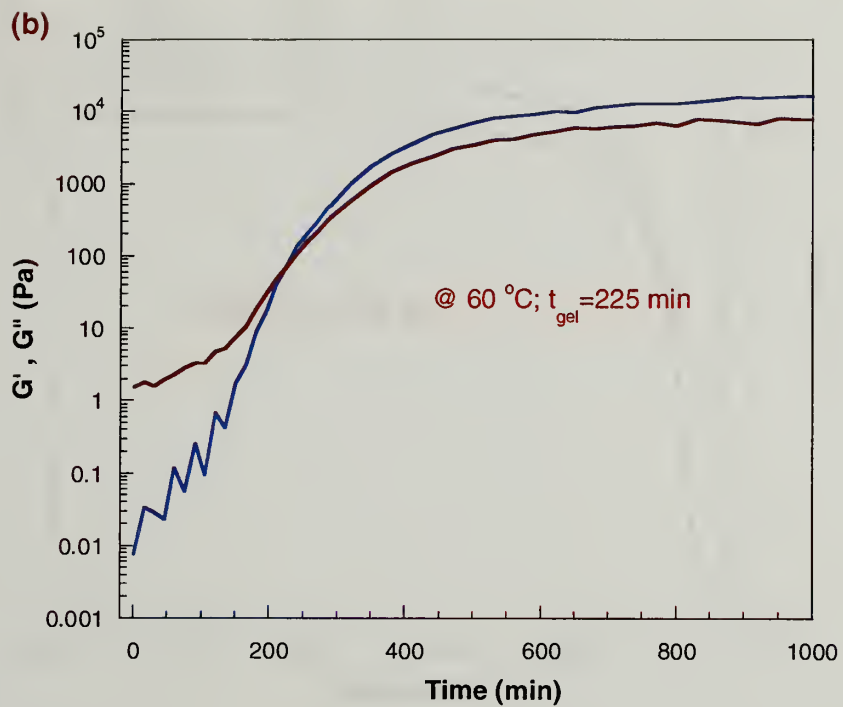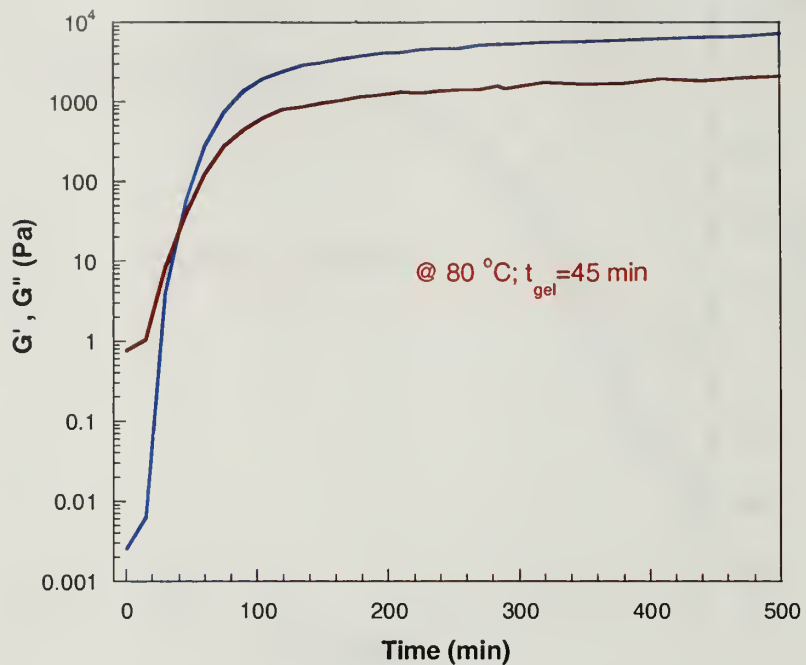
Figure 3.7 Curing kinetics of PPG prepolymer with NH_4HCO_3 as followed by the rheological studies for (a) RC/NCO = 2 and (b) RC/NCO =4. Curing temperature and gelation time, t_{gel}, are given for each curing kinetics curve. — denotes G' and — denotes G".

(a)

@ 60 °C; t_{gel} = 36 min

@ 70 °C; t_{gel} = 22 min

@ 80 °C;

(b)

@ 50 °C; t_{gel}=58 min

57
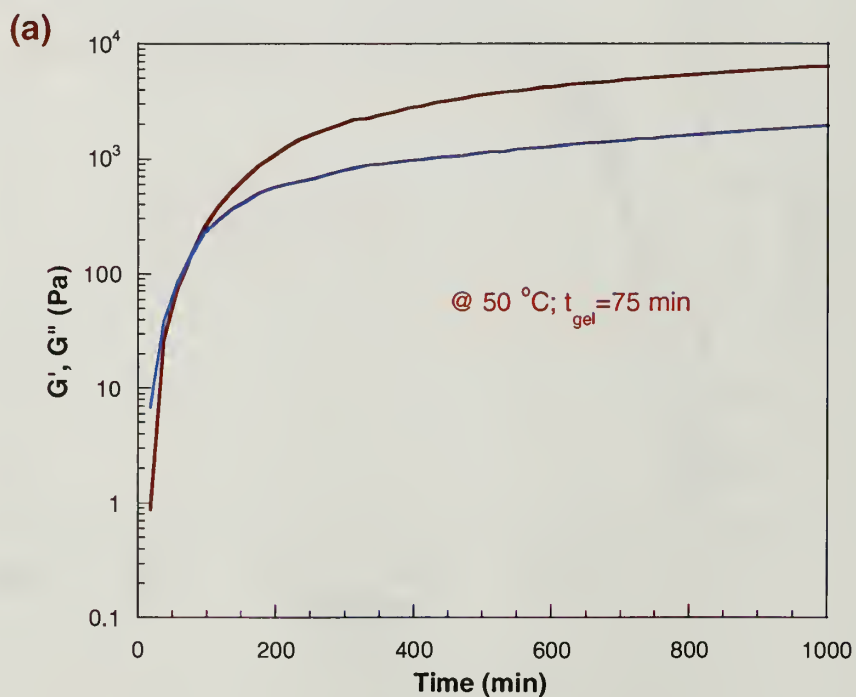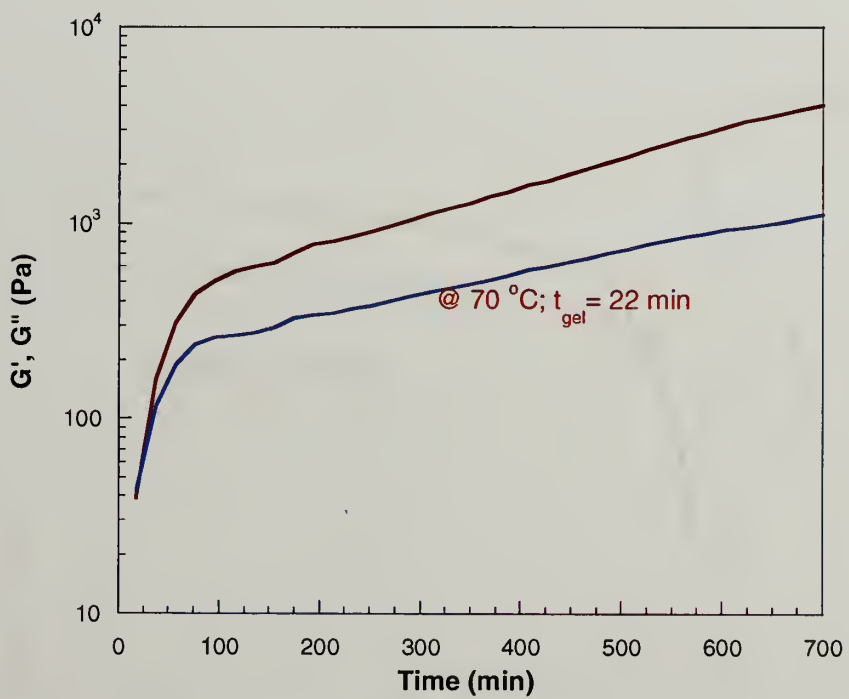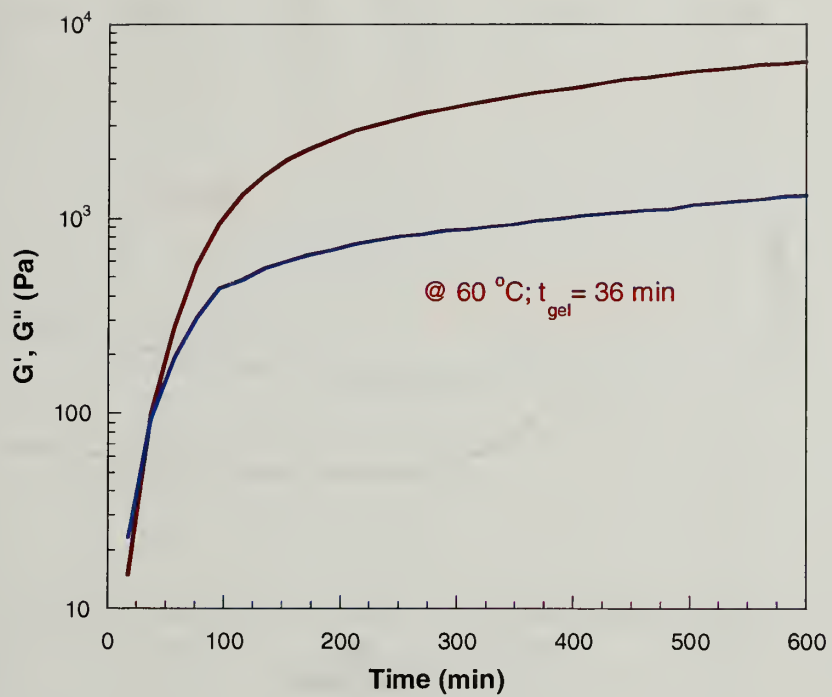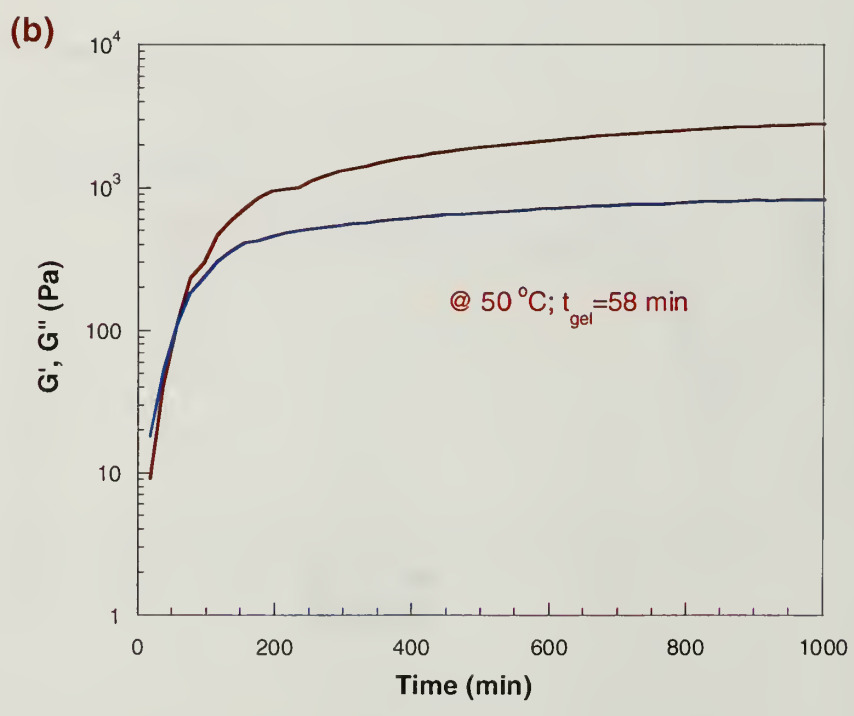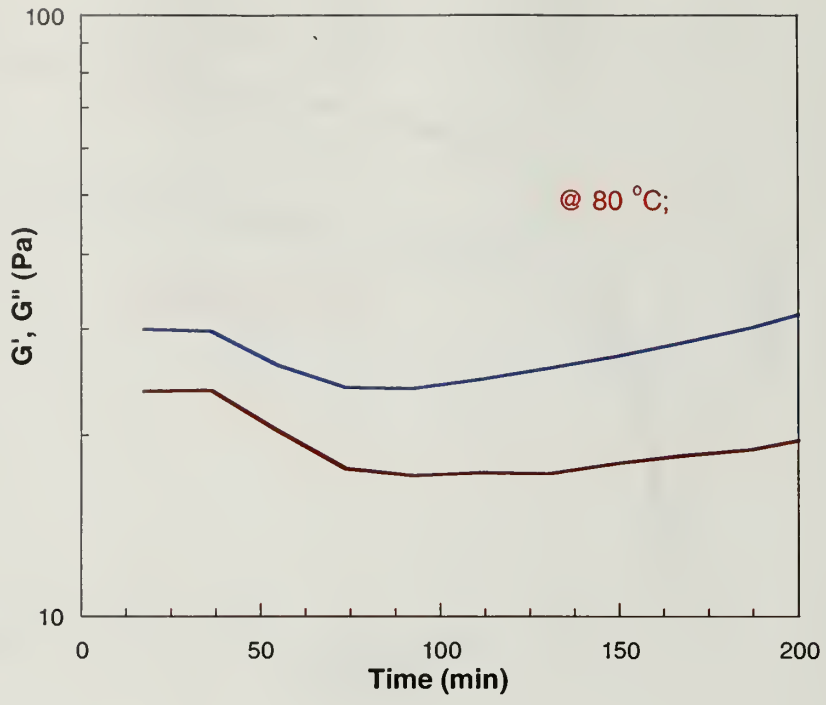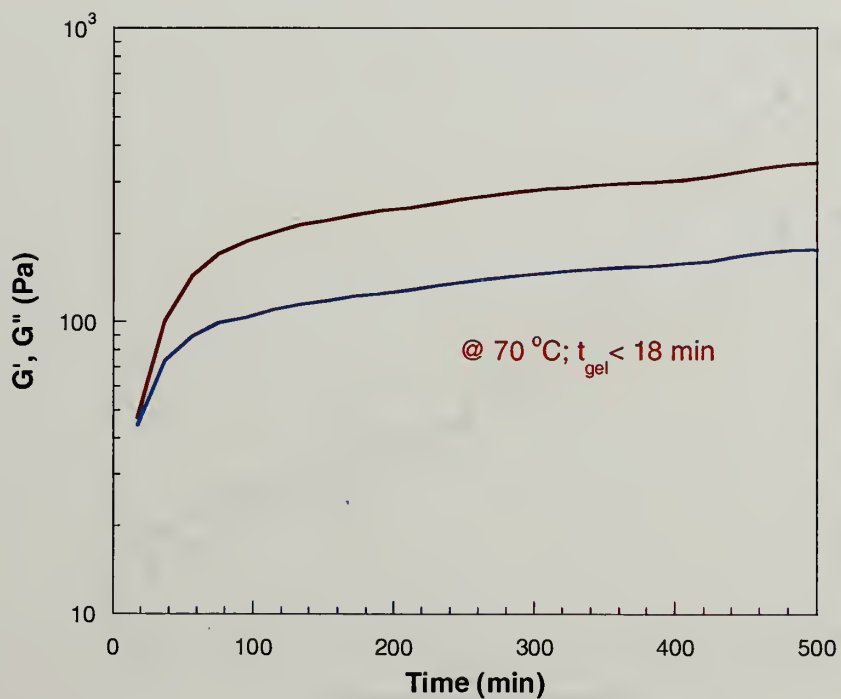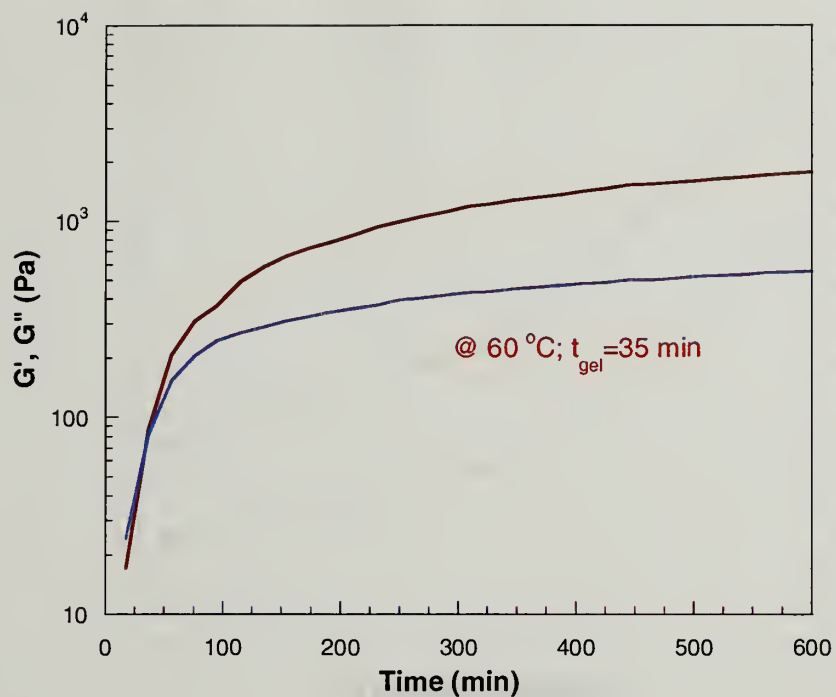
Figure 3.8 Curing kinetics of PPG prepolymer with NH_2COONH_4 as followed by the rheological studies for (a) RC/NCO = 2 and (b) RC/NCO = 4. Curing temperature and gelation time, t_{gel}, are given for each curing kinetics curve. −− denotes G' and −− denotes G".
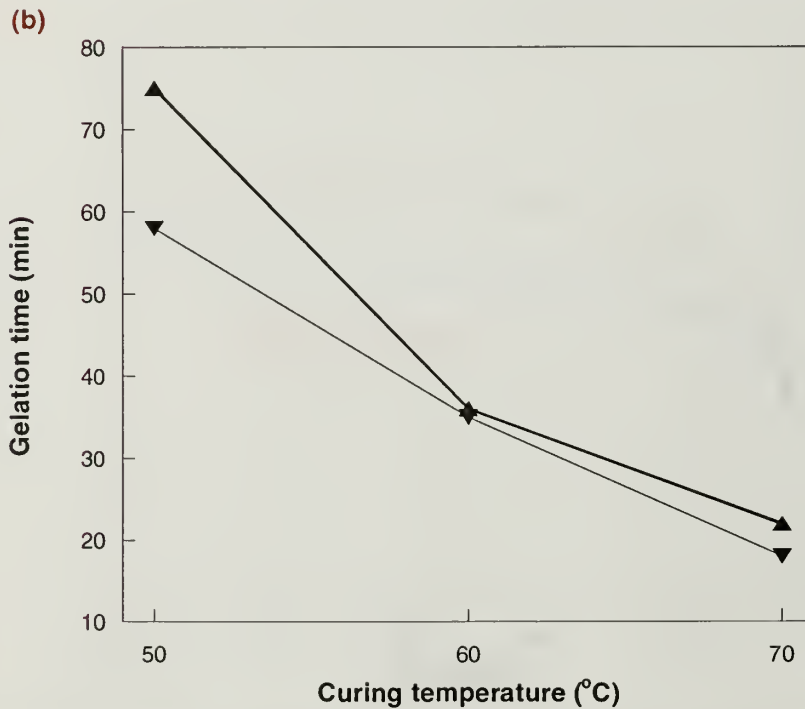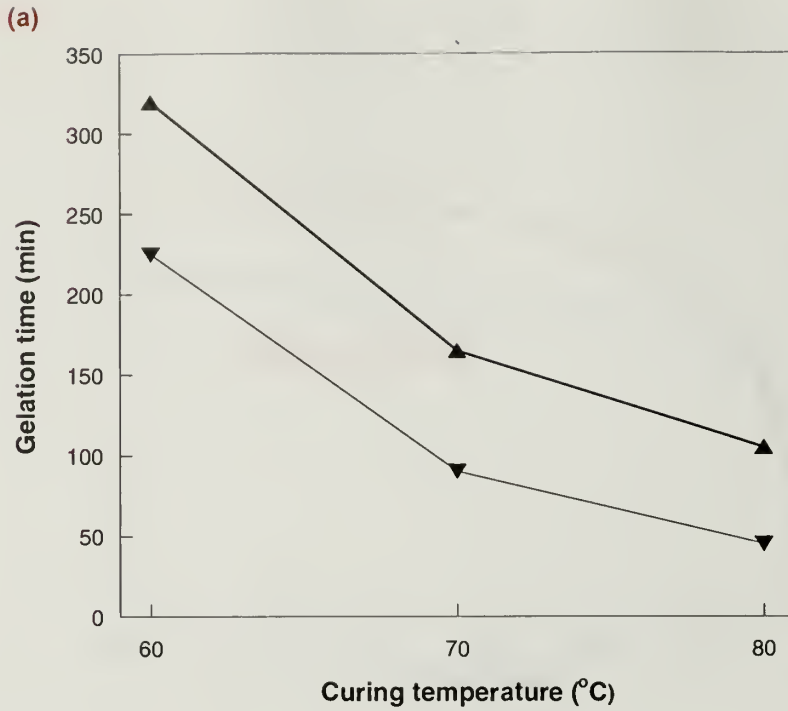
Figure 3.9 Dependence of gelation time on curing temperature when (a) NH_4HCO_3 and (b) NH_2COONH_4 are used as curing agents : (▲) RC/NCO = 2 and (▼) RC/NCO = 4.

Figure 3.8 shows the curing kinetics of isocyanate-terminated PPG prepolymer by the decomposition of NH_2COONH_4. As with NH_4HCO_3-promoted curing, curing kinetics is influenced by temperature and RC/NCO. The important thing to notice with NH_2COONH_4 is the t_{gel}. Gelation time of NH_2COONH_4-promoted curing is less than the one promoted by NH_4HCO_3. This is due to the faster decomposition rate of NH_2COONH_4 compared to NH_4HCO_3. In fact, at 80 °C, decomposition of NH_2COONH_4 is so fast (as seen in TGA studies) that gelation is not observed at all due to either too high or too low a conversion of NCO groups by reaction with NH_3. Apart from the decomposition rate, the mechanical properties of the materials prepared by NH_2COONH_4-induced curing are inferior to those prepared by NH_4HCO_3-induced curing. This may be due to two reasons. The first one is due to the reactivity difference between NH_3 and H_2O. NH_3 being stronger base/better nucleophile than H_2O, NH_3 should react faster than H_2O with NCO. But the physical states of the RCs also play a role as gaseous NH_3 can escape from the reaction medium faster than H_2O. The second reason is due to the relative ease of formation of crosslinks by the RCs. When NH_4HCO_3 is used as curing agent, both H_2O and NH_3 act as RCs whereas with NH_2COONH_4, only NH_3 reacts with NCO. Thus the faster decomposition rate of NH_2COONH_4 and less ease in the formation of crosslinks (hence lower crosslink density) affect the mechanical properties of NH_2COONH_4 promoted curing. Figure 3.9 compiles the impact of curing temperature on the gelation time for the isocyanate-terminated PPG prepolymer for the different concentrations of RCs.
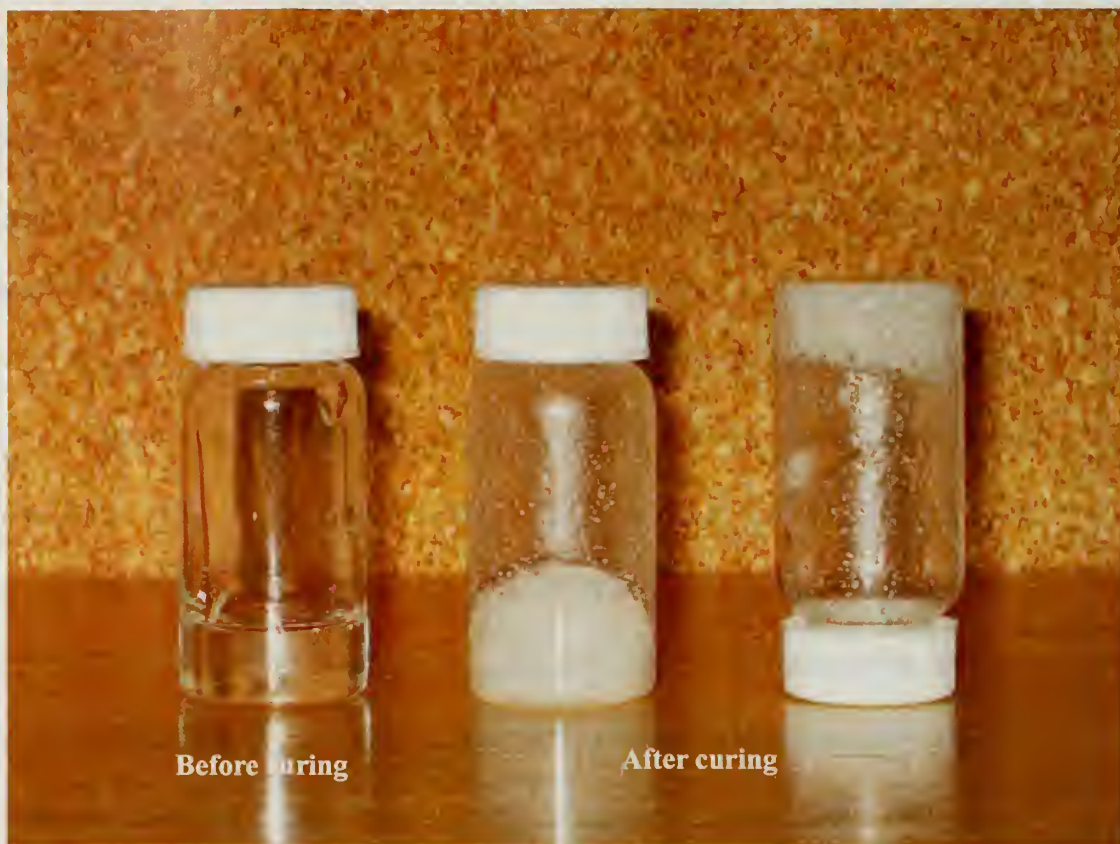
Figure 3.10 Physical state of PPG prepolymer before curing (liquid-like) and gel state of NH$_4$HCO$_3$-cured PPG-based polyurethane polymer.

The gel state of the cured polyurethane polymer due to crosslink formation is shown in Figure 3.10. PPG prepolymer is a viscous liquid and upon curing, a solid-like, gel state is obtained.

(a)

(b)

(c)
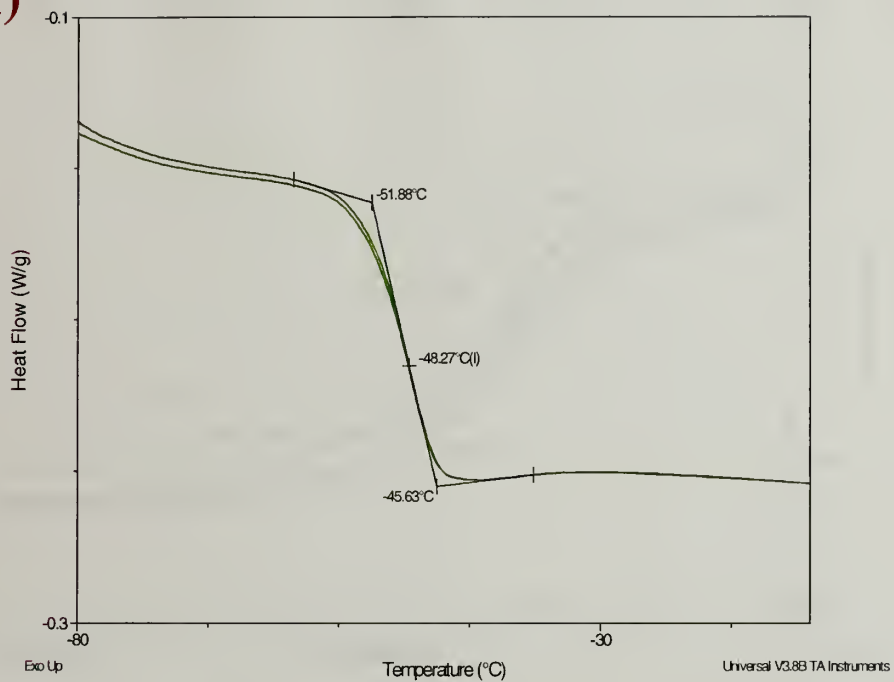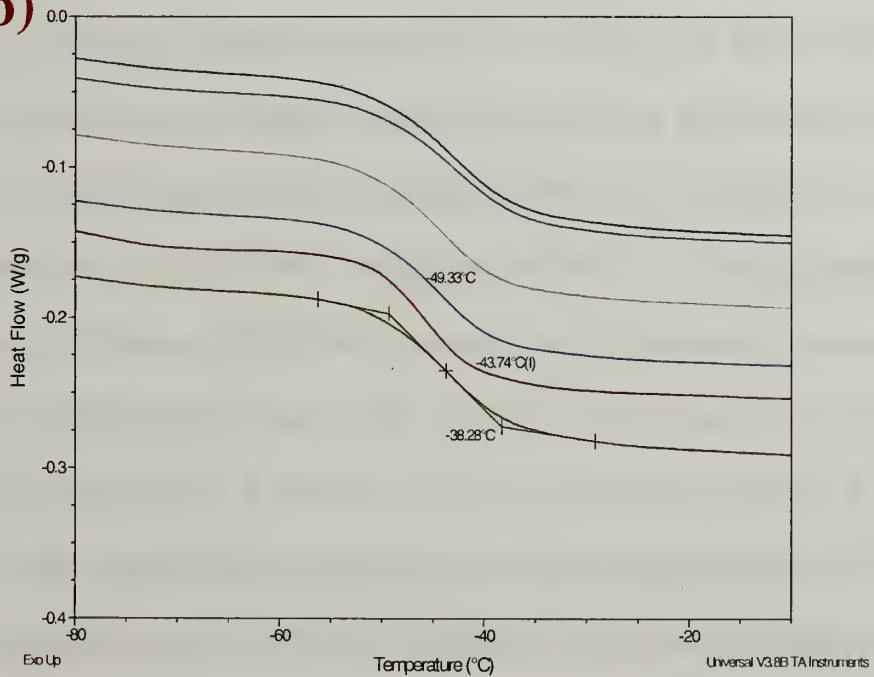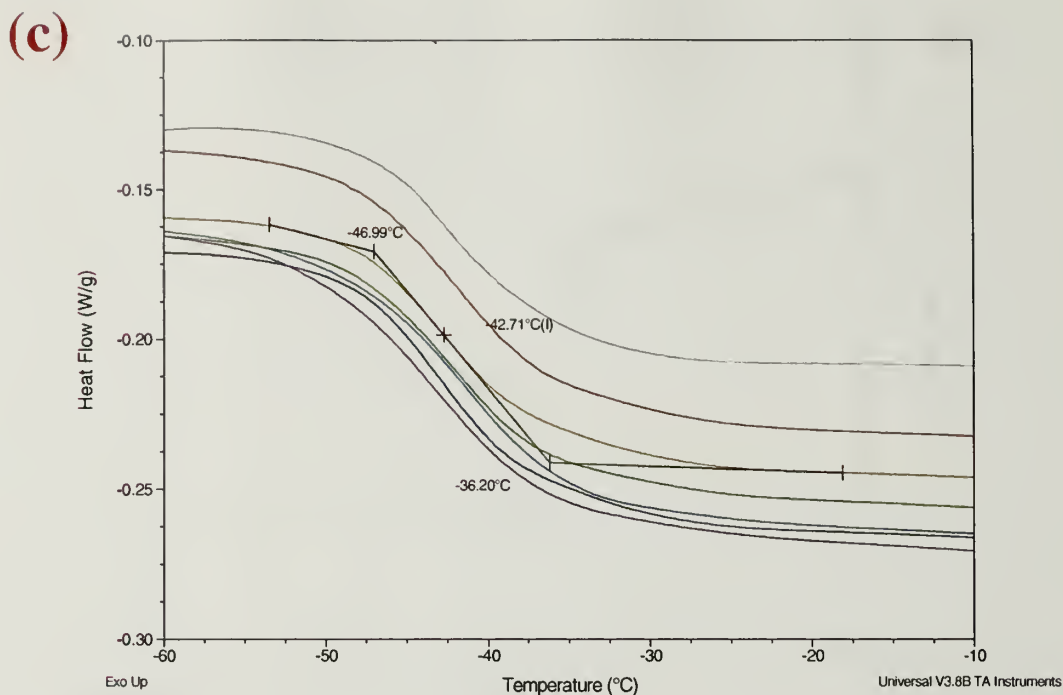
Figure 3.11 DSC studies of (a) PPG prepolymer (b) PPG prepolymer cured by
NH₄HCO₃ and (c) PPG prepolymer cured by NH₂COONH₄.

DSC studies were carried out to confirm the presence of crosslinks. T_g should

increase on crosslinking and the crosslink density dictates the extent of increase in T_g.

Figure 3.11 compares the T_g of PPG prepolymer and the ammonium salts-cured

polyurethane polymer. T_g of the PPG prepolymer is -48.27 ˚C. On curing with the

ammonium salts, increases in T_g are observed. For NH_4HCO_3-cured PPG prepolymer,

T_g is found to be in the range of -44.8 ˚C to -42.7 ˚C and for NH_2COONH_4-cured

polymer, T_g is found in the range of -43.08 ˚C to -41.27 ˚C. The increase in T_g for

NH_2COONH_4-cured polymer is higher than NH_4HCO_3-cured polymer. This is

surprising because the mechanical properties of NH_4HCO_3-cured polymer are superior

to the mechanical properties of NH_2COONH_4-cured polymer. This anomaly can be

explained by considering the possible products formed by the reaction of RCs with

NCO. Reaction of H_2O with NCO can result in a maximum of just one crosslink at the junction point whereas reaction with NH_3 can lead to more than one crosslink at the junction point. Apart from that, molecular weight between the crosslink junctions can also be different as the reactivity and physical state of RCs are also different. All these variables make the comparative studies irrelevant. One thing to note in the NH_2COONH_4-assisted curing is that at 80 °C and RC/NCO = 2, a gel point was not reached after 200 min, but the T_g of the cured sample increased compared to the PPG prepolymer. This may be due to low conversion of NCO by the reaction with gaseous NH_3 (at 80 °C, decomposition of the salt is abrupt), in the initial time period, in the rheometer not leading to gelation. But, over a period of time, reaction of NCO with monosubstituted urea (formed by the reaction of NCO with NH_3) can occur, leading to an increase in T_g when DSC studies were carried out.

3.4 Conclusions

A new approach to cure isocyanate-terminated prepolymer by a trigger mechanism has been studied. Addition of an ammonium salt that is stable at room temperature but decomposes on heating to release products that cure the prepolymer is presented. This mechanism makes the curing process independent of environmental conditions. Curing kinetics of the prepolymer were followed by rheological studies. Curing by the decomposition of NH_4HCO_3 yields better mechanical properties than by the decomposition of NH_2COONH_4. Differences in the mechanical properties and thermal properties are explained in terms of reactivity, physical state of the RCs and the properties of crosslinks formed by the reaction between NCO and the RCs.

3.5 References

(1)   Chen, D. B.; Qi, X.; Zhou, Z. H.; Zhong, A. Y.; Du, Z. Y. "Curing behavior of acrylate-urethane system" *Journal of Applied Polymer Science* **1996**, *62*, 1715-1721.

(2)   Cui, Y. J.; Hong, L.; Wang, X. L.; Tang, X. Z. "Evaluation of the cure kinetics of isocyanate reactive hot-melt adhesives with differential scanning calorimetry" *Journal of Applied Polymer Science* **2003**, *89*, 2708-2713.

(3)   Dimier, F.; Sbirrazzuoli, N.; Vergnes, B.; Vincent, M. "Curing kinetics and chemorheological analysis of polyurethane formation" *Polymer Engineering and Science* **2004**, *44*, 518-527.

(4)   Lepene, B. S.; Long, T. E.; Meyer, A.; Kranbuehl, D. E. "Moisture-curing kinetics of isocyanate prepolymer adhesives" *Journal of Adhesion* **2002**, *78*, 297-312.

(5)   Sun, X. D.; Sung, C. S. P. "Cure characterization in polyurethane and model urethane reactions by an intrinsic fluorescence technique" *Macromolecules* **1996**, *29*, 3198-3202.

(6)   Comyn, J.; Brady, F.; Dust, R. A.; Graham, M.; Haward, A. "Mechanism of moisture-cure of isocyanate reactive hot melt adhesives" *International Journal of Adhesion and Adhesives* **1998**, *18*, 51-60.

(7)   Jeong, Y. G.; Hashida, T.; Hsu, S. L.; Paul, C. W. "Factors influencing curing Behavior in phase-separated structures" *Macromolecules* **2005**, *38*, 2889-2896.

(8)   Wicks, D. A.; Wicks, Z. W. "Blocked isocyanates III: Part A. Mechanisms and chemistry" *Progress in Organic Coatings* **1999**, *36*, 148-172.

(9)   Chambon, F.; Petrovic, Z. S.; Macknight, W. J.; Winter, H. H. "Rheology of Model Polyurethanes at the Gel Point" *Macromolecules* **1986**, *19*, 2146-2149.

CHAPTER 4

MULTILAYER FORMATION USING HYDROPHOBIC INTERACTIONS

4.1 Introduction

Multilayer thin film preparation has progressed significantly in many ways since Blodgett's deposition of calcium stearate films on glass slides.[1] The Langmuir-Blodgett (LB) technique has been well studied, but practical issues - that it is sensitive to contaminants, substrate geometry and the kinetics of monolayer film transfer, have limited its utility.[2-4] A limited amount of relatively early research was reported that adopted chemical means to construct multilayer films to try to circumvent problems inherent to the LB technique, and then the relative dormancy in this field was replaced with a very active period following the seminal work of Decher and co-workers.[5-7] Their work revived interest in layer-by-layer deposition (LbL) primarily through the use of electrostatic interactions between polycation and polyanion layers. Although this preparative technique was versatile, in terms of the wide choice of polyelectrolyte materials and that pH, ionic strength and counterion identity of adsorption solutions could control layer structure, it was limited by the lack of applicability to neutral molecules. Hence, hydrogen bonding, charge transfer, repetitive adsorption/drying, biological interactions and various complex formation methods were studied for LbL multilayer film construction.[8-13] Although these methods extend multilayer assembly to neutral molecules with specific interactions, they individually lack latitude in terms of substrate choice and multilayer functionality and collectively do not comprise a versatile method, but rather a collection of specific syntheses. In McCarthy's lab, LbL

adsorption was studied with the goal of turning any polymer surface into "the same surface" so that interface problems could be solved generically.[14-17] This failed because "memory effects" over length scale of the substrates (interactions being inversely proportional to l^n where l is length and n is determined by the type of interaction) persisted over all subsequent adsorptions steps.

Supported thin films (coatings) require a range of bulk and surface properties for specific applications and need to be applied to a range of substrates. An objective of the work studied here is to establish a technique that can be used for any substrate and can be adapted to permit wide latitude of chemical structure manipulation, both in individual layers and at the free surface of the resulting material. This has been accomplished by using the hydrophobic interactions that occur between most polymers that are soluble in water and hydrophobic, low energy surfaces in contact with these aqueous solutions.

Hydrophobic interaction is an entropy-driven phenomenon in which an adsorbate adsorbs at the solid-water (or liquid-water) interface to reduce the interfacial energy. Entropy gained by the release of water molecules from the interface drives the adsorption process.[18] Although most polymers adsorb at aqueous interfaces with hydrophobic solids, the stability of such coatings based on this process is questionable due to the reversible nature of many adsorptions. Numerous biopolymers, particularly proteins, have been shown to irreversibly adsorb to hydrophobic solids. The fact that proteins denature (change conformation and become insoluble) upon adsorption makes the process irreversible. It has been shown that proteins can adsorb irreversibly even on a negatively charged surface with the hydrophobic interactions overcoming coulombic

repulsions.[19] In spite of the facile irreversible adsorption of many biopolymers, only a few synthetic polymers have been shown to adsorb irreversibly (cannot be washed off with water) from aqueous solution. Poly(L-lysine) adsorbs to fluoropolymers and the irreversibility is proposed to be due to the unfolding of the α-helix structure.[20] Poly(vinyl alcohol) (PVOH) adsorbs to hydrophobic surfaces and crystallization, in conjunction with hydrophobic interactions, is proposed to be responsible for the irreversibility.[21-23] It has been suggested that the PVOH adsorption occurs from water on all sufficiently hydrophobic surfaces and the effects of temperature, time, PVOH concentration, degree of hydrolysis, salt concentration and the type of salt on the adsorption of PVOH have been reported.[22,23] Hence to have a stable coating (water insoluble), it is necessary to couple hydrophobic interactions with a secondary interaction that is more more stable (unfolding, denaturization, crystallization).

Hydrophobic interactions most certainly play a role in most LbL techniques. Ionic interactions are the most important driving force for multilayer formation using polyelectrolytes, but hydrophobic interactions are also involved in the process. Water molecules in the solvation sphere are released when a cation binds to an anion leading to increase in entropy. Serizawa *et. al.* studied PVOH adsorption on a (likely hydrophobic) gold surface and showed that surface reconstruction on drying facilitates subsequent PVOH adsorption at the solid-liquid interface.[11] This argument can be extended to other LbL techniques and we argue that most of the LbL techniques involve hydrophobic interactions as a secondary effect for multilayer formation.

In the research described in this chapter, we discuss using hydrophobic interactions as the primary force in multilayer formation. PVOH is adsorbed to a

hydrophobic substrate to form a reproducible ~2 nm thick layer that is stabilized (at room temperature) by crystallization. Chemical reaction of this thin semicrystalline layer in the vapor phase can produce a hydrophobic coating that is susceptible to adsorption by a second exposure to PVOH solution. The 2-step process can be repeated to form multilayer films. The preparation of multilayer films with ester, urethane and acetal functionalities is described here.

4.2 Experimental Section

4.2.1 Materials

Poly(vinyl alcohol) (99+% hydrolyzed, $M_w = 89000 - 98000$ g/mol), heptafluorobutyryl chloride, hexanoyl chloride and octanoyl chloride were purchased from Aldrich and used as received. Silicon wafers (100 orientation) were obtained from International Wafer Service (P/B doped; resistivity, 20-40 Ω cm; thickness 450-575 μm). Propyldimethylchlorosilane was obtained from Gelest and used as received. House purified water (reverse osmosis) was further purified using a Millipore Milli-Q system that involves reverse osmosis, ion-exchange, and filtration steps. Other reagents and solvents were obtained from Aldrich or Fisher and used as received.

4.2.2 Characterization

X-ray photoelectron spectra (XPS) were recorded with a Physical Electronics Quantum 2000 with Al K_α excitation (15 KV, 25 W). Spectra were obtained at take off angles of 15° and 75° (between the plane of the surface and the entrance lens of the detector optics). Contact angle measurements were made with a Ramè-Hart telescopic

goniometer and a Gilmont syringe with a 24-gauge flat-tipped needle. The probe fluid was water, purified as described above. Dynamic advancing angle (θ_A) and receding angle (θ_R) were recorded as water was added to or withdrawn from the drop, respectively. The values reported are averages of 3-5 measurements made on different areas of the sample surface. Ellipsometric measurements were made with a Rudolph Research model SL-II automatic ellipsometer with an angle of incidence of 70° from the normal. The light source was a He-Ne laser with λ = 632.8 nm. Measurements were performed on 3-5 different locations on each sample. Thickness of the layers was calculated from the ellipsometric parameters (Δ and Ψ) using DafIBM software. Calculations were performed for the transparent double layer model (Si substrate/SiO_X + alkylsilane layer / PVOH (derivatized PVOH) / air) with the following parameters: air, n_o = 1; PVOH, n_1 = 1.54; SiO_X + propyldimethylsilane layer, n_2 = 1.462 (the thickness of this layer varied from 2.3-2.6 nm); silicon substrate, n_s = 3.858, k_s = 0.018 (imaginary part of refractive index); poly (vinyl heptafluorobutyrate), n_3 = 1.3019; poly (vinyl hexanoate), n_4 = 1.4073; poly (vinyl octanoate), n_5 = 1.4178. The refractive indices of the monomers of the PVOH derivatives were used for the calculation of the thickness of the corresponding PVOH derivative. Though refractive index of the functionalized layer is used assuming 100% conversion of hydroxyl groups of PVOH to ester, in reality it is found not to be the case. This introduces certain degree of error in the calculation of thickness which is included in the error bar in the figures. The AFM images were obtained with a Digital Instruments Dimension 3100 scanning probe microscope with a Nanoscope III controller operated in tapping mode.

4.2.3 Preparation of Si-supported substrates

Silicon wafers were cut into 1.2 cm x 1.2 cm samples, rinsed with water and dried in air before treatment with oxygen plasma for 5 minutes at a pressure of 100 mtorr (Harrick Plasma Cleaner). Silanization reactions were carried out immediately on the plasma-cleaned wafers. Silanization with propyldimethylchlorosilane was performed in the vapor phase at 70 °C for 72h.[24] After silanization, wafers were rinsed with toluene, ethanol, ethanol/water (1:1) and water (in this order).

4.2.4 PVOH solutions

PVOH aqueous solutions were prepared by heating the polymer-water suspension for 1 hour at 85-100 °C in a water bath and allowing it to cool. The solutions were allowed to equilibrate for at least 3 days before the adsorption experiments. Concentrations used in this study were 0.1% and 1.0% w/v.

4.2.5 Adsorption experiments

Hydrophobized silicon wafers were submerged in polymer solutions for 2h, removed, and rinsed with copious amounts of water and dried under reduced pressure overnite. To eliminate any possibility of LB film transfer during removal of samples through the solution-air interface, adsorption solutions were diluted repetitively after adsorption and the samples were removed from pure water.[22,23]

4.2.6 Reaction of adsorbed PVOH with acyl chlorides

Samples containing PVOH layers on silicon-supported propyldimethylchlorosilane-derived monolayers were allowed to react with the acyl

chlorides in vapor phase. Kinetics studies were performed by carrying out the reaction for different time periods at a predetermined temperature and measuring the thickness of the ester layer by ellipsometric studies. From the kinetics studies, the reaction time was chosen to maximize conversion. Exposure to heptafluorobutyryl chloride was for 4 h at room temperature. Hexanoyl chloride was allowed to react at 75 °C for 6 h for the 0.1% PVOH multilayer system and for 2 h for the 1.0% multilayer system. Octanoyl chloride was allowed to react at 100 °C for 12 h for the 0.1% multilayer system and for 3 h for the 1.0% multilayer system. All of the esterified surfaces were rinsed with copious amounts of water and dried at reduced pressure overnite.

4.2.7 Reaction of adsorbed PVOH with butyl isocyanate

Adsorbed PVOH was reacted with butyl isocyanate (0.25 M) in the presence of dibutyltin dilaurate (0.025 M) in anhydrous toluene for 4 h at 60 °C. Wafers were removed from the solution by repetitive dilution of the solution by toluene and then rinsed with toluene and dried by blowing compressed air and under reduced pressure overnite.

4.2.8 Reaction of adsorbed PVOH with butanal

Butanal (0.15 M) in the presence of 0.2 M H_2SO_4 in water was reacted with adsorbed PVOH for 18 h at 50 °C. Wafers were removed from the solution by repetitive dilution of the solution by water and then rinsed with water and dried by blowing compressed air and under reduced pressure overnite.

4.3 Results and Discussion

The spontaneous and irreversible adsorption of PVOH from aqueous solution to hydrophobic solids that is in contact with the solution has been demonstrated to occur for a range of hydrophobic solids.[21-23] This adsorption takes place on all hydrophobic materials and detailed studies of this adsorption for a silicon-supported perfluoroalkyl monolayer has been reported.[23] In this study, propyldimethylchlorosilane-derived hydrophobic silicon wafers were chosen as the substrate because these samples can be reproducibly prepared using an uncatalyzed vapor phase reaction and they do not contain fluorine. The experiments described here involve the multilayer build up of esters, urethane and acetal of polyvinyl alcohol prepared by reacting PVOH layers with acid chlorides, butyl isocyanate and butanal respectively.
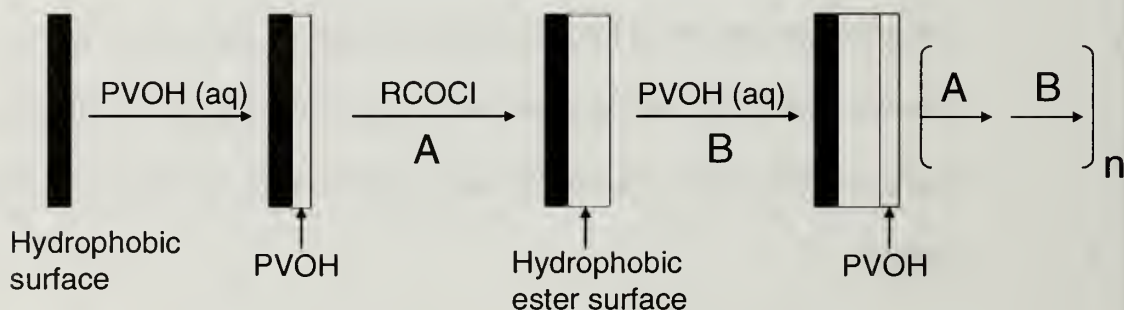
Figure 4.1. Multilayer formation by the repetitive process of adsorption and chemical reaction of PVOH.

Figure 4.1 shows the general strategy for multilayer assembly beginning with a hydrophobic solid. PVOH is adsorbed to the solid from aqueous solution, and after isolation and drying is exposed to the vapor of a carboxylic acid chloride, chosen to convert the hydrophilic PVOH layer to a hydrophobic ester surface. Figure 4.1 deliberately indicates that the thickness of this layer increases as the result of the

73

esterification reaction. The formed hydrophobic solid is exposed again to aqueous PVOH and a second layer of PVOH film is formed. Cycling steps A and B in Figure 4.1 allows build up of a multilayer film. 5 points are made in regard to this sequential scheme, some of which are followed up below: (1) The thickness of the first PVOH layer will be a function of the hydrophobicity (and perhaps other properties) of the hydrophobic solid. It has been shown that less hydrophobic solids are coated with thinner layers of PVOH.[22] (2) The thickness and structure (in particular, percent crystallinity) of this layer can also be controlled by PVOH concentration, molecular weight and degree of hydrolysis and as well by adsorption temperature and solution ionic strength.[23] (3) The thickness of the functionalized layer resulting from reaction of PVOH with other reactants will be the result of the reaction yield and the identity of alkyl group of the reactant. This thickness can likely be controlled by choice of reagent. (4) The wettability of the hydrophobic layer will also be controlled by the choice of reactants. This will affect the thickness of the subsequent layer of PVOH that adsorbs. (5) Different reactants could be used in a single multilayer film to give alternating, gradient or evenly spaced layers, which might be useful for a particular application.

4.3.1 Multilayer ester formation with heptafluorobutyryl chloride (HFBC)

The process described in Figure 4.1 was carried out using HFBC. This acid chloride was chosen to modify PVOH (and form poly(vinyl heptafluorobutyrate)) for several reasons: (1) The fluorine in HFBC acts as a sensitive label for XPS studies and facilitates the calculation of the degree of conversion. (2) The high vapor pressure of HFBC (b.p. 40 °C) enables esterification in the gas phase at room temperature. (3) The

74

reactivity of fluorinated acid chlorides is enhanced over other acid chlorides because of the electron withdrawing effect of the perfluoroalkyl group. (4) The perfluoroalkyl group should impart hydrophobicity and promote the adsorption of subsequent layers of PVOH. Two different concentration solutions of PVOH, 0.1% and 1.0% w/v, were used for adsorption experiments. The rationale behind using two concentrations was to study the impact of PVOH crystallinity on multilayer formation. A concentration of 0.1% PVOH solution is below the entanglement concentration and adsorption using this concentration leads to PVOH with a high degree of crystallinity.[23] The 1.0% PVOH solution is above the entanglement concentration and leads to a less crystalline and more amorphous layer.
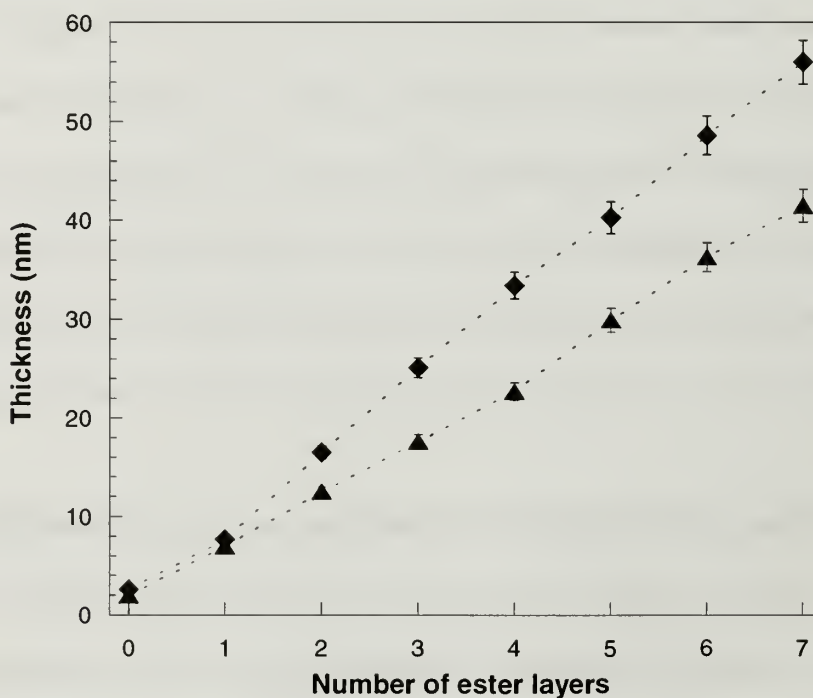
Figure 4.2. Ellipsometric thickness of multilayer films prepared by sequential adsorption of PVOH followed by esterification with HFBC. PVOH solution concentration was 0.1% (▲) and 1.0% (♦).

Figure 4.2 shows plots of the thickness of multilayer films (measured by ellipsometry) versus the number of ester layers formed. The data at 0 layers represent the thicknesses of the initial PVOH layer formed on the silicon-supported propyldimethylsilyl monolayer. The values are 2.0 ± 0.2 nm for the 0.1% PVOH solution and 2.6 ± 0.2 nm for the 1.0% PVOH solution. The thicknesses increase to 7.0 nm and 7.7 nm, respectively, after reaction of these layers with HFBC vapor. Subsequent sequential adsorption of PVOH and reaction with HFBC produces multilayer films of increasing thickness. From the slope of the plots in Figure 4.2, the average thickness increase per ester layer is determined to be 5.8 nm for 0.1% PVOH and 8.0 nm for 1% PVOH. The differences between these thickness values for films prepared with different concentration PVOH solutions can be attributed to either thicker PVOH layers formed with the higher concentration solution, greater reaction yield with HFBC for the less crystalline PVOH formed with the higher concentration solution or both of these effects. The thickness of the adsorbed PVOH layer is dependent on the hydrophobicity of the solid surface as well as the concentration of PVOH in the solution. Attempts were made to measure ellipsometric thicknesses of samples with PVOH as the outer layer to distinguish between these possibilities, but the scatter in the data was too great to make any conclusions as water adsorption/absorption on/in the hydrophilic layers complicates the measurement. Contact angle and XPS data gave more insight into this issue.
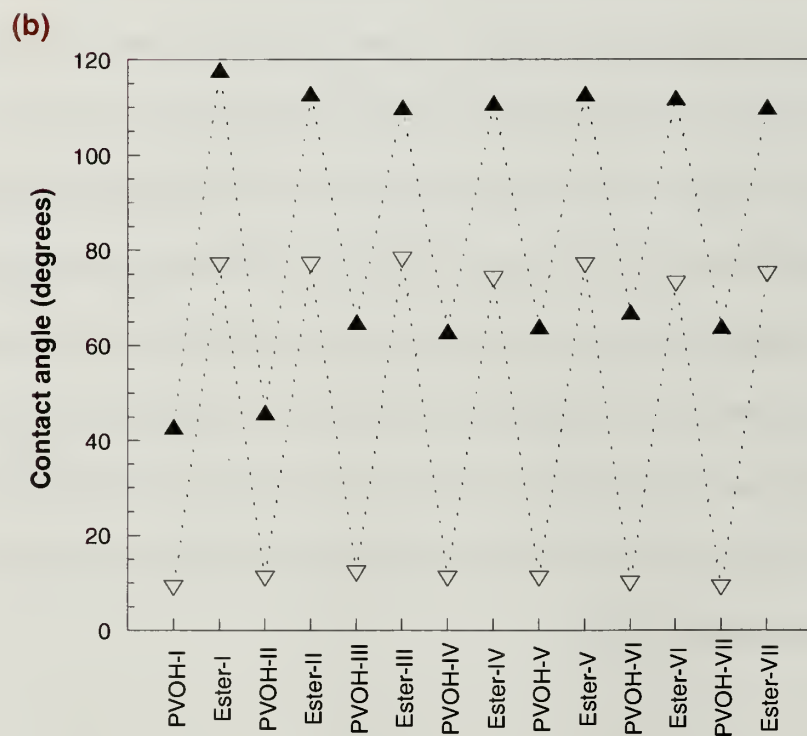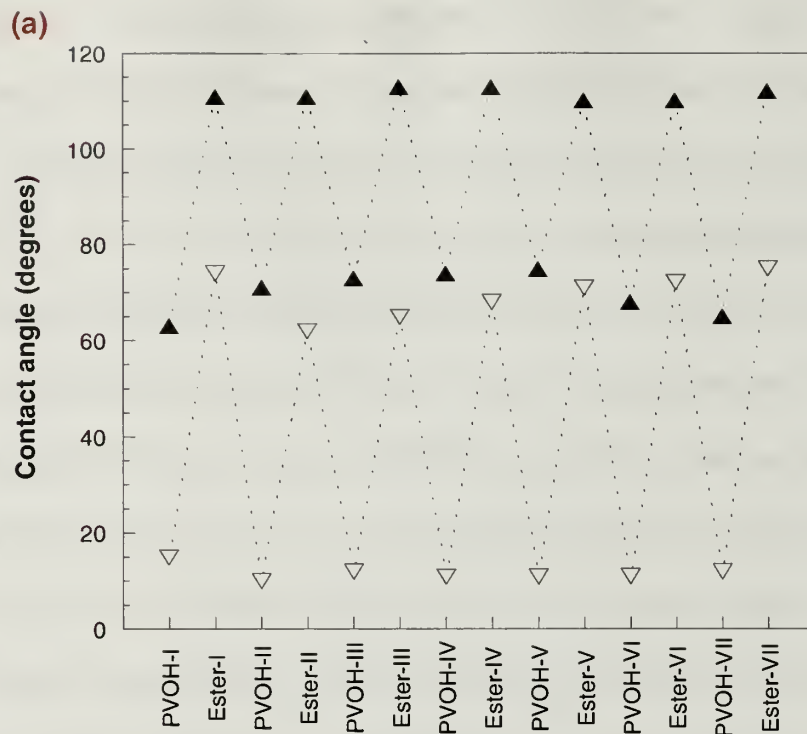
Figure 4.3 Dynamic water contact angle measurements for surfaces formed using (a) 0.1% PVOH and (b) 1.0% PVOH and HFBC: (▲) advancing angles, (∇) receding angles.

Contact angle analysis (Figure 4.3) of the deposition process supports the view

of multilayer build-up depicted in Figure 4.1. The alternate hydrophilization and

hydrophobization by PVOH and HFBC treatments is apparent from the zig-zag profile

of advancing and receding water contact angles. The propyldimethylsilyl monolayer

surface exhibits water contact angles of $\theta_A/\theta_R = 104°/93°$ which decrease to $63°/15°$ and

$43°/9°$ upon adsorption of PVOH from 0.1% and 1.0% PVOH solutions, respectively.

After reaction with HFBC, θ_A/θ_R values increase to $111°/74°$ and $118°/77°$ for 0.1% and

1.0% PVOH-treated surfaces, respectively. The oscillating data between hydrophobic

and hydrophilic is obvious from the plots in Figure 4.3 and the scatter in the data is

largely due to the fact that each θ_A/θ_R value was determined on separate samples that

were prepared by multiple synthetic steps. The receding contact angle data for the

fluorinated ester surfaces is in general lower for samples prepared using the lower

concentration PVOH solution. This may contribute to the thinner layers observed in

samples prepared with the less concentrated PVOH solution. It is also interesting to note

that these perfluoroalkyl surfaces exhibit lower contact angles and greater hysteresis

than covalently attached perfluoroalkyl monolayers.[23] The presence of unreacted

alcohols and ester functionality in the region of contact angle sensitivity is suggested.

Surface roughness can also influence contact angle hysteresis, but these samples

exhibited smooth surfaces as assessed by AFM. Figure 4.4 shows the AFM images of

the final ester surface prepared using different concentrations of PVOH. The maximum

root mean square roughness for the surfaces shown in Figure 4.4 was 0.757 nm for 0.1%

PVOH samples and 1.034 nm for 1.0% PVOH samples.
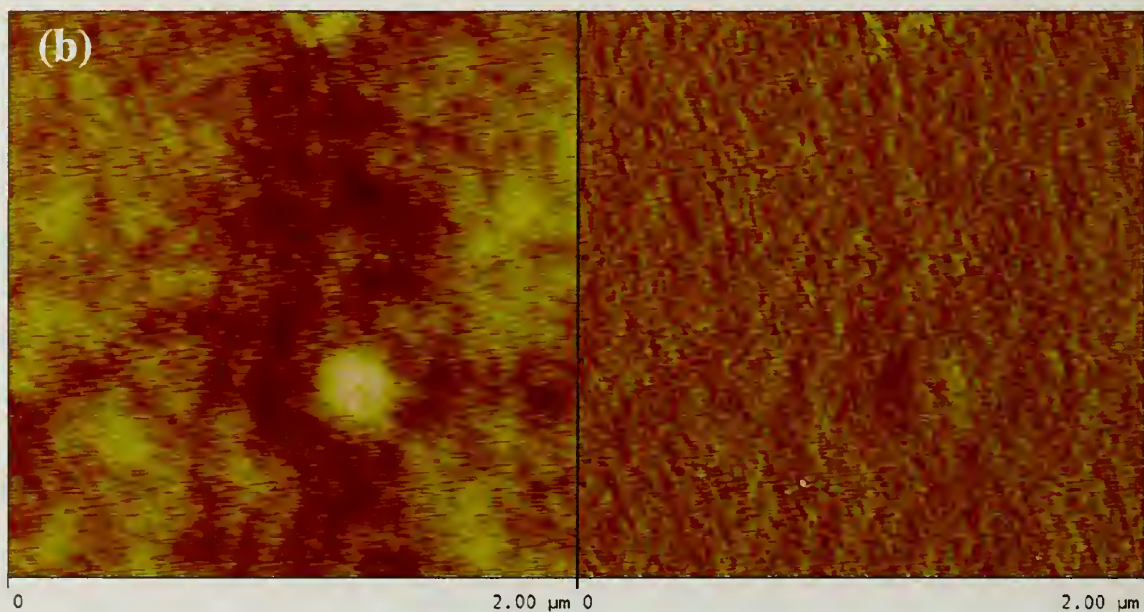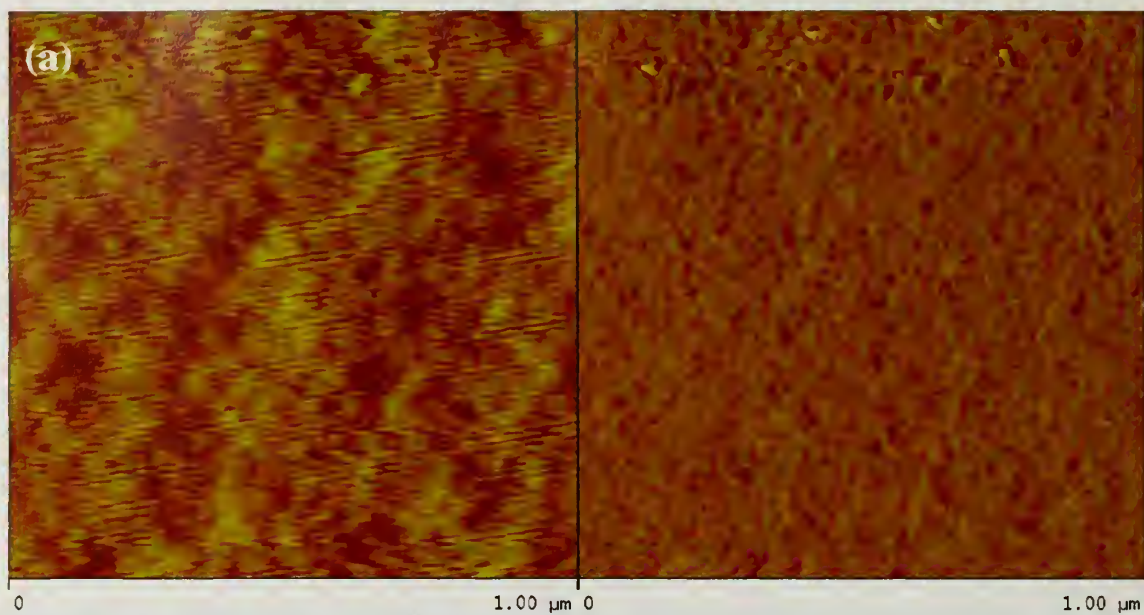
Figure 4.4. AFM analyses showing height (left image) and phase (right image) profile for ester surfaces formed by the reaction of HFBC with the thin layer formed by (a) 0.1% PVOH and (b) 1.0% PVOH.
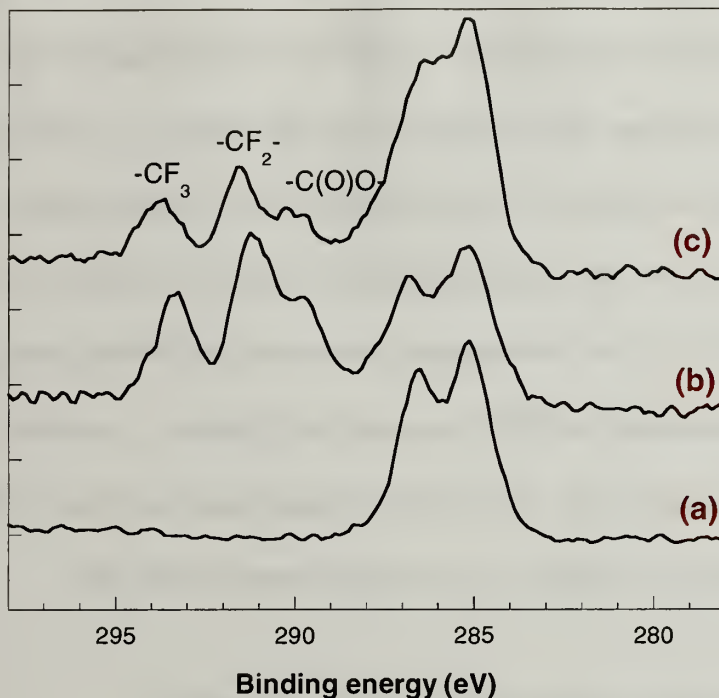
Figure 4.5 C$_{1s}$ spectra recorded at 15° takeoff angle for (a) a single PVOH layer adsorbed on a propyldimethylsilyl monolayer, (b) a single HFBC-reacted PVOH layer and (c) PVOH adsorbed on a single HFBC-derived ester layer.

XPS data were recorded for all samples and were consistent with the ellipsometry and contact angle data just described. It did permit us to make estimates for the yields of reaction with HFBC. Figure 4.5 shows C$_{1s}$ region spectra for the first 3 steps of preparing a multilayer film using 0.1% PVOH solution. The sample containing the first layer of PVOH shows two peaks for the 2 carbons present in -CH$_2$-CH(OH)-, at relatively low binding energy. Some contribution from the propyldimethylsilyl monolayer is not ruled out. Upon reaction with HFBC, carbon signals at higher binding energy appear, indicating the presence of CF$_3$CF$_2$CF$_2$C(O)O- groups. Adsorption of the second layer of PVOH increases the relative intensity of the low binding energy peaks. The degree of conversion of alcohol to ester can be calculated from the XPS data to give

estimates of reaction yield. From the F/C ratio of multilayer esterified surfaces, yields of 60-70% for 0.1% PVOH and 80-90% for 1.0% PVOH were observed. The XPS data used for these calculations was recorded at a take off angle of 75° which provides information on the outermost 5-10 nm of samples. This is roughly equal to the average thickness per ester layer. We attribute the higher degree of conversion for 1% PVOH than for 0.1% PVOH to the lower degree of crystallinity of PVOH layers prepared from higher concentrated solutions. HFBC can rapidly diffuse into ~2 nm thick films. The average thickness per layer for 1.0% PVOH is higher than that of the 0.1% PVOH because of the lower crystallinity and thus higher esterification yield.

4.3.2 Multilayer ester formation with n-alkanoyl chlorides

The generality of this multilayer assembly method was shown using two additional acid chlorides, hexanoyl chloride and octanoyl chloride, which were chosen to ensure sufficient hydrophobicity of the resulting ester surfaces for PVOH adsorption. Vapor phase reactions were again carried out, however at temperatures of 75 °C and 100 °C for hexanoyl chloride and octanoyl chloride, respectively, to compensate for their lower vapor pressures and higher boiling points (150 and 250 °C at 1 atm).
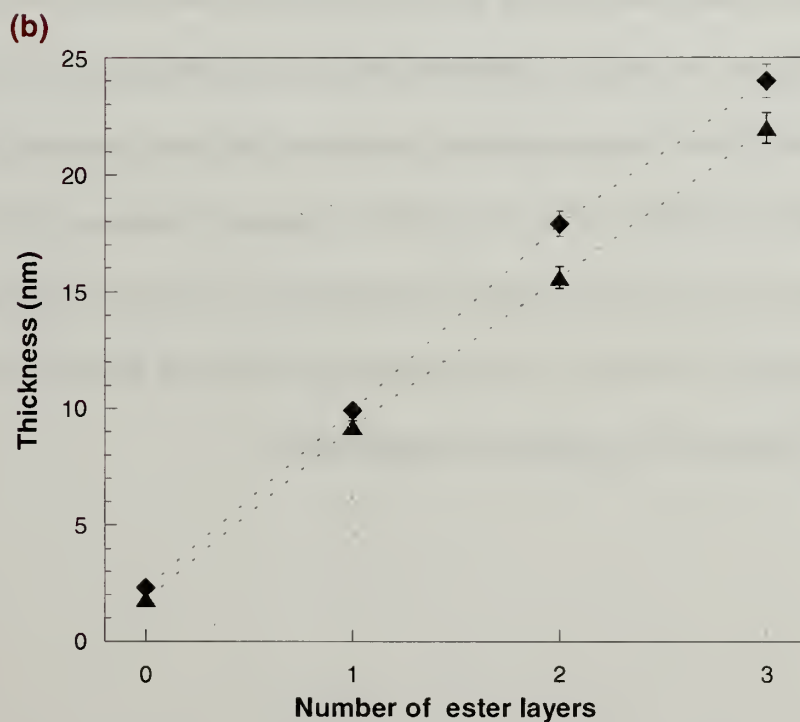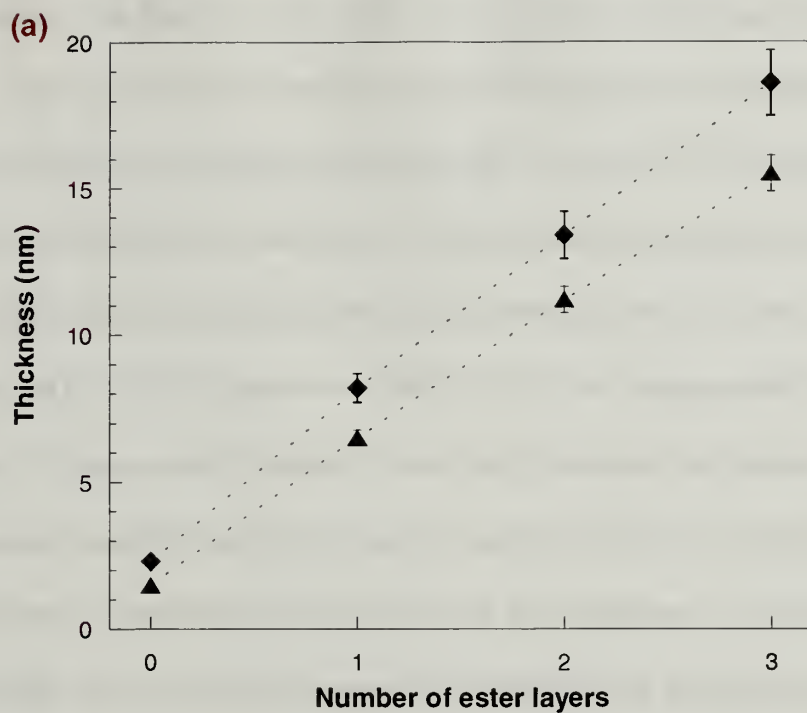
Figure 4.6 Ellipsometric thickness of multilayer films prepared by sequential adsorption of PVOH followed by esterification with hexanoyl chloride (a) and octanoyl chloride (b) PVOH solution concentration was 0.1% (▲) and 1.0% (◆).

Films were prepared with 1, 2 and 3 ester layers for each acid chloride and, as was described above for HFBC; PVOH was adsorbed from solutions with concentrations of 0.1% and 1.0%. Figure 4.6 shows ellipsometric thickness data for the hexanoate and octanoate multilayer films. As was the case for HFBC, the thickness increases linearly with the number of ester layers applied and the thickness was slightly greater for films prepared with 1.0% PVOH than with 0.1% PVOH. The average thickness increase per hexanoate layer was 4.5 nm and 5.2 nm using 0.1% and 1.0% PVOH, respectively. For the octanoate system, the average thickness increase per layer was 6.4 nm and 7.1 nm using 0.1% and 1.0% PVOH, respectively. These differences between the hexanoate and octanoate thicknesses could be due to the different alkyl chain lengths of the esters or to the relative yields of the esterification reactions.

XPS data was used to estimate the yields of the esterification reactions. The C_{1s} spectra of all of the alkanoate multilayer samples exhibit three prominent peaks that correspond to -C=O (288.2 eV), -C-O (285.9 eV) and alkyl carbons (284.2 eV). Taking ratios of the area of the carbonyl peak to the total area of the carbon signal gave reaction yield values of 35-45% for 0.1% PVOH and 40-55% for 1.0% PVOH for formation of the esters. These must be regarded as rough estimates.

Figure 4.7 Dynamic water contact angle measurements for surfaces formed using (a) 0.1% PVOH and (b) 1.0% PVOH and $C_5H_{11}COCl$: (▲) advancing angles, (∇) receding angles.

Figure 4.8 Dynamic water contact angle measurements for surfaces formed using (a) 0.1% PVOH and (b) 1.0% PVOH and $C_7H_{15}COCl$: (▲) advancing angles, (∇) receding angles.

Dynamic water contact angle data for the multilayers prepared with PVOH and either hexanoyl chloride or octanoyl chloride are qualitatively similar to those of HFBC-derived ester surfaces and are shown in Figure 4.7 and Figure 4.8 respectively. Receding contact angles show the pronounced zig-zag patterns as the surfaces change from hydrophilic ($\theta_R \sim 10°$) to hydrophobic ($\theta_R \sim 45°$ for 0.1% PVOH and $\sim 60°$ for 1.0% PVOH). The zig-zag patterns are evident, but less pronounced in the advancing contact angle data, changing from $\theta_A \sim 110°$ for hydrophobic surfaces to $\theta_A \sim 95°$ after PVOH is adsorbed to an ester surface. The pronounced hysteresis is not due to roughness as all surfaces are smooth as evidenced by AFM. Figures 4.9 and 4.10 shows the AFM images of the final poly(vinyl hexanoate) and poly(vinyl octanoate) surfaces respectively. The highest value RMS roughness measured is lower than 1 nm for all the samples
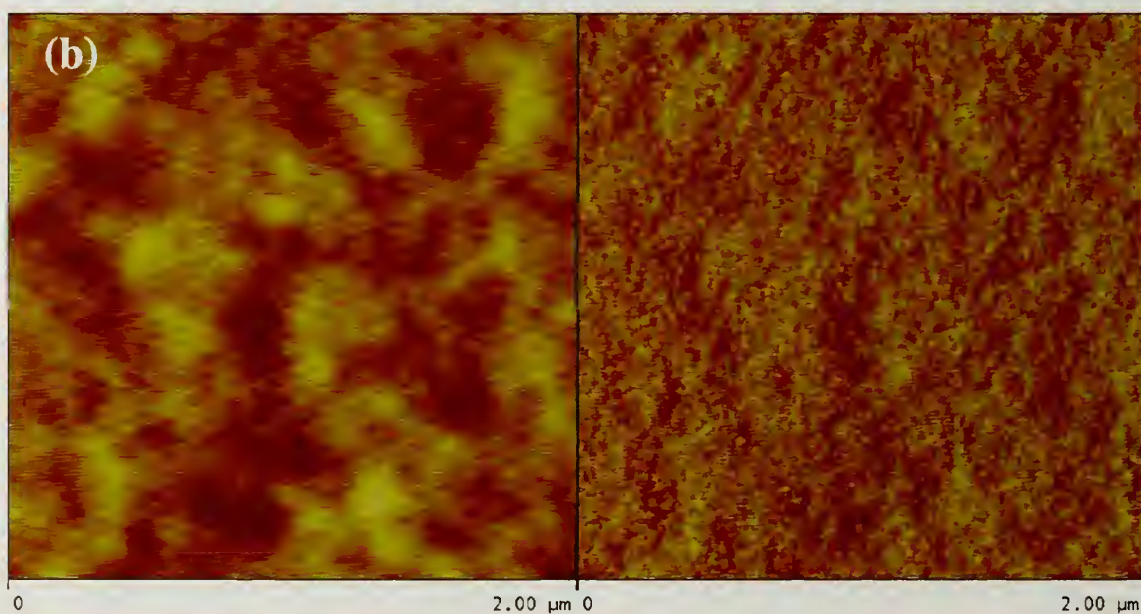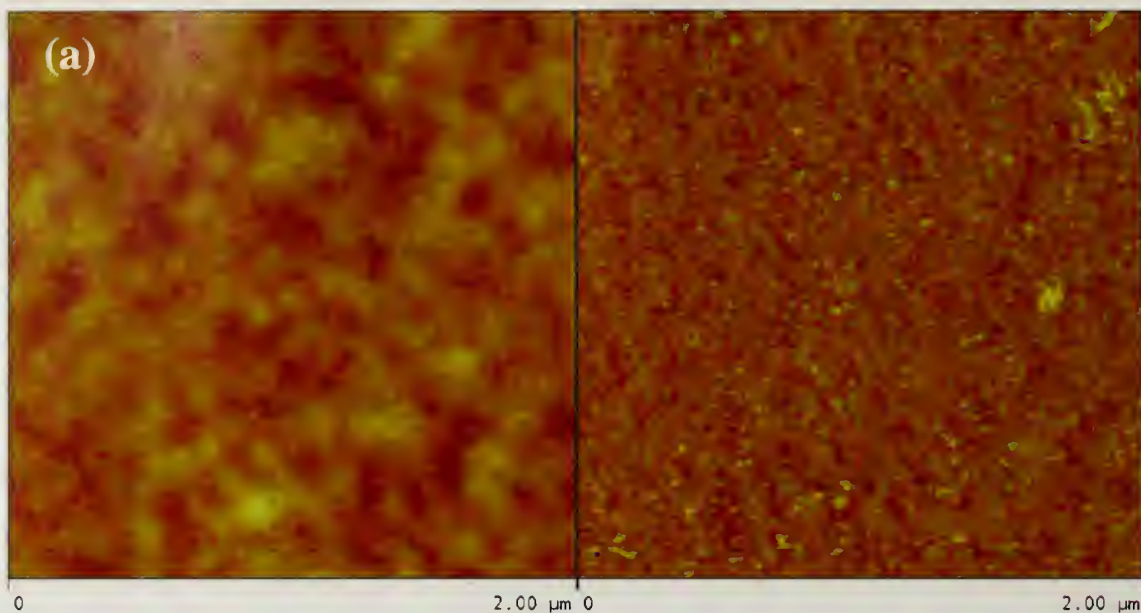
Figure 4.9 AFM analyses showing height (left image) and phase (right image) profile for ester surfaces formed by the reaction of $C_5H_{11}COCl$ with the thin layer formed by (a) 0.1% PVOH and (b) 1.0% PVOH.
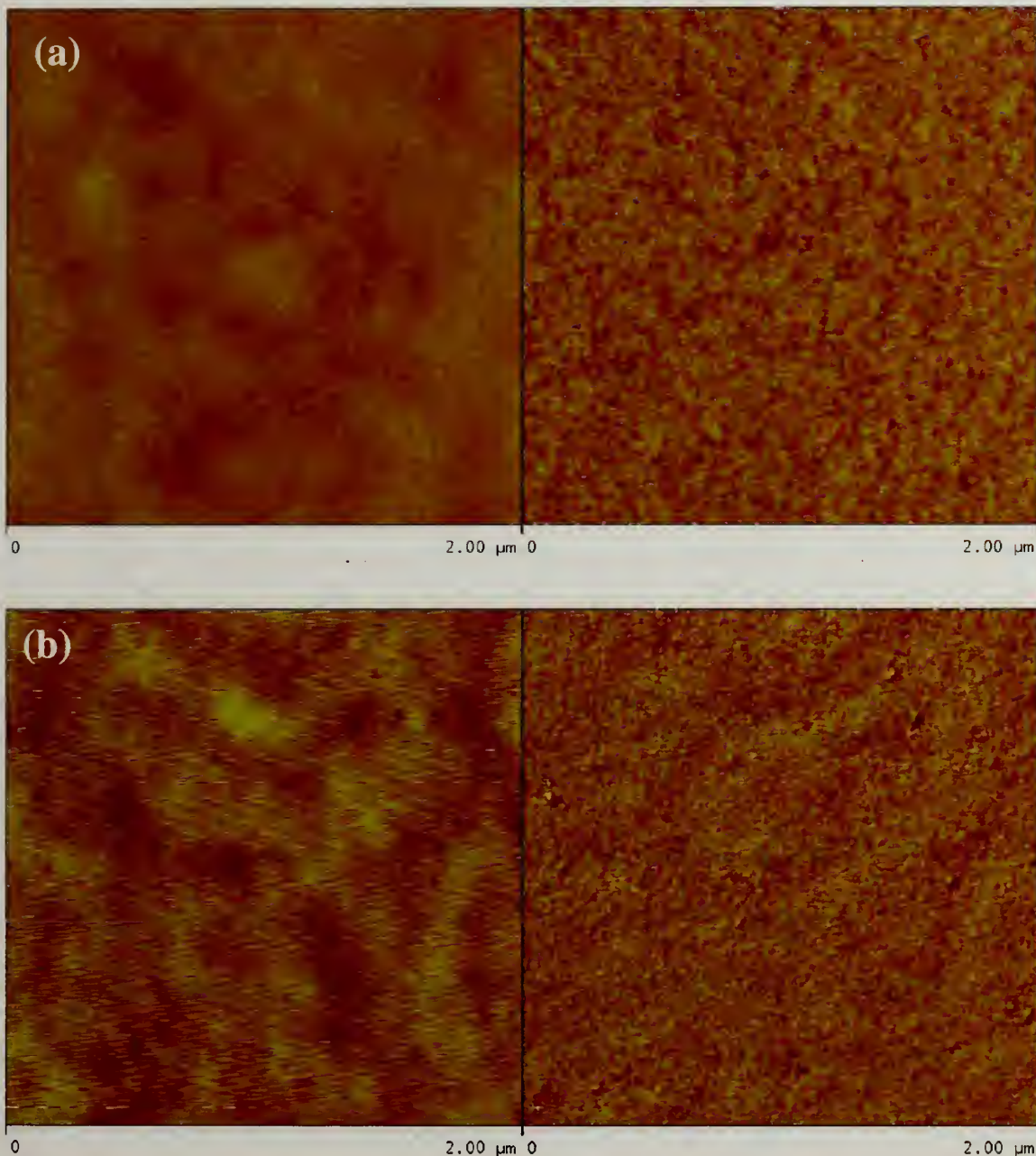
Figure 4.10 AFM analyses showing height (left image) and phase (right image) profile for ester surfaces formed by the reaction of $C_7H_{15}COCl$ with the thin layer formed by (a) 0.1% PVOH and (b) 1.0% PVOH.
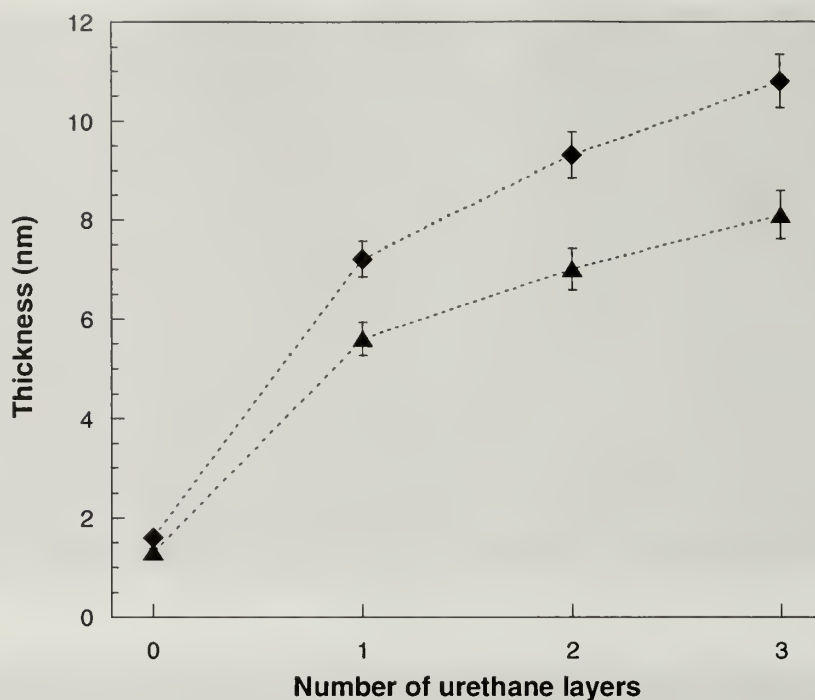
Figure 4.11 Ellipsometric thickness of multilayer films prepared by sequential adsorption of PVOH followed by reaction with C_4H_9NCO. PVOH solution concentration was 0.1% (▲) and 1.0% (◆)

4.3.3 Multilayer urethane formation with butyl isocyanate

Adsorbed PVOH was reacted with butyl isocyanate in the presence of dibutyltin dilaurate to form poly (N-butylvinyl carbamate) (PBVC), an urethane layer. A plot of ellipsometric thickness vs. number of layers is shown in Figure 4.11. The thicknesses of the first functionalized layers derived from nascent PVOH are 5.6 nm and 7.2 nm for 0.1% PVOH and 1.0% PVOH respectively. Thickness increase per layer is ~1.3 nm for 0.1% PVOH and ~1.8 nm for 1.0% PVOH. Such low thickness increases are attributed to very thin films of PVOH adsorbed on the urethane surfaces. The urethane functionality is more hydrophilic than the esters and this decrease in hydrophobicity reduces the amount of PVOH adsorbed, eventually resulting in low thickness increases

per layer. Contact angle measurements follow the expected trend of alternating hydrophilicity and hydrophobicity as shown in Figure 4.12. It is observed that θ_A for the urethane surface is lower than θ_A for ester surfaces because urethane functionality is more hydrophilic than the esters and this observation also supports the low thickness increase per layer. Figure 4.13 shows the AFM images of the final functionalized surfaces prepared using 0.1% PVOH and 1.0% PVOH. It is apparent from the height section that the films are very rough relative to the thickness of the samples. RMS roughness is 2.5 nm for a 8.1 nm thick urethane film obtained using 0.1% PVOH and 1.9 nm for a 10.8 nm thick urethane film obtained using 1.0% PVOH. The combination of lower hydrophobicity and high roughness explains the trend observed in ellipsometric measurements.
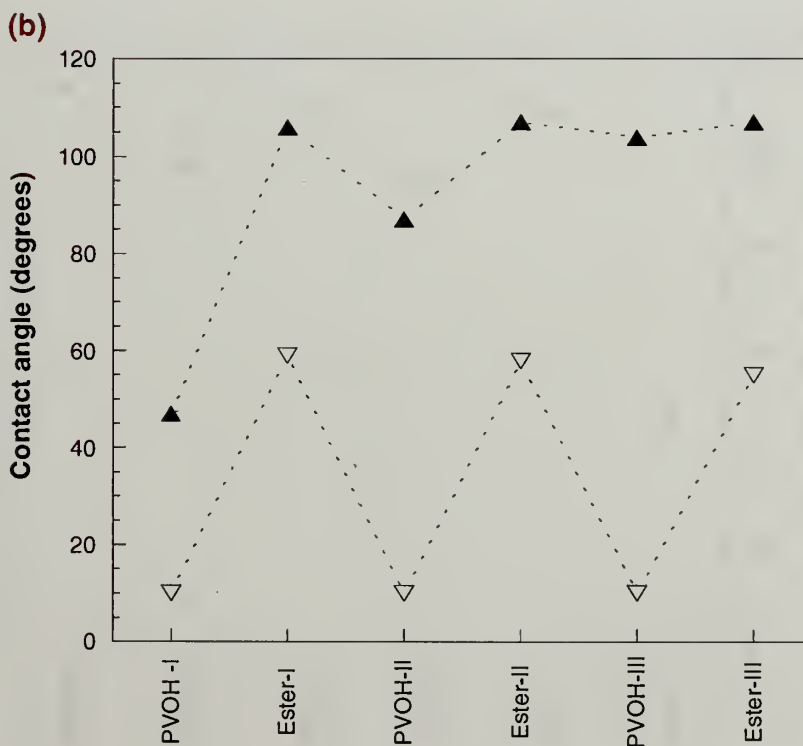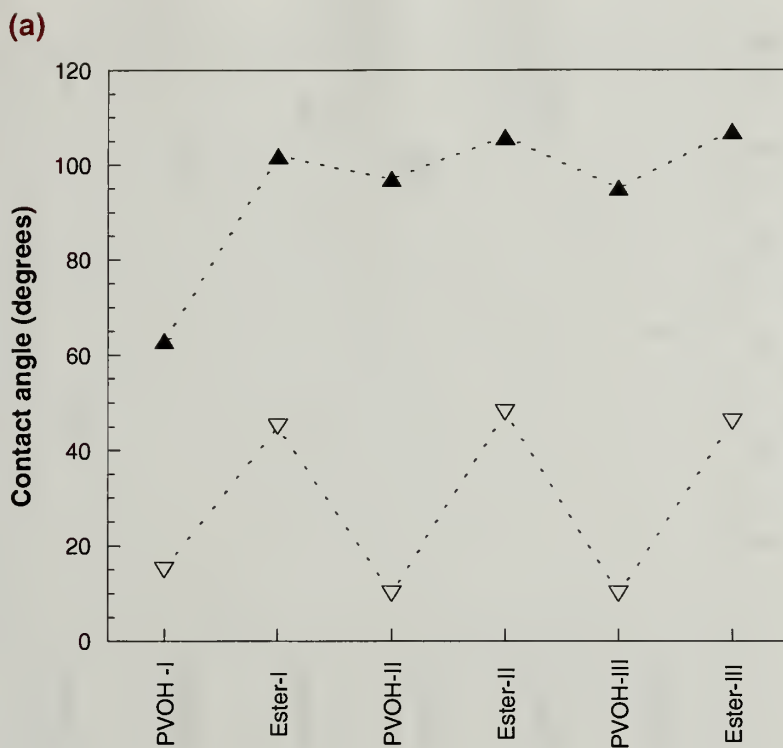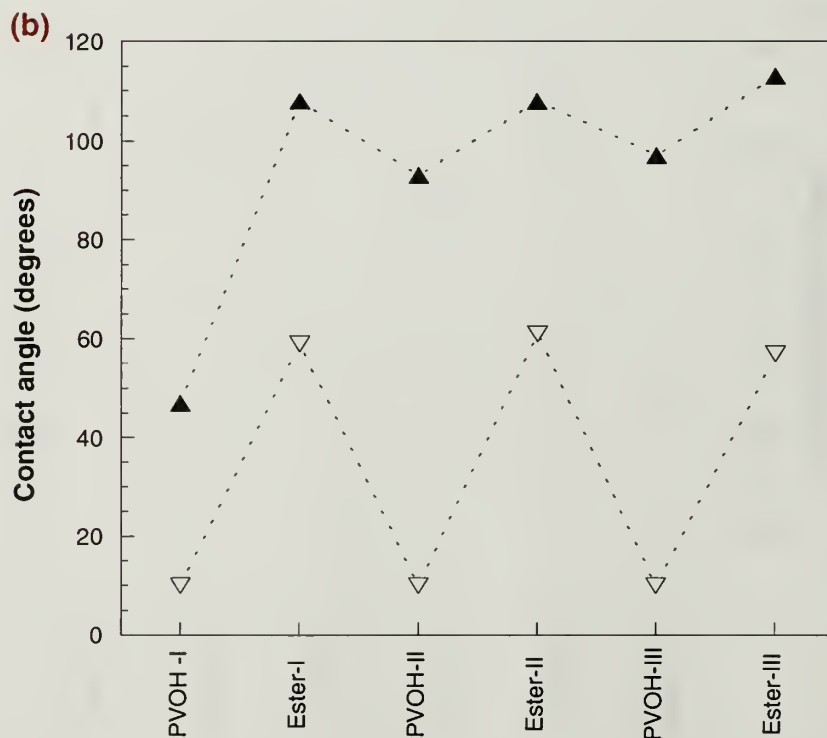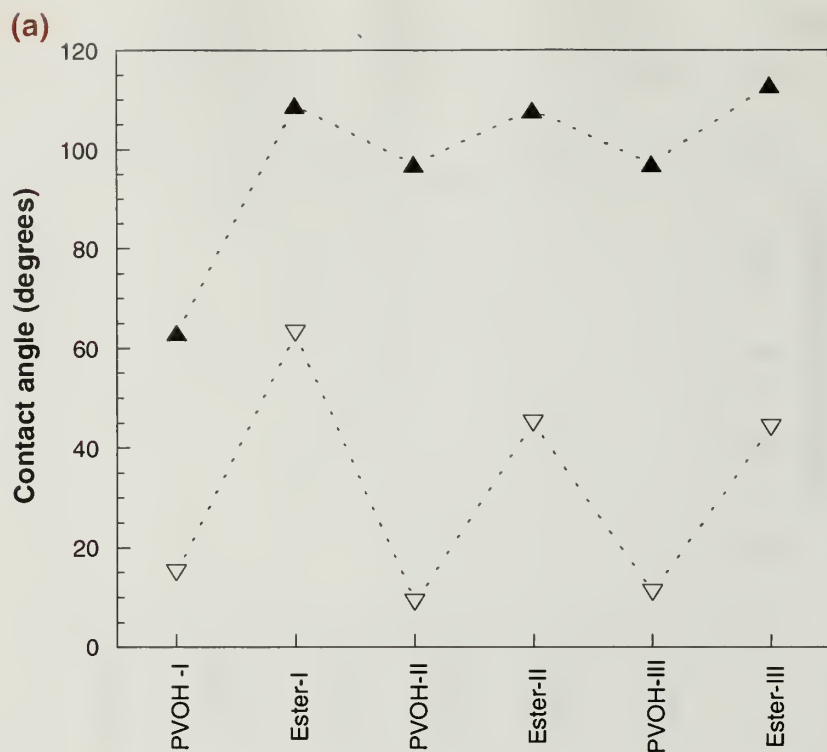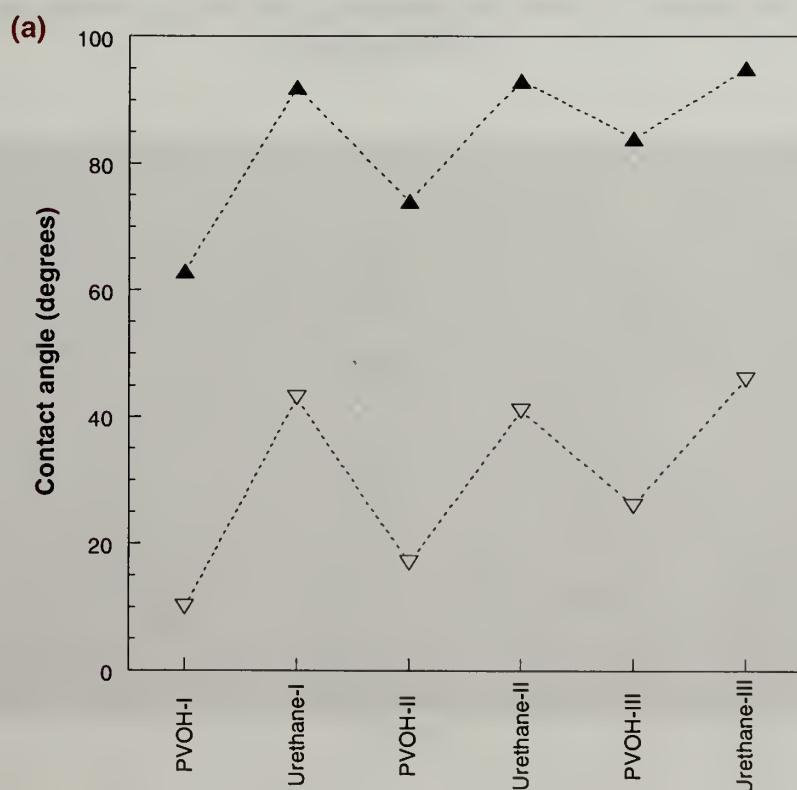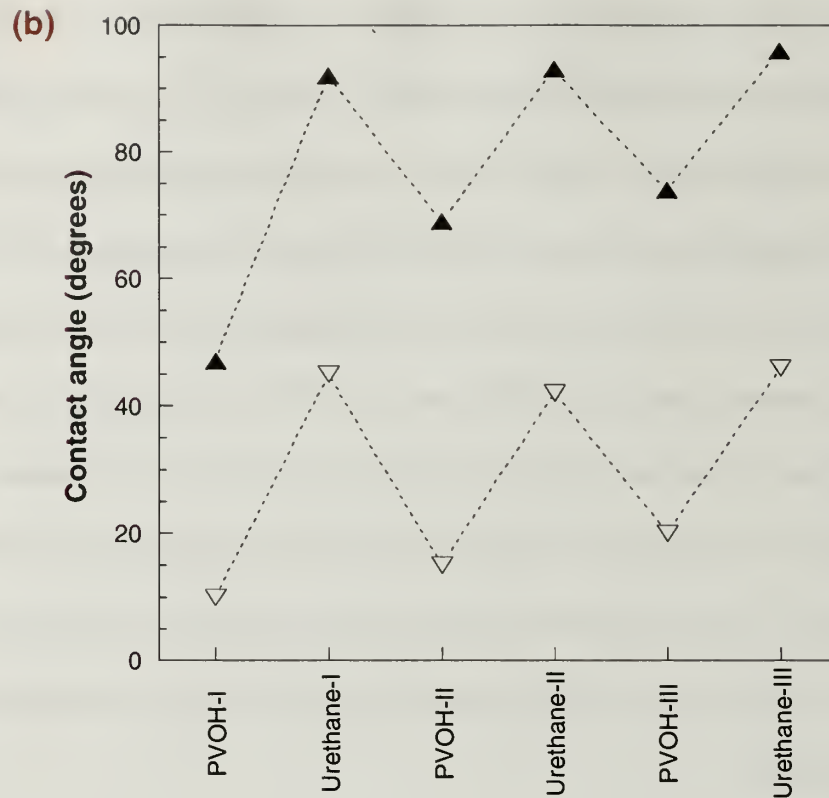
Figure 4.12 Dynamic water contact angle measurements for surfaces formed using (a) 0.1% PVOH and (b) 1.0% PVOH and C_4H_9NCO : (▲) advancing angles, (∇) receding angles.
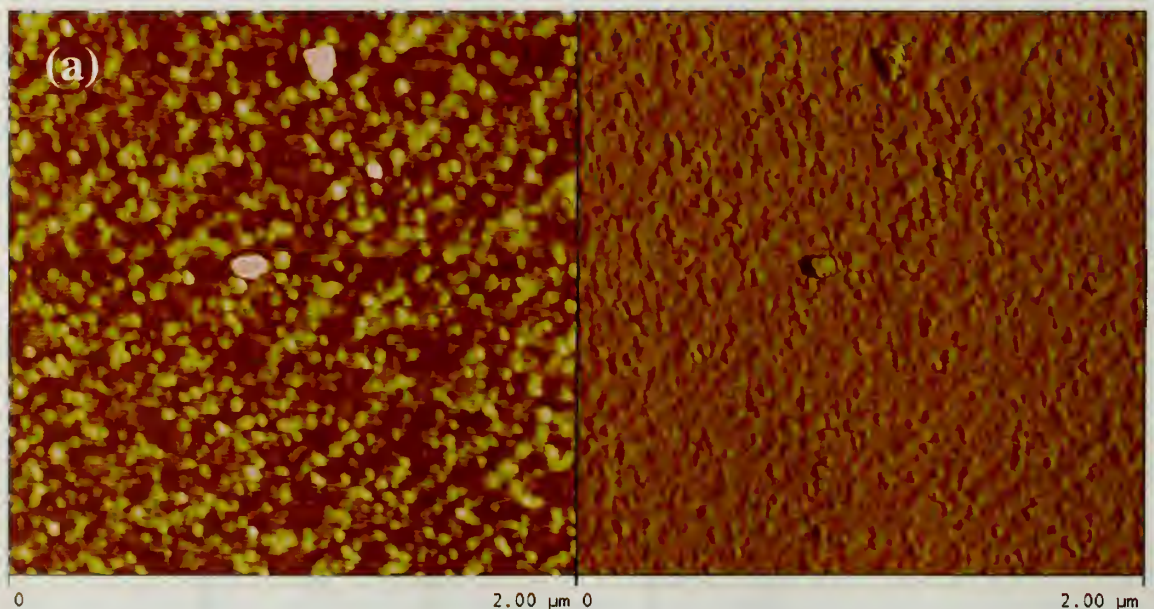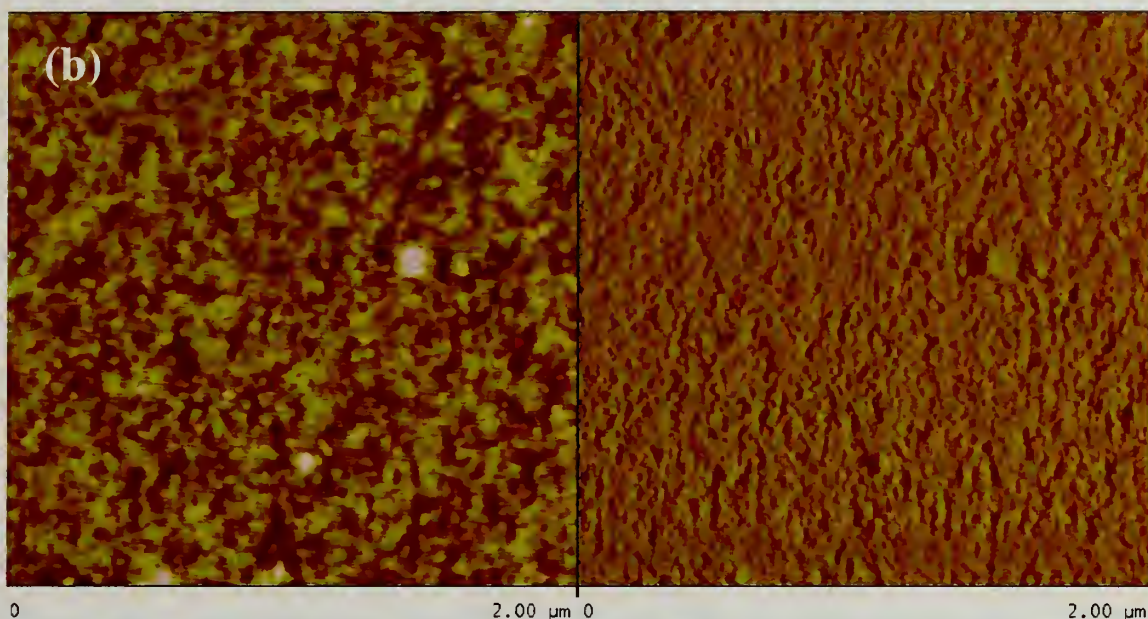
Figure 4.13 AFM analyses showing height (left image) and phase (right image) profile for urethane surfaces formed using (a) 0.1% PVOH and (b) 1.0% PVOH.
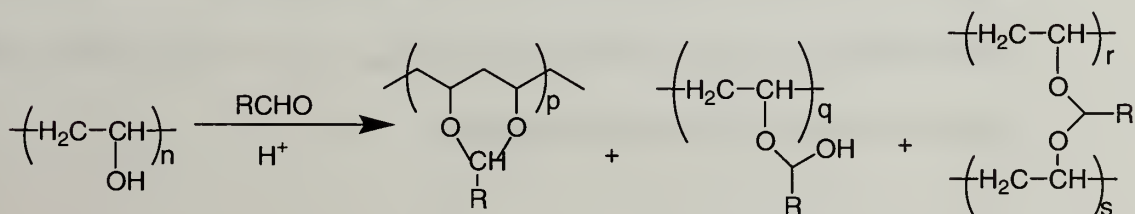
Figure 4.14 Possible products formed by the reaction of PVOH with an aldehyde in acid medium.

4.3.4 Multilayer acetal formation with butanal

Adsorbed PVOH is reacted with butanal in the presence of H_2SO_4 to form an acetal surface. Reaction of PVOH with butanal could lead to various products as shown in Figure 4.14. Products formed are not as hydrophobic as the ester surfaces.

Ellipsometric thickness vs. number of layers is shown in Figure 4.15 for the multilayer system formed using 0.1% PVOH. Thickness of the first functionalized layer derived from nascent PVOH is 5.9 nm. However, subsequent increase in thickness is very low as the thickness reaches 7.0 nm after three cycles of adsorption/reaction. Such a low thickness increase is due to the low hydrophobicity of the acetal surface and hence low adsorption of PVOH. Low hydrophobicity of the acetal surface is supported by contact angle studies as shown in Figure 4.16. The advancing angle does not change much when PVOH is adsorbed onto the acetal surface whereas receding angle shows the characteristic zig-zag pattern between acetal and PVOH surfaces. The advancing angle of the acetal surface is ~90°. This is not sufficiently hydrophobic to cause substantial adsorption of PVOH. To understand the contact angle hysteresis, XPS and AFM studies were carried out. XPS of the surface, as shown in Figure 4. 17, shows a broad tail which suggests that a variety of products form. AFM analysis of the final acetal surface is shown in Figure 4.18. For the 7.0 nm thick film, R_{rms} is 1.5 nm. Thus XPS and AFM explain the reasons for contact angle hysteresis.
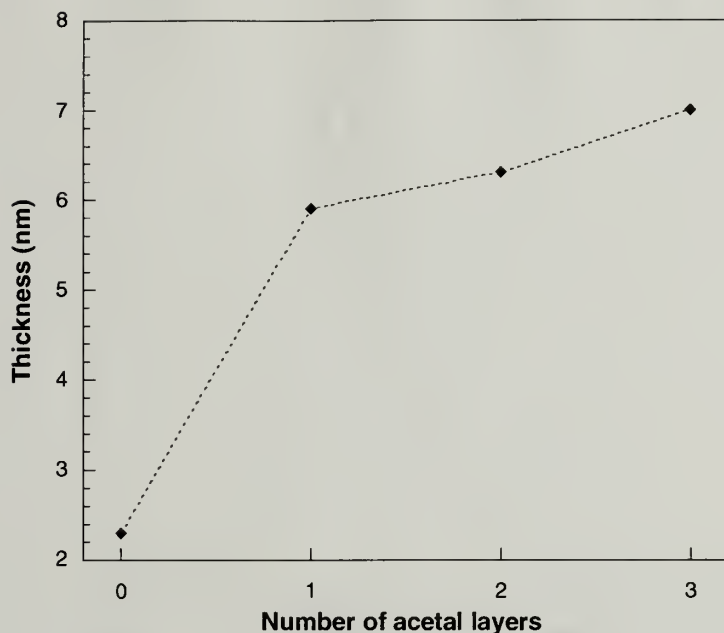
Figure 4.15 Ellipsometric thickness of multilayer films prepared by sequential adsorption of PVOH followed by reaction with butanal.
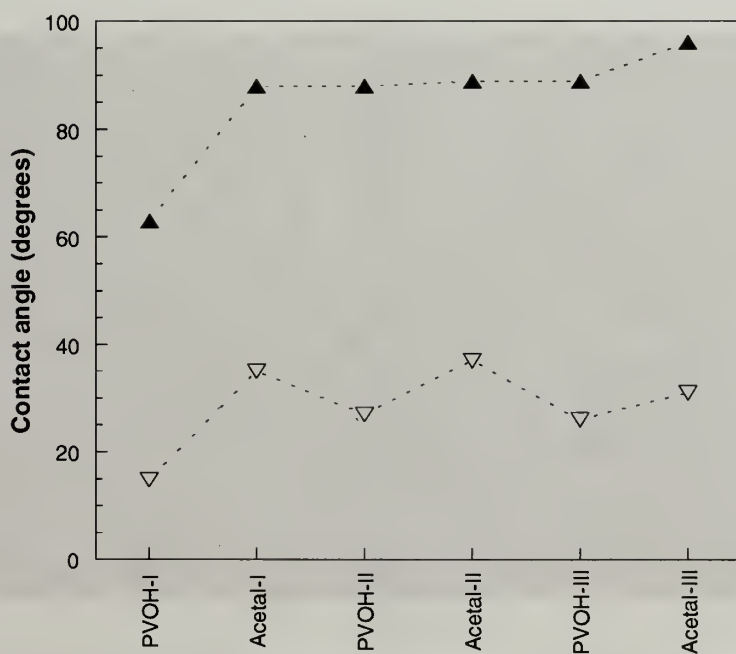
Figure 4.16 Dynamic water contact angle measurements for surfaces formed using 0.1% PVOH and C_3H_7CHO : (▲) advancing angles, (▽) receding angles.
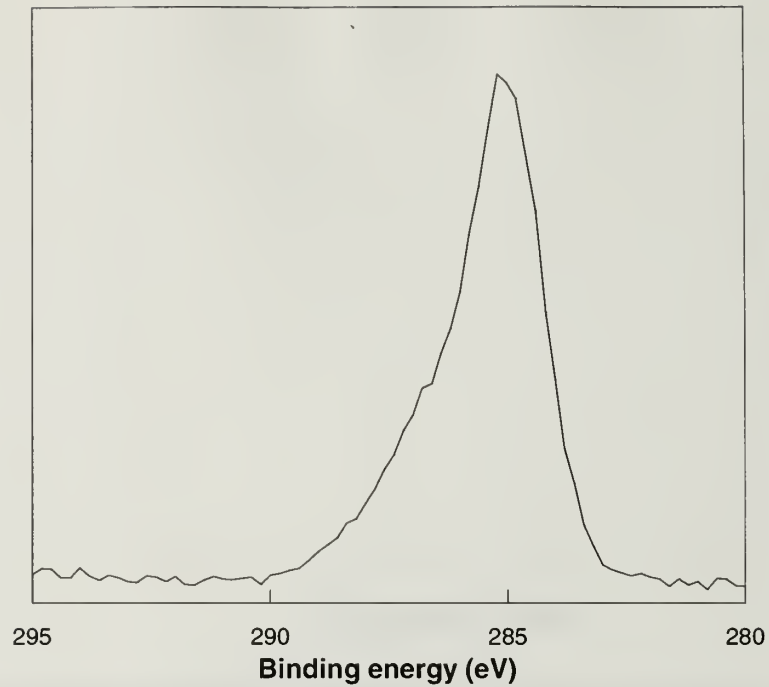
Figure 4.17 C$_{1s}$ spectra recorded at 75° takeoff angle for the acetal surface.
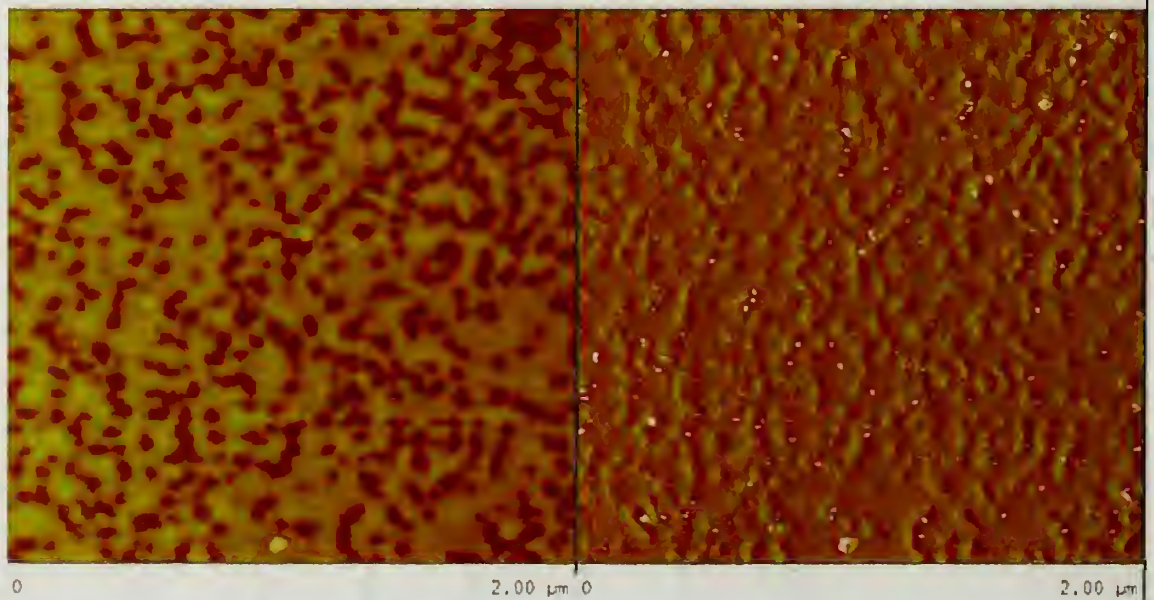
Figure 4.18 AFM analyses showing height (left image) and phase (right image) profile for acetal surface formed using 0.1% PVOH.

4.4 Conclusions

A new method for layer-by-layer assembly that uses hydrophobic interactions to adsorb PVOH followed by chemical modification to regenerate a hydrophobic surface that another layer of PVOH can adsorb to has been presented. This technique is general in that it can be used on any hydrophobic substrate and versatile in that different hydrophobic functionalities can be incorporated. Vapor phase reaction of acid chloride with PVOH is found to yield better results than the solution phase reaction of PVOH with isocyanate and butanal.

4.5 References

(1)   Blodgett, K. B. "Films built by depositing successive monomolecular layers on a solid surface" *Journal of the American Chemical Society* **1935**, *57*, 1007-1022.

(2)   Gaines, G. L. "From Monolayer to Multilayer - Some Unanswered Questions" *Thin Solid Films* **1980**, *68*, 1-5.

(3)   Honig, E. P. "Molecular Constitution of X-Type and Y-Type Langmuir-Blodgett Films" *Journal of Colloid and Interface Science* **1973**, *43*, 66-72.

(4)   Kopp, F.; Fringeli, U. P.; Muhlethaler, K.; Gunthard, H. H. "Instability of Langmuir-Blodgett Layers of Barium Stearate, Cadmium Arachidate and Tripalmitin, Studied by Means of Electron-Microscopy and Infrared Spectroscopy" *Biophysics of Structure and Mechanism* **1975**, *1*, 75-96.

(5)   Lee, H.; Kepley, L. J.; Hong, H. G.; Mallouk, T. E. "Inorganic Analogs of Langmuir-Blodgett Films - Adsorption of Ordered Zirconium 1,10-Decanebisphosphonate Multilayers on Silicon Surfaces" *Journal of the American Chemical Society* **1988**, *110*, 618-620.

(6)   Netzer, L.; Sagiv, J. "A New Approach to Construction of Artificial Monolayer Assemblies" *Journal of the American Chemical Society* **1983**, *105*, 674-676.

(7)   Decher, G.; Hong, J. D.; Schmitt, J. "Buildup of Ultrathin Multilayer Films by a Self-Assembly Process .3. Consecutively Alternating Adsorption of Anionic and Cationic Polyelectrolytes on Charged Surfaces" *Thin Solid Films* **1992**, *210*, 831-835.

(8)   Stockton, W. B.; Rubner, M. F. "Molecular-level processing of conjugated polymers .4. Layer-by-layer manipulation of polyaniline via hydrogen-bonding interactions" *Macromolecules* **1997**, *30*, 2717-2725.

(9)   Wang, L. Y.; Wang, Z. Q.; Zhang, X.; Shen, J. C.; Chi, L. F.; Fuchs, H. "A new approach for the fabrication of an alternating multilayer film of poly(4-vinylpyridine) and poly(acrylic acid) based on hydrogen bonding" *Macromolecular Rapid Communications* **1997**, *18*, 509-514.

(10)   Shimazaki, Y.; Mitsuishi, M.; Ito, S.; Yamamoto, M. "Preparation of the layer-by-layer deposited ultrathin film based on the charge-transfer interaction" *Langmuir* **1997**, *13*, 1385-1387.

(11)   Serizawa, T.; Hashiguchi, S.; Akashi, M. "Stepwise assembly of ultrathin poly(vinyl alcohol) films on a gold substrate by repetitive adsorption/drying processes" *Langmuir* **1999**, *15*, 5363-5368.

(12)   Decher, G.; Lehr, B.; Lowack, K.; Lvov, Y.; Schmitt, J. "New Nanocomposite Films for Biosensors - Layer-by-Layer Adsorbed Films of Polyelectrolytes, Proteins or DNA" *Biosens Bioelectron* **1994**, *9*, 677-684.

(13)   Serizawa, T.; Hamada, K.; Kitayama, T.; Fujimoto, N.; Hatada, K.; Akashi, M. "Stepwise stereocomplex assembly of stereoregular poly(methyl methacrylate)s on a substrate" *Journal of the American Chemical Society* **2000**, *122*, 1891-1899.

(14)   Chen, W.; McCarthy, T. J. "Layer-by-layer deposition: A tool for polymer surface modification" *Macromolecules* **1997**, *30*, 78-86.

(15)   Levasalmi, J. M.; McCarthy, T. J. "Poly(4-methyl-1-pentene)-supported polyelectrolyte multilayer films: Preparation and gas permeability" *Macromolecules* **1997**, *30*, 1752-1757.

(16)   Hsieh, M. C.; Farris, R. J.; McCarthy, T. J. "Surface "priming" for layer-by-layer deposition: Polyelectrolyte multilayer formation on allylamine plasma-modified poly(tetrafluoroethylene)" *Macromolecules* **1997**, *30*, 8453-8458.

(17)   Phuvanartnuruks, V.; McCarthy, T. J. "Stepwise polymer surface modification: Chemistry-layer-by-layer deposition" *Macromolecules* **1998**, *31*, 1906-1914.

(18)   Chandler, D. "Interfaces and the driving force of hydrophobic assembly" *Nature* **2005**, *437*, 640-647.

(19)   Norde, W.; Lyklema, J. "Adsorption of Human-Plasma Albumin and Bovine Pancreas Ribonuclease at Negatively Charged Polystyrene Surfaces .1. Adsorption Isotherms. Effects of Charge, Ionic-Strength, and Temperature" *Journal of Colloid and Interface Science* **1978**, *66*, 257-265.

(20)   Shoichet, M. S.; McCarthy, T. J. "Surface Modification of Poly(Tetrafluoroethylene-Co-Hexafluoropropylene) Film by Adsorption of Poly(L-Lysine) from Aqueous-Solution" *Macromolecules* **1991**, *24*, 1441-1442.

(21)   Coupe, B.; Chen, W. "A new approach to surface functionalization of fluoropolymers" *Macromolecules* **2001**, *34*, 1533-1535.

(22)   Kozlov, M.; Quarmyne, M.; Chen, W.; McCarthy, T. J. "Adsorption of poly(vinyl alcohol) onto hydrophobic substrates. A general approach for hydrophilizing and chemically activating surfaces" *Macromolecules* **2003**, *36*, 6054-6059.

(23)   Kozlov, M.; McCarthy, T. J. "Adsorption of poly(vinyl alcohol) from water to a hydrophobic surface: Effects of molecular weight, degree of hydrolysis, salt, and temperature" *Langmuir* **2004**, *20*, 9170-9176.

(24)   Fadeev, A. Y.; McCarthy, T. J. "Trialkylsilane monolayers covalently attached to silicon surfaces: Wettability studies indicating that molecular topography contributes to contact angle hysteresis" *Langmuir* **1999**, *15*, 3759-3766.

CHAPTER 5

SYNTHESIS AND ADSORPTION OF HEMI-TELECHELIC BLOCK

COPOLYMERS

5.1 Introduction

Adsorption is a phenomenon in which there exists concentration gradient of the adsorbate at the interface. Adsorption of polymer to solid surfaces is of technological significance in colloidal stabilization, lubrication, adhesion and coating applications. Adsorption of polymers onto a solid surface is influenced by variety of factors including polymer molecular weight, polydispersity, chain stiffness, solvent quality and chemical interactions.[1] Upon adsorption, polymer molecules can adopt various configurations, like trains, loops and tails. Adsorption of polymers leads to loss of translational entropy, polymer/solvent interactions and solvent/adsorbent interactions. However, if there exists an environment, like poor solvent or a favorable enthalpic interaction between the polymer and the adsorbent, adsorption can occur.

Many studies have been carried out that deal with adsorption of polymers onto solid surfaces.[2,3] This chapter describes the synthesis of hemi-telechelic block copolymers of poly(styrene-*b*-isoprene) with different compositions and attachment of the functional group, -COOH at different positions. Adsorption studies of the polymers on alumina and silica surfaces were also carried out. The aim of the project is to carry out preliminary studies so that these functionalized polymers can be used in controlling the morphology of block copolymers in the pores of alumina membranes

5.2 Experimental section

5.2.1 Materials

All reagents were purchased from Aldrich and purified as mentioned below. All the distillations were preformed using a trap-to-trap technique. Styrene was distilled from CaH_2 into dibutyl magnesium and redistilled under low pressure at 40 °C. Isoprene was distilled from CaH_2 into 1°- butyl lithium and redistilled at 0 °C under low pressure. Cyclohexane was first distilled from CaH_2. To further purify cyclohexane, a solution containing 2°- butyl lithium/cyclohexane and few drops of styrene was made. This solution was added to distilled cyclohexane and it was redistilled. All the distilled reagents/solvent were stored under nitrogen. Tetrahydrofuran was distilled from sodium/benzophenone. Isopropanol was degassed by a freeze and thaw technique.
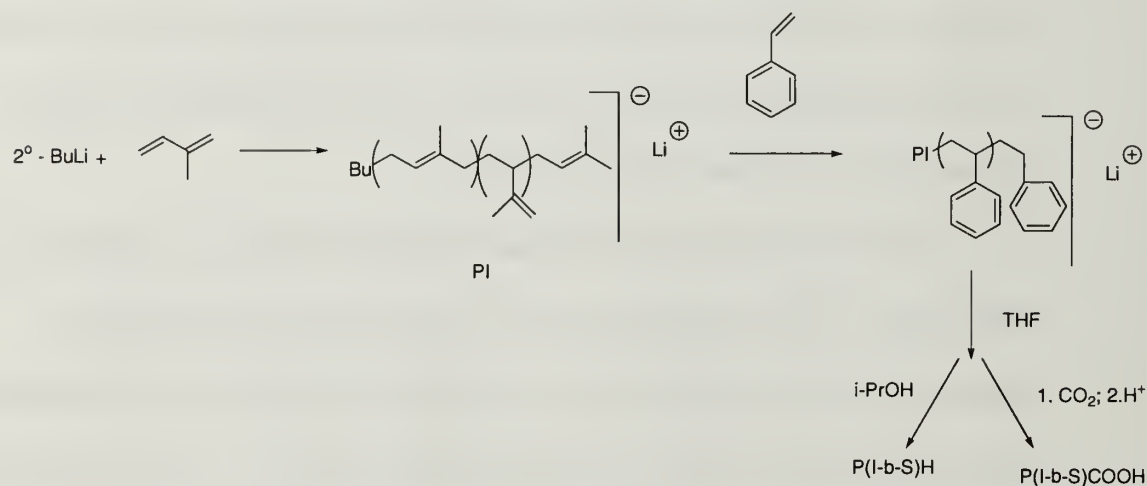
Figure 5.1 Representative synthesis of hemi telechelic block copolymer P(I-*b*-S).

5.2.2 Block copolymer synthesis

Hemitelechelic block copolymers of poly (styrene-co-isoprene) were synthesized in cyclohexane medium. Figure 5.1 shows a representative synthesis of functionalized block copolymer with the COOH group attached to the polystyrene end. To cyclohexane, a few drops of 2°- butyl lithium/styrene were added until a pale yellow color persists, indicating an impurities-free reaction medium. A calculated amount of 2°- butyl lithium was added followed by isoprene and the reaction was allowed to proceed for 17 hours at room temperature. Then, a calculated amount of styrene was added and allowed to react for 4 hours. To this block copolymer anion, distilled THF containing a few drops of 2°- butyl lithium/styrene was added to separate the aggregated anion. This solution was separated into two parts with one part terminated with isopropanol and the other part purged with CO_2 till the color of the solution changes from reddish orange to colorless. Block copolymer was precipitated in acidified ethanol and filtered. Block copolymers thus obtained were stored in amber-colored bottles under nitrogen. Calculations for the volume composition of the copolymer were based on the densities of monomer and polymer with isoprene (0.68 g/ml), poly(isoprene) (0.91 g/ml), styrene (0.906 g/ml) and poly(styrene) (1.05 g/ml).

5.2.3 Adsorption experiments

Alumina or silica substrates were submerged in block copolymer solutions in distilled toluene (25 mg / 5ml) for 17 h, removed, and rinsed with copious amounts of toluene. Substrates were dried under reduced pressure overnite.

5.2.4 Characterization

A Bruker DPX300 spectrometer (300 MHz ^{1}H NMR) was used to record NMR spectra to determine the volume fraction of polyisoprene and polystyrene. $CDCl_3$ was used as solvent. The molecular weight distribution was obtained using a Waters GPC equipped with a differential refractometer using THF as the eluent at a flow rate of 1.0 mL/min and the molecular weight determined using polystyrene standards. Thin Layer Chromatography (TLC) was performed using benzene as mobile phase and silica gel 60 Å as stationary phase. UV light was used to monitor the elution after drying the TLC plate. X-ray photoelectron spectra (XPS) were recorded with a Physical Electronics Quantum 2000 with Al K_α excitation. Spectra were obtained at different take off angles of 15°, 45° and 75° (between the plane of the surface and the entrance lens of the detector optics).

5.3 Results and discussion

5.3.1 Synthesis and characterization of the block copolymer

Block copolymers of different composition with the functional group attached to either isoprene end or styrene end were synthesized. Table 5.1 summarizes the properties of the block copolymer synthesized.

Table 5.1 Molecular properties of the polymer synthesized. F denotes either H or COOH.

Polymer	Volume % of styrene (± 4%)	M_w (Kg/mol)	PDI
P(S-*b*-I)F	50	29	1.05
P(I-*b*-S)F	50	36	1.08
P(S-*b*-I)F	30	16	1.03
P(I-*b*-S)F	70	19	1.29

Conventional synthesis of carboxylic acid-terminated polymers synthesized by living anionic polymerization using alkyl lithium in apolar solvent involves using tetramethylethylene diamine (TMEDA) as base to disaggregate the lithium clusters.[4,5] In the synthesis scheme used here, instead of using TMEDA, THF was used as the base to disaggregate the cluster. Along with that, carbonation was carried out by sparging CO_2 rather than by the conventional freeze-dry technique.[6]
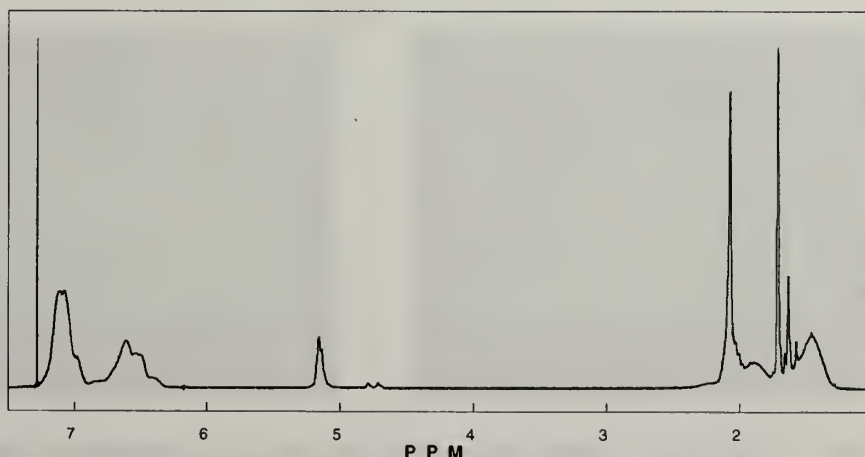
Figure 5.2 Representative NMR spectrum of P(S-*b*-I) copolymer
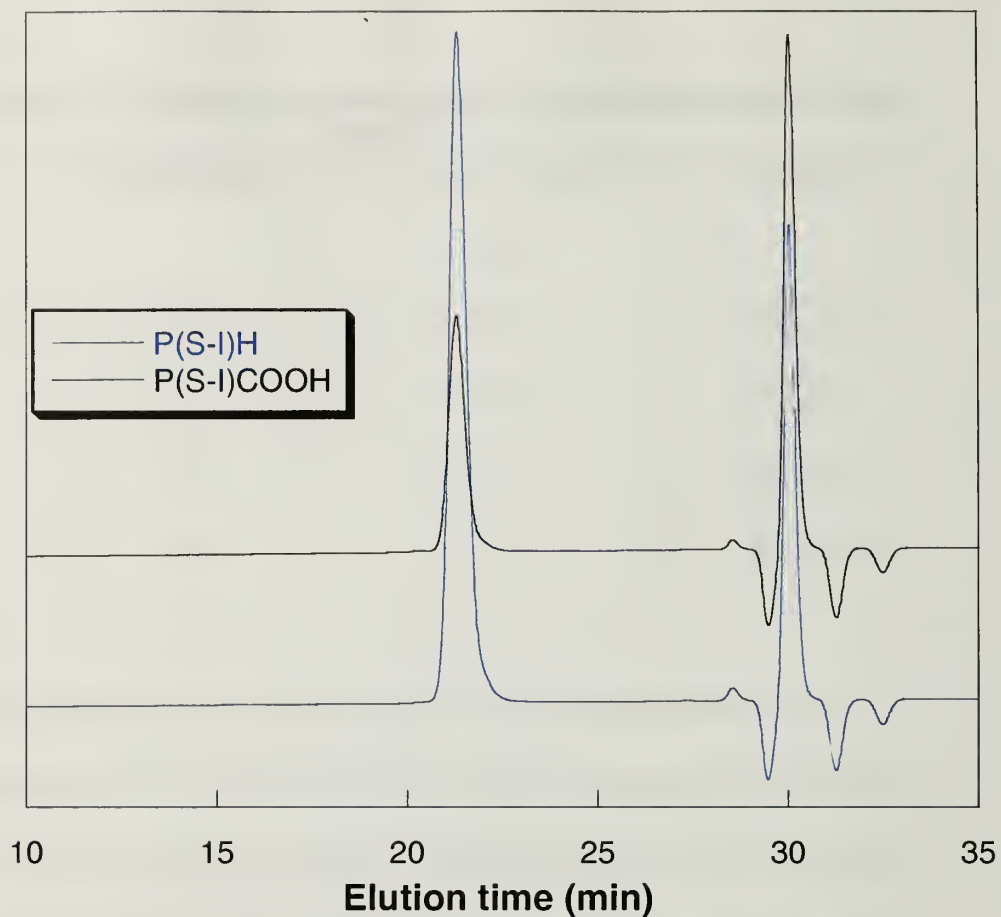
Figure 5.3 Representative GPC spectrum of COOH and H-terminated P(S-*b*-I) copolymer
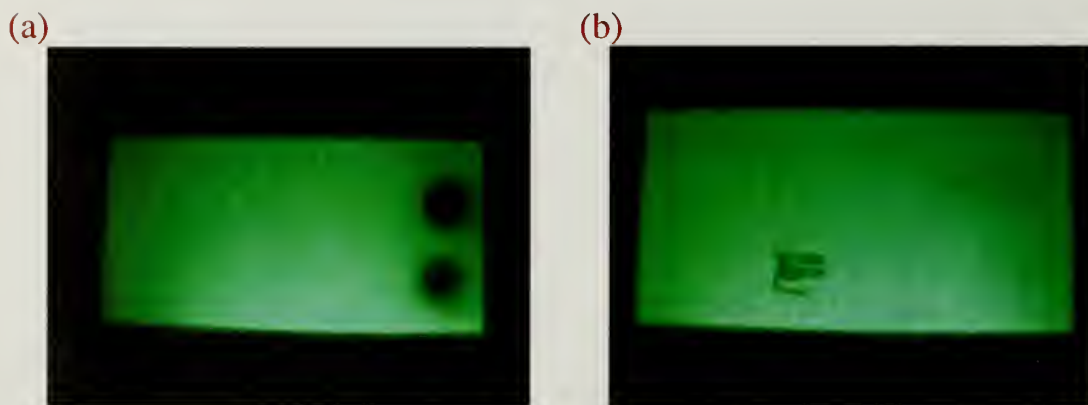
Figure 5.4 Thin layer chromatogram on fluorescence indicator-containing silica plate of COOH and H-terminated copolymer for (a) before elution and (b) after elution.

Block copolymers obtained were characterized by NMR to determine the volume composition of the components, GPC for molecular weight distribution and TLC to confirm the presence of functionalized end group. Figure 5.2 shows a representative NMR spectrum of a block copolymer. Use of apolar solvent for polymerization results in the thermodynamic product 1,4-isoprene compared to the kinetic product, 3,4-isoprene that is favored in polar solvents. In the NMR spectrum, the alkenic proton of the 1,4 product is at 5.15 ppm and the alkenic protons of the 3,4 product are at 4.7-4.8 ppm. Figure 5.3 compares the MWD of the –COOH terminated polymer and the H-terminated polymer. GPC confirms the ability of THF addition to successfully obtain monodisperse hemi-telechelic block copolymers. Presence of carboxylic acid group at the end of the polymer chain was confirmed by TLC studies. Figure 5.4 shows the chromatogram before and after elution for the carboxylic acid and hydrogen terminated block copolymer. H-terminated copolymer elutes completely by reaching the top of the solvent front (R_f =1) whereas the carboxylic acid terminated polymer leaves 2 distinct features, one at the solvent front due to the presence of H-terminated impurities and the second with a trail of COOH-terminated copolymer. Elution (or in general adsorption) is a dynamic process involving adsorption and desorption of the adsorbate/polymer from the surface. The presence of –COOH group affects the adsorption and desorption process, making the –COOH functionalized copolymer elute slower than the H-terminated copolymer.

5.3.2 Adsorption studies on alumina and silica substrates

Toluene (solubility parameter, $\delta = 18.5$ MPa$^{1/2}$) was chosen as the solvent for

adsorption studies as it is neutral to polystyrene ($\delta = 19.0$ MPa$^{1/2}$) and polyisoprene ($\delta =$

15.1 MPa$^{1/2}$) blocks. Figure 5.5 shows the XPS spectrum of the various alumina

surfaces in the adsorption experiments. The shakeup peak, corresponding to π to π^*

transition in polystyrene, is seen for P(S-b-I)COOH ($M_w = 29$ kG/mol) adsorbed on

alumina surface at higher binding energy, aroung 290 eV, in Figure 5.5(c). For H-

terminated copolymer, in Figure 5.5(b), no such shake-up peak is observed. The C_{1s} peak

observed in H-terminated peak is due to adsorption of carbonaceous impurities/solvent

on the high surface energy alumina surface. Such carbon is also observed for plasma-

treated alumina before adsorption experiments. It is also observed that when the

molecular weight of the copolymer is high, for P(I-b-S)F (36 Kg/mol), adsorption does

not occur as seen in Figure 5.6 (d) and (e). This is because, after a critical molecular

weight, an entropic penalty due to adsorption outweighs the enthalpic interaction

between COOH and alumina. These results are consistent with that observed by Iyengar

et. al. for functionalized polystyrenes where polymers above 37 Kg/mol did not show

any functionality effects.[2] Figure 5.6 shows the XPS spectra for the adsorption

experiments conducted on silica surfaces. As can be seen from the XPS studies, end

functionality does not have any impact on the adsorption characteristics of the

copolymer on silica. This is because the -COOH group interacts with the adsorbents in

different manner. Between alumina and carboxylic acid group, chemisorption with a

transfer of proton takes place whereas with silica, physisorption occurs.[7,8] This

difference in enthalpic interaction due to type of adsorption explains the adsorption of
hemi-telechelic block copolymer onto alumina and silica substrates.

(a)
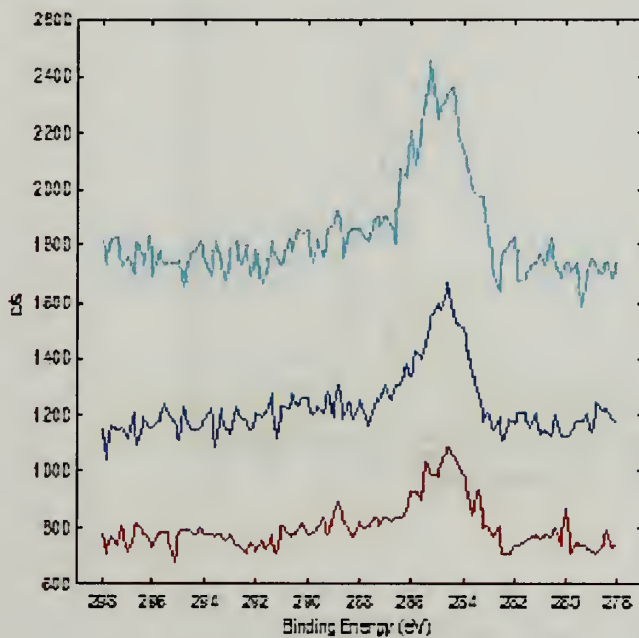
(b)
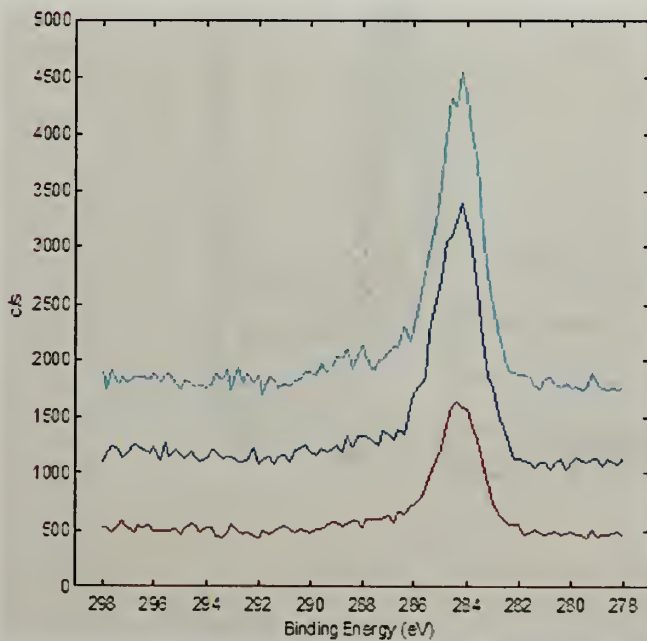
(c)
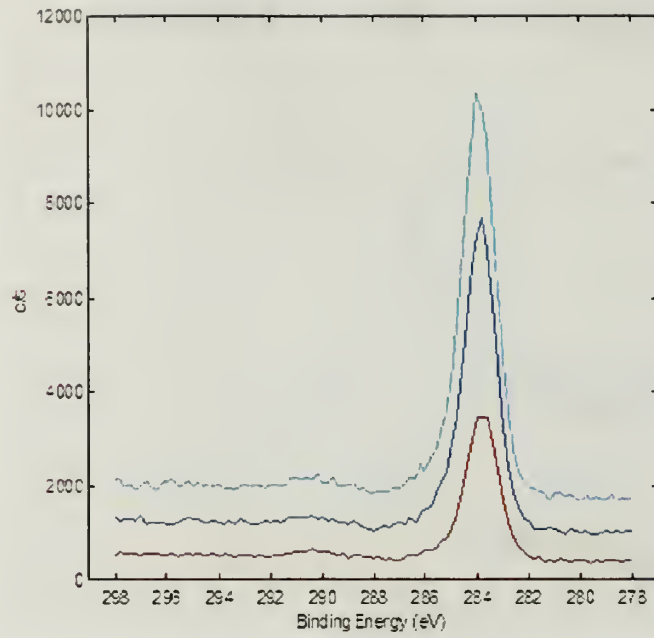
(d)
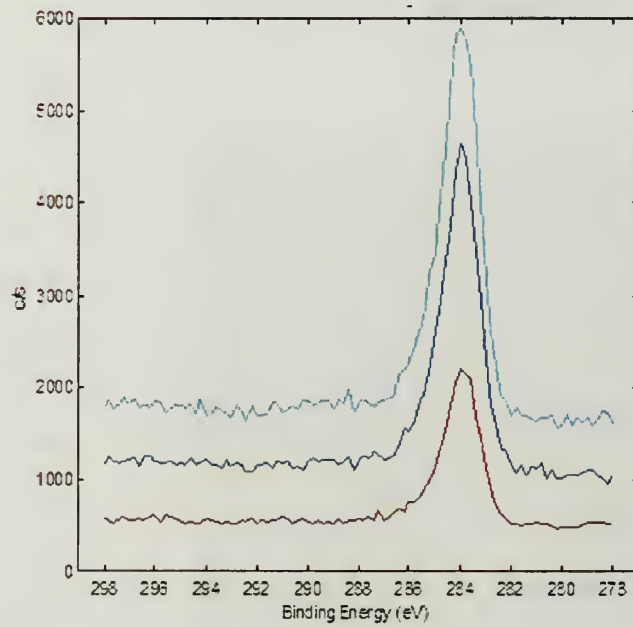
(e)
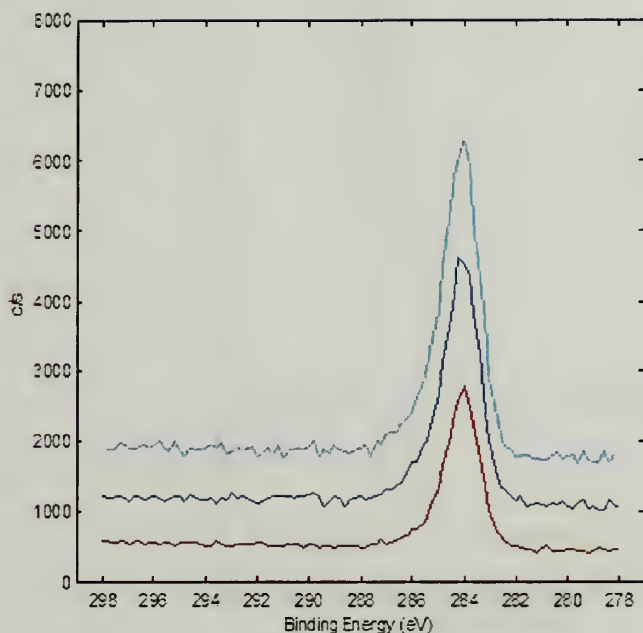
Figure 5.5 C_{1s} XPS spectrum of (a) plasma-treated alumina and alumina surfaces adsorbed with (b) P(S-*b*-I)H (M_w =29 Kg/mol) (c) P(S-*b*-I)COOH (M_w =29 Kg/mol) (d) P(I-*b*-S)H (M_w =36 Kg/mol) and (e) P(I-*b*-S)COOH (M_w =36 Kg/mol). Take off angles of 15° (red), 45° (blue) and 75° (turquoise) were used for XPS studies.

(a)
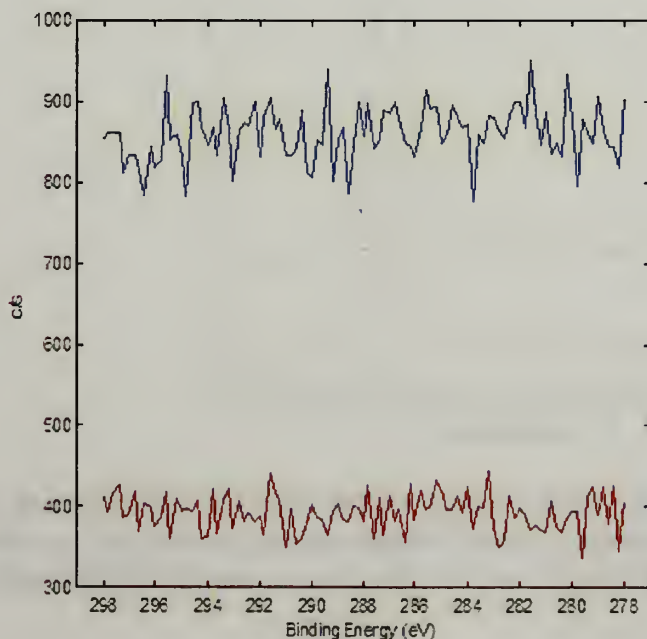
(b)
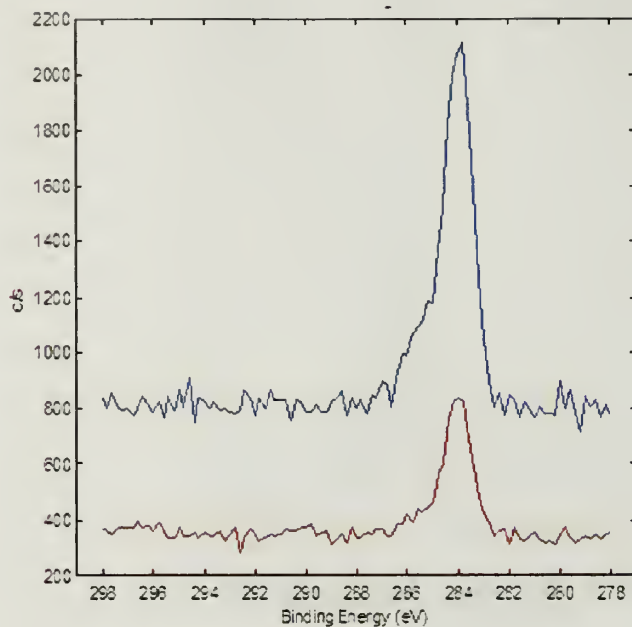
(c)
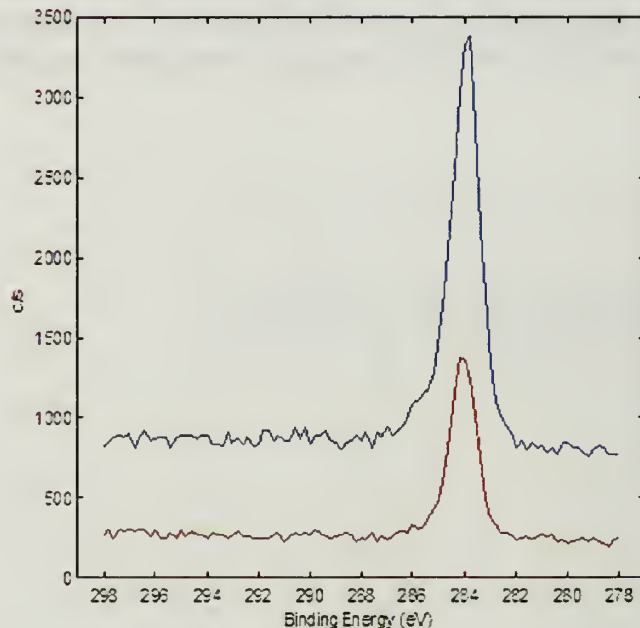
Figure 5.6 C_{1s} spectrum of (a) plasma treated silica (b) adsorption of H-terminated copolymer and (c) adsorption of COOH-terminated copolymer on silica. Take off angles of 15° (red), and 75° (blue) were used for XPS studies.

5.4 Conclusions

Poly(styrene-*b*-isoprene) copolymers end-functionalized with carboxylic acids were synthesized and characterized by NMR, GPC and TLC. Adsorption studies of the synthesized copolymers were carried out on silica and alumina. Adsorption of functionalized copolymer is influenced by the substrate, molecular weight of the copolymer and solvent quality. For future studies, these copolymers will be used in porous alumina membranes to control the copolymer morphology by varying the end functionality.

5.5 References

(1)   Adamson, A. W.; Gast, A. P. *Physical chemistry of surfaces*, 1997.

(2)   Iyengar, D. R.; Mccarthy, T. J. "Trends in Adsorption of End-Functionalized Polystyrenes by Thin-Layer Chromatography" *Macromolecules* **1990**, *23*, 4344-4346.

(3)   Stouffer, J. M.; Mccarthy, T. J. "Polymer Monolayers Prepared by the Spontaneous Adsorption of Sulfur-Functionalized Polystyrene on Gold Surfaces" *Macromolecules* **1988**, *21*, 1204-1208.

(4)   Quirk, R. P.; Yin, J.; Fetters, L. J. "Carbonation and Related Reactions of Poly(Styryl)Lithium" *Macromolecules* **1989**, *22*, 85-90.

(5)   Schulz, G. O.; Milkovich, R. "Graft Polymers with Macromonomers .1. Synthesis from Methacrylate-Terminated Polystyrene" *Journal of Applied Polymer Science* **1982**, *27*, 4773-4786.

(6)   Ji, H. N.; Nonidez, W. K.; Advincula, R. C.; Smith, G. D.; Kilbey, S. M.; Dadmun, M. D.; Mays, J. W. "MALDI-TOF MS characterization of carboxyl-end-capped polystyrenes synthesized using anionic polymerization" *Macromolecules* **2005**, *38*, 9950-9956.

(7)   Allara, D. L.; Nuzzo, R. G. "Spontaneously Organized Molecular Assemblies .1. Formation, Dynamics, and Physical-Properties of Normal-Alkanoic Acids Adsorbed from Solution on an Oxidized Aluminum Surface" *Langmuir* **1985**, *1*, 45-52.

(8)   Iler, R. K. *The chemistry of silica*; Wiley, 1979.

CHAPTER 6

CONCLUSIONS AND FUTURE WORK

6.1 Studies on reactive, hot-melt polyurethane adhesives

In the first part, influence of copolymer formed by the reaction of polyols, PHMA and PPG (1:1 by mass) with diisocyanate on morphology and crystallization kinetics is studied. Presence of copolymer of PPG-PHMA whose PPG contribution is 12% of the total mass of the polyurethane prepolymer has compatibilizing effect on the otherwise phase-separated blend of PPG prepolymer and PHMA prepolymer. From the crystallization kinetics study of PHMA, followed by time-dependent IR studies, it is observed that nucleation rate in PPG prepolymer/PHMA prepolymer blend and polyurethane prepolymer are almost equal at same degree of supercooling. But growth in polyurethane prepolymer is slower due to reduced domain size formed by the compatibilizing action of PPG-PHMA copolymer. Transport of PHMA to the crystallization growth front is affected by the presence of PPG 'defects'. This observation on crystallization kinetics is explained in terms of de Gennes' reptation model.

In the second part, a novel approach to cure isocyanate-terminated prepolymer, inspired by 'Trojan horse strategy' is implemented. Ammonium salts that are stable at room temperature but decompose on heating to evolve active hydrogen-containing compounds on heating or decompose over longer period of time (in days) at room temperature are used as triggers. Ammonium carbamate in the dispersion of PPG prepolymer/ammonium salt is more stable than ammonium bicarbonate at room

temperature but the decomposition rate of carbamate is faster than bicarbonate. Rate at which the active hydrogen-containing compounds are released determines the mechanical properties of the final product. Chemical crosslinks in the cured, polyurethane product is confirmed by the increase in T_g from DSC studies.

6.2 Adsorption studies using different interactions

Repetition of adsorption of PVOH on hydrophobic substrates by hydrophobic interactions followed by chemical modification of PVOH to generate hydrophobic substrate is used to form thickness-controlled, wettability-controlled, functionalized multilayer. Multilayers have been made using ester, urethane and acetal functionalities. Ability to successfully form the multilayer is contingent upon hydrophobicity of PVOH derived product. Hydrophobicity of PVOH derivative is in the order of ester > urethane > acetal. Multilayer-formation is also affected by the concentration of PVOH used for adsorption studies. Concentration of PVOH above entanglement concentration results in predominantly amorphous layer. This translates to thicker functionalized layers.

In the second part of this study, presence of functionality at the end of poly (styrene-*b*-isoprene) is used to control the adsorption properties of the polymer on alumina and silica substrates. Hemi-telechelic block copolymers, end-terminated with carboxylic acid or hydrogen, has been synthesized by living anionic polymerization. Enthalpic interaction between alumina and carboxylic acid overcomes the loss of translational entropy on adsorption, solvent/alumina interactions and polymer/solvent interactions. Thus, carboxylic acid-terminated polymer adsorbs onto alumina whereas hydrogen-containing polymer does not.

6.3 Future work

Curing studies by 'Trojan horse approach' involves using isocyanate-terminated PPG prepolymer ($T_g \sim$ -48 °C) as model prepolymer. However, actual, reactive, hot-melt polyurethane adhesive is a multicomponent system containing high T_g components (T_g up to 100 °C). This requires the adhesive to be melted before application. Ammonium salts used in this study can not withstand such high temperature. Future studies will involve developing new trigger systems or different ways of implementing the 'controlled curing' using ammonium carbamate or ammonium bicarbonate. Mechanical studies will also be performed to verify the suitability of these techniques to multicomponent systems.

Hemi-telechelic block copolymers will be used to control the morphology in the pores of alumina membrane. Studies will be carried out to verify if the enthalpic interaction between alumina and carboxylic acid group can overcome the interfacial interactions. Controlled positioning of carboxylic acid group in poly(styrene-*b*-isoprene) will help to study the competing factors.

BIBLIOGRAPHY

Adamson, A. W.; Gast, A. P. *Physical chemistry of surfaces*, 1997.

Allara, D. L.; Nuzzo, R. G. "Spontaneously Organized Molecular Assemblies .1. Formation, Dynamics, and Physical-Properties of Normal-Alkanoic Acids Adsorbed from Solution on an Oxidized Aluminum Surface" *Langmuir* **1985**, *1*, 45-52.

Blodgett, K. B. "Films built by depositing successive monomolecular layers on a solid surface" *Journal of the American Chemical Society* **1935**, *57*, 1007-1022.

Brame, E. G.; Ferguson, R. C.; Thomas, G. J. "Identification of Polyurethanes by High Resolution Nuclear Magnetic Resonance Spectrometry" *Anal Chem* **1967**, *39*, 517.

Campbell, J. R.; Hobbs, S. Y.; Shea, T. J.; Watkins, V. H. "Poly(Phenylene Oxide) Polyamide Blends Via Reactive Extrusion" *Polym Eng Sci* **1990**, *30*, 1056.

Chambon, F.; Petrovic, Z. S.; Macknight, W. J.; Winter, H. H. "Rheology of Model Polyurethanes at the Gel Point" *Macromolecules* **1986**, *19*, 2146-2149.

Chan, C.-M. *Polymer surface modification and characterization*; Hanser Publishers.

Chandler, D. "Interfaces and the driving force of hydrophobic assembly" *Nature* **2005**, *437*, 640-647.

Chen, D. B.; Qi, X.; Zhou, Z. H.; Zhong, A. Y.; Du, Z. Y. "Curing behavior of acrylate-urethane system" *J Appl Polym Sci* **1996**, *62*, 1715-1721.

Chen, W.; McCarthy, T. J. "Layer-by-layer deposition: A tool for polymer surface modification" *Macromolecules* **1997**, *30*, 78-86.

Chokki, Y. "Studies on Structure of Polyurethane Elastomers, .4. Nmr-Spectra of Linear Polyurethane Based on 2,4-Tolylenediisocyanate" *Makromol Chem* **1974**, *175*, 3425.

Chokki, Y.; Sumi, M.; Nakabaya.M. "Studies on Structure of Polyurethane Elastomers .3. Characterization of Linear Polyurethanes by Nmr-Spectroscopy - Components and Molecular-Weight" *Makromolekul Chem* **1972**, *153*, 189.

Comyn, J.; Brady, F.; Dust, R. A.; Graham, M.; Haward, A. "Mechanism of moisture-cure of isocyanate reactive hot melt adhesives" *International Journal of Adhesion and Adhesives* **1998**, *18*, 51-60.

Coupe, B.; Chen, W. "A new approach to surface functionalization of fluoropolymers" *Macromolecules* **2001**, *34*, 1533-1535.

Cui, Y. J.; Hong, L.; Wang, X. L.; Tang, X. Z. "Evaluation of the cure kinetics of isocyanate reactive hot-melt adhesives with differential scanning calorimetry" *Journal of Applied Polymer Science* **2003**, *89*, 2708-2713.

de Gennes, P. G. "Dynamics of Entangled Polymer-Solutions .1. Rouse Model" *Macromolecules* **1976**, *9*, 587.

de Gennes, P. G. "Reptation of a Polymer Chain in Presence of Fixed Obstacles" *J Chem Phys* **1971**, *55*, 572.

Decher, G.; Hong, J. D.; Schmitt, J. "Buildup of Ultrathin Multilayer Films by a Self-Assembly Process .3. Consecutively Alternating Adsorption of Anionic and Cationic Polyelectrolytes on Charged Surfaces" *Thin Solid Films* **1992**, *210*, 831-835.

Decher, G.; Lehr, B.; Lowack, K.; Lvov, Y.; Schmitt, J. "New Nanocomposite Films for Biosensors - Layer-by-Layer Adsorbed Films of Polyelectrolytes, Proteins or DNA" *Biosens Bioelectron* **1994**, *9*, 677-684.

Dimier, F.; Sbirrazzuoli, N.; Vergnes, B.; Vincent, M. "Curing kinetics and chemorheological analysis of polyurethane formation" *Polymer Engineering and Science* **2004**, *44*, 518-527.

Duffy, D. J.; Heintz, A. M.; Stidham, H. D.; Hsu, S. L.; Suen, W.; Chu, W.; Paul, C. W. "Influence of polymer structure on melt miscibility of ternary polymer blends: A model for high performance polyurethane adhesives and coatings" *Journal of Adhesion* **2003**, *79*, 1091-1107.

Duffy, D. J.; Heintz, A. M.; Stidham, H. D.; Hsu, S. L.; Suen, W.; Paul, C. W. "The competitive influence of specific interactions and extent of reaction on the miscibility of ternary reactive polymer blends: model for polyurethane adhesives" *International Journal of Adhesion and Adhesives* **2005**, *25*, 39-46.

Duffy, D. J.; Stidham, H. D.; Hsu, S. L.; Sasaki, S.; Takahara, A.; Kajiyama, T. "Effect of polyester structure on the interaction parameters and morphology development of ternary blends: Model for high performance adhesives and coatings" *J Mater Sci* **2002**, *37*, 4851-4859.

Fadeev, A. Y.; McCarthy, T. J. "Trialkylsilane monolayers covalently attached to silicon surfaces: Wettability studies indicating that molecular topography contributes to contact angle hysteresis" *Langmuir* **1999**, *15*, 3759-3766.

Folkes, M. J.; Hope, P. S. *Polymer blends and alloys*; Chapman & Hall, 1993.

Forschner, T. C.; Gwyn, D. E.; Xiao, H. X.; Suthar, B.; Sun, L. Q.; Frisch, K. C. "Polyurethane hot melt adhesives based on 1,3-PDO" *Adhes Age* **1999**, *42*, 20.

Freluche, M.; Iliopoulos, I.; Millequant, M.; Flat, J. J.; Leibler, L. "Graft copolymers of poly(methyl methacrylate) and polyamide-6: Synthesis by reactive blending and characterization" *Macromolecules* **2006**, *39*, 6905-6912.

Gaines, G. L. "From Monolayer to Multilayer - Some Unanswered Questions" *Thin Solid Films* **1980**, *68*, 1-5.

Guegan, P.; Macosko, C. W.; Ishizone, T.; Hirao, A.; Nakahama, S. "Kinetics of Chain Coupling at Melt Interfaces" *Macromolecules* **1994**, *27*, 4993.

Hashida, T.; Jeong, Y. G.; Hua, Y.; Hsu, S. L.; Paul, C. W. "Spectroscopic study on morphology evolution in polymer blends" *Macromolecules* **2005**, *38*, 2876.

Heintz, A. M. *Ph. D Thesis, University of Massachusetts, 2003*.

Heintz, A. M.; Duffy, D. J.; Hsu, S. L.; Suen, W.; Chu, W.; Paul, C. W. "Effects of reaction temperature on the formation of polyurethane prepolymer structures" *Macromolecules* **2003**, *36*, 2695.

Helfand, E.; Tagami, Y. "Theory of Interface between Immiscible Polymers" *Journal of Polymer Science Part B-Polymer Letters* **1971**, *9*, 741.

Honig, E. P. "Molecular Constitution of X-Type and Y-Type Langmuir-Blodgett Films" *Journal of Colloid and Interface Science* **1973**, *43*, 66-72.

Hsieh, M. C.; Farris, R. J.; McCarthy, T. J. "Surface "priming" for layer-by-layer deposition: Polyelectrolyte multilayer formation on allylamine plasma-modified poly(tetrafluoroethylene)" *Macromolecules* **1997**, *30*, 8453-8458.

Ide, F.; Hasegawa, A. "Studies on Polymer Blend of Nylon-6 and Polypropylene or Nylon-6 and Polystyrene Using Reaction of Polymer" *J Appl Polym Sci* **1974**, *18*, 963.

Ikkala, O. T.; Holstimiettinen, R. M.; Seppala, J. "Effects of Compatibilization on Fractionated Crystallization of PA6/PP Blends" *J Appl Polym Sci* **1993**, *49*, 1165.

Iler, R. K. *The chemistry of silica*; Wiley, 1979.

Iyengar, D. R.; Mccarthy, T. J. "Trends in Adsorption of End-Functionalized Polystyrenes by Thin-Layer Chromatography" *Macromolecules* **1990**, *23*, 4344-4346.

Jeong, Y. G.; Hashida, T.; Hsu, S. L.; Paul, C. W. "Factors influencing curing Behavior in phase-separated structures" *Macromolecules* **2005**, *38*, 2889-2896.

Jeong, Y. G.; Hashida, T.; Nelson, C. M.; Hsu, S. L.; Paul, C. W. "Morphology evolution and associated curing kinetics in reactive blends" *International Journal of Adhesion and Adhesives* **2006**, *26*, 600-608.

Jeong, Y. G.; Hashida, T.; Wu, G. L.; Hsu, S. L.; Paul, C. W. "Analysis of the multistep solidification process in polymer blends" *Macromolecules* **2006**, *39*, 274-280.

Jeong, Y. G.; Pagodina, N. V.; Jiang, C.; Hsu, S. L.; Paul, C. W. "Effects of polyester-poor phase microstructures on viscosity development of polymer blends" *Macromolecules* **2006**, *39*, 4907-4913.

Jeong, Y. G.; Ramalingam, S.; Archer, J.; Hsu, S. L.; Paul, C. W. "Influence of copolymer configuration on the phase behavior of ternary blends" *J Phys Chem B* **2006**, *110*, 2541-2548.

Ji, H. N.; Nonidez, W. K.; Advincula, R. C.; Smith, G. D.; Kilbey, S. M.; Dadmun, M. D.; Mays, J. W. "MALDI-TOF MS characterization of carboxyl-end-capped polystyrenes synthesized using anionic polymerization" *Macromolecules* **2005**, *38*, 9950-9956.

Kopp, F.; Fringeli, U. P.; Muhlethaler, K.; Gunthard, H. H. "Instability of Langmuir-Blodgett Layers of Barium Stearate, Cadmium Arachidate and Tripalmitin, Studied by Means of Electron-Microscopy and Infrared Spectroscopy" *Biophysics of Structure and Mechanism* **1975**, *1*, 75-96.

Kozlov, M.; Quarmyne, M.; Chen, W.; McCarthy, T. J. "Adsorption of poly(vinyl alcohol) onto hydrophobic substrates. A general approach for hydrophilizing and chemically activating surfaces" *Macromolecules* **2003**, *36*, 6054-6059.

Kozlov, M.; McCarthy, T. J. "Adsorption of poly(vinyl alcohol) from water to a hydrophobic surface: Effects of molecular weight, degree of hydrolysis, salt, and temperature" *Langmuir* **2004**, *20*, 9170-9176.

Lee, H.; Kepley, L. J.; Hong, H. G.; Mallouk, T. E. "Inorganic Analogs of Langmuir-Blodgett Films - Adsorption of Ordered Zirconium 1,10-Decanebisphosphonate Multilayers on Silicon Surfaces" *Journal of the American Chemical Society* **1988**, *110*, 618-620.

Leibler, L.; Orland, H.; Wheeler, J. C. "Theory of Critical Micelle Concentration for Solutions of Block Co-Polymers" *J Chem Phys* **1983**, *79*, 3550.

Lepene, B. S.; Long, T. E.; Meyer, A.; Kranbuehl, D. E. "Moisture-curing kinetics of isocyanate prepolymer adhesives" *Journal of Adhesion* **2002**, *78*, 297-312.

Levasalmi, J. M.; McCarthy, T. J. "Poly(4-methyl-1-pentene)-supported polyelectrolyte multilayer films: Preparation and gas permeability" *Macromolecules* **1997**, *30*, 1752-1757.

Mehl, J. T.; Murgasova, R.; Dong, X.; Hercules, D. M.; Nefzger, H. "Characterization of polyether and polyester polyurethane soft blocks using MALDI mass spectrometry" *Anal Chem* **2000**, *72*, 2490.

Murgasova, R.; Brantley, E. L.; Hercules, D. M. "Characterization of polyester-polyurethane soft and hard blocks by a combination of MALDI, SEC, and chemical degradation" *Macromolecules* **2002**, *35*, 8338.

Netzer, L.; Sagiv, J. "A New Approach to Construction of Artificial Monolayer Assemblies" *Journal of the American Chemical Society* **1983**, *105*, 674-676.

Noolandi, J.; Hong, K. M. "Interfacial Properties of Immiscible Homopolymer Blends in the Presence of Block Copolymers" *Macromolecules* **1982**, *15*, 482-492.

Norde, W.; Lyklema, J. "Adsorption of Human-Plasma Albumin and Bovine Pancreas Ribonuclease at Negatively Charged Polystyrene Surfaces .1. Adsorption Isotherms. Effects of Charge, Ionic-Strength, and Temperature" *Journal of Colloid and Interface Science* **1978**, *66*, 257-265.

Okuto, H. "Studies on Structure of Polyurethane Elastomers .2. High Resolution Nmr Spectroscopic Determination of Allophanate and Biuret Linkages in Cured Polyurethane Elastomer - Degradation by Amine" *Makromolekul Chem* **1966**, *98*, 148.

Otterson, D. M.; Kim, B. H.; Lavengood, R. E. "The Effect of Compatibilizer Level on the Mechanical-Properties of a Nylon 6/Abs Polymer Blend" *J Mater Sci* **1991**, *26*, 1478-1484.

Park, D. W.; Roe, R. J. "Effect of Added Block Copolymer on the Phase-Separation Kinetics of a Polymer Blend .2. Optical Microscopic Observations" *Macromolecules* **1991**, *24*, 5324.

Paul, D. R. *Polymer Blends (Eds. D. R. Paul and S. Newmann), Vol. 1, Academic Press* **2000**.

Pegoraro, M.; Galbiati, A.; Ricca, G. "H-1 nuclear magnetic resonance study of polyurethane prepolymers from toluene diisocyanate and polypropylene glycol" *J Appl Polym Sci* **2003**, *87*, 347.

Pernot, H.; Baumert, M.; Court, F.; Leibler, L. "Design and properties of co-continuous nanostructured polymers by reactive blending" *Nat Mater* **2002**, *1*, 54-58.

Phuvanartnuruks, V.; McCarthy, T. J. "Stepwise polymer surface modification: Chemistry-layer-by-layer deposition" *Macromolecules* **1998**, *31*, 1906-1914.

Prabhakar, A.; Chattopadhyay, D. K.; Jagadeesh, B.; Raju, K. V. S. N. "Structural investigations of polypropylene glycol (PPG) and isophorone diisocyanate (IPDI)-based polyurethane prepolymer by 1D and 2D NMR spectroscopy" *J Polym Sci Pol Chem* **2005**, *43*, 1196.

Qiao, L.; Leibig, C.; Hahn, S. F.; Winey, K. I. "Isolating the effects of morphology and chain architecture on the mechanical properties of triblock copolymers" *Ind Eng Chem Res* **2006**, *45*, 5598-5602.

Quirk, R. P.; Yin, J.; Fetters, L. J. "Carbonation and Related Reactions of Poly(Styryl)Lithium" *Macromolecules* **1989**, *22*, 85-90.

Schulz, G. O.; Milkovich, R. "Graft Polymers with Macromonomers .1. Synthesis from Methacrylate-Terminated Polystyrene" *Journal of Applied Polymer Science* **1982**, *27*, 4773-4786.

Serizawa, T.; Hamada, K.; Kitayama, T.; Fujimoto, N.; Hatada, K.; Akashi, M. "Stepwise stereocomplex assembly of stereoregular poly(methyl methacrylate)s on a substrate" *Journal of the American Chemical Society* **2000**, *122*, 1891-1899.

Serizawa, T.; Hashiguchi, S.; Akashi, M. "Stepwise assembly of ultrathin poly(vinyl alcohol) films on a gold substrate by repetitive adsorption/drying processes" *Langmuir* **1999**, *15*, 5363-5368.

Shimazaki, Y.; Mitsuishi, M.; Ito, S.; Yamamoto, M. "Preparation of the layer-by-layer deposited ultrathin film based on the charge-transfer interaction" *Langmuir* **1997**, *13*, 1385-1387.

Shoichet, M. S.; McCarthy, T. J. "Surface Modification of Poly(Tetrafluoroethylene-Co-Hexafluoropropylene) Film by Adsorption of Poly(L-Lysine) from Aqueous-Solution" *Macromolecules* **1991**, *24*, 1441-1442.

Stockton, W. B.; Rubner, M. F. "Molecular-level processing of conjugated polymers .4. Layer-by-layer manipulation of polyaniline via hydrogen-bonding interactions" *Macromolecules* **1997**, *30*, 2717-2725.

Stouffer, J. M.; Mccarthy, T. J. "Polymer Monolayers Prepared by the Spontaneous Adsorption of Sulfur-Functionalized Polystyrene on Gold Surfaces" *Macromolecules* **1988**, *21*, 1204-1208.

Sumi, M.; Chokki, Y.; Nakai, Y.; Nakabayashi, M.; Kanzawa, T. "Studies on the Structure of Polyurethane Elastomers .1. Nmr Spectra of the Model Compounds and Some Linear Polyurethanes" *Makromolekul Chem* **1964**, *78*, 146.

Sun, X. D.; Sung, C. S. P. "Cure characterization in polyurethane and model urethane reactions by an intrinsic fluorescence technique" *Macromolecules* **1996**, *29*, 3198-3202.

Szycher , M. *Handbook of Polyurethanes*, Chapter 4.

Tol, R. T.; Mathot, V. B. F.; Groeninckx, G. "Confined crystallization phenomena in immiscible polymer blends with dispersed micro- and nanometer sized PA6 droplets, part 2: reactively compatibilized PS/PA6 and (PPE/PS)/PA6 blends" *Polymer* **2005**, *46*, 383.

Vanderweij, F. W. "Kinetics and Mechanism of Urethane Formation Catalyzed by Organotin Compounds .1. The Reaction of Phenyl Isocyanate with Methanol in Dibutyl Ether under the Action of Dibutyltin Diacetate" *J Polym Sci Pol Chem* **1981**, *19*, 381.

Vanderweij, F. W. "Kinetics and Mechanism of Urethane Formation Catalyzed by Organotin Compounds .2. The Reaction of Phenyl Isocyanate with Methanol in Dmf and Cyclohexane under the Action of Dibutyltin Diacetate" *J Polym Sci Pol Chem* **1981**, *19*, 3063.

Vick, C. B.; Okkonen, E. A. "Strength and durability of one-part polyurethane adhesive bonds to wood" *Forest Prod J* **1998**, *48*, 71.

Wang, L. Y.; Wang, Z. Q.; Zhang, X.; Shen, J. C.; Chi, L. F.; Fuchs, H. "A new approach for the fabrication of an alternating multilayer film of poly(4-vinylpyridine) and poly(acrylic acid) based on hydrogen bonding" *Macromolecular Rapid Communications* **1997**, *18*, 509-514.

Wicks, D. A.; Wicks, Z. W. "Blocked isocyanates III: Part A. Mechanisms and chemistry" *Progress in Organic Coatings* **1999**, *36*, 148-172.

Wong, S. W.; Frisch, K. C. "Catalysis in Competing Isocyanate Reactions .2. Competing Phenyl Isocyanate Reactions Catalyzed with N,N',N"-Pentamethyldipropylenetriamine" *J Polym Sci Pol Chem* **1986**, *24*, 2877.

Yeager, F. W.; Becker, J. W. "Determination of Composition and Molecular-Weight of Polyester Urethanes by High-Resolution Proton Magnetic-Resonance Spectrometry" *Anal Chem* **1977**, *49*, 722.